Geology and geochemistry of regolith carbonate accumulations of the southwestern Curnamona Province, SA: Implications for mineral exploration

P.D. WITTWER

CRC LEME, School of Earth & Environmental Sciences, Geology & Geophysics, Mawson Laboratories, University of Adelaide, SA, 5005.
e-mail: paul.wittwer@student.adelaide.edu.au

Supervisors: Dr K.M. BAROVICH and Dr S.M. HILL

Date: 27th day of October, 2004

TABLE OF CONTENTS

LIST OF FIGURES

LIST OF TABLES

ABSTRACT

Although regolith carbonate accumulations (RCAs) have been extensively used in mineral exploration programs in the regolith-dominated terrains of the Yilgarn and Gawler Cratons, their use has so far been limited within the Curnamona Province, SA. This study shows how the detailed characterisation of RCAs in the southwestern Curnamona Province enhances their use in mineral exploration programs at the regional to prospect scales. A regional RCA distribution map for the study area shows that RCAs are generally widespread, although certain RCA morphological facies are dominant in different parts of the landscape, and in some areas RCAs are absent or at best a very minor component of the regolith. A dataset of whole rock geochemical assays of RCAs provides the basis of graphical presentations and geochemical maps that highlight the chemical characteristics of RCAs proximal to areas of known Au mineralisation in contrast to more distal samples. Several Au pathfinder elements in RCA assays were found to include As, W, Bi, and Mo, and greatly assist in further anomaly definition when used in conjunction with Au assays. Major element composition (e.g. Ca, Mg, Fe) showed little relationship to local landform setting, however, landscape setting appears to be a more important control on Au assay results both at the regional and prospect scales. Gold distribution in the area was independent of the presence of major elements such as calcium and magnesium. Microprobe analysis showed that Au was rare and invisible at the resolution of the analysis and existed in the calcium carbonate matrix as well as in detrital material. The composition of the underlying rock lithologies was also compared to the whole rock chemistry of the RCAs, and showed the possibilities of this technique to aid geological mapping in regolith-dominated terrains and to assist in locating mineralised systems.

KEY WORDS: Gold, regolith, calcrete, mineral exploration, Curnamona Province

INTRODUCTION

The use of regolith carbonate accumulations (RCAs) in Australian mineral exploration programs has increased greatly in the past decade (e.g. McQueen *et al*. 1999; Lintern 2002). The main application of RCAs has been as a geochemical sampling media for the detection of Au mineralisation within regolith-dominated terrains. The technique has been responsible for mineral discoveries in the Yilgarn (e.g. Lintern & Butt 1993; Anand *et al*. 1997) and Gawler Cratons (e.g. Lintern & Sheard 1999; Lintern 2001), but to date has had limited application in other Precambrian terranes, such as the Curnamona Province.

The aim of this study is to characterise RCAs in the Olary Domain in the southwestern part of the Curnamona Province (CP). The study is designed to give an insight into whether RCAs are an effective tool for detecting mineralisation and distinguishing it from 'background' settings at both a regional and a tenement or prospect scale. Additionally, an evaluation is made of the potential for RCA geochemical assays to serve as an aid to geological mapping, in areas of shallow (< 10 m) transported cover.

The area for the RCA study (Figure 1) was chosen because it has historically been prospective for Au, including the Luxemburg, Wilkins, and Green and Gold Cu-Au mines (Drew 1992). The region is also a target area for ongoing exploration for Au mineralisation, particularly after the recent discovery of the White Dam Au-Cu deposit

(Brown & Hill 2003; Busuttil & Bargman 2003; Cooke 2003). This study has implications for the further development of exploration techniques for large areas of the central and northern Curnamona Province, where there is minor exposure of rocks that host mineralisation. The results from this study can also be linked with other research in the area, such as remote sensing, regolith-landform mapping at various scales (e.g. Crooks 2002; Brown & Hill 2003; Lau 2004), and other regolith geochemical investigations (e.g. Brown *et al*. 2002) and biogeochemical studies (e.g. Hulme & Hill 2003).

SETTING

Geological setting

The Curnamona Province is located in eastern South Australia and western New South Wales (Figure 1). It is composed of Palaeoproterozoic metasedimentary and metaigneous rocks intruded by early Mesoproterozoic granitic intrusives and felsic volcanics. Extensive Neoproterozoic and early Palaeozoic sequences unconformably overlie basement. Cainozoic sediments associated with the Murray Basin to the south (e.g. Fabris 2002) and the Lake Eyre Basin to the north (e.g. Alley 1998) are widespread across the entire region.

Mineralisation at each of the Luxemburg, Green and Gold, White Dam and Wilkins areas occurs near the top of the lower Willyama Supergroup (including Thackaringa and Curnamona Groups), in mainly albitic and calc-albitic metasedimentary rocks, in

discordant zones or a stratabound fashion (Skirrow & Ashley 2000). The major geological and alteration features of each are briefly described in Table 1.

Landscape setting, vegetation and regolith materials

Although the landscape of the study may at first appear to be a relatively simple assemblage of undulating landforms, in detail it contains considerable local complexity. Topographic elevations in the area ranges between over 370 m above sea level near MacDonald Hill in the west to approximately 200 m above sea level along tributaries of the Mingary Creek system in the north. The area contains the generally east-west trending regional drainage divide between the Murray Basin to the south and the Lake Eyre Basin to the north. To the south the drainage is mostly associated with the Olary Creek system, whereas to the north it includes tributaries of the Mingary Creek system.

The dominant landforms of the area are bedrock-dominated erosional low hills, rises and plains, and transported regolith-dominated plains, drainage depressions and channels. The southern and western areas tend to be associated with higher relief parts of the landscape, including erosional rises (9 – 30 m relief) and low hills (30 – 90 m relief). Alluvial drainage depressions have incised into many of the erosional landforms and deliver sediment into the larger depositional plains associated with major valley systems (Figure 2).

There are also major variations in regolith materials, associated with the differences in landform setting. The dominant regolith units on the plains are sheet flow sediments

with minor aeolian accessions. The sediments are typically red-brown silts and sands within the areas of high relief, and grade laterally towards red clays as the relief decreases within the depositional plains. The southern and western parts of the area are dominated by exposures of Willyama Supergroup and Adelaidean rocks. The bedrock is slightly to moderately weathered, and generally flanked by colluvial sediment. Alluvial lithic and quartzose, silts, sands and gravels dominate the drainage depressions.

The main vegetation community is a chenopod shrubland, which extends across most of the area. The dominant plants include *Maireana spp.* (pearl bluebush and black bluebush) and *Atriplex spp.* (bladder saltbush and pop saltbush). Scattered trees of *Alectrylon oleofolius* (rosewood), *Casuarina pauper* (belah) and stumps (with only occasional living specimens) of *Acacia aneura* (mulga) occur within these shrublands. The undergrowth consists of copper burr and some grasses, as well as cryptogam mats (combination of lichens, mosses and algae) colonising the surface soils. The species composition of the chenopod shrubland closely relates to the landform and regolith setting. There is a general transition from pearl bluebush to black bluebush to bladder saltbush between high to low lying settings (Figure 3). A riparian woodland of *Eucalyptus camaldulensis* (river red gums) occurs along the upper tributaries of Bulloo Creek in the north of the area.

Climate and land use

The climate in the area is semi-arid, with an annual precipitation of around 150 mm. In summer the temperature can reach 47° C and drop as low as –6° C on winter nights

(www.bom.com.au). The study area hosts three sheep grazing stations – 'Tikalina' in the south and east central parts, 'Wiawera' in the southwest and 'Bulloo Creek' in the north.

METHODS

Mapping

Regolith-landform mapping was completed at both the regional and detailed scales. A regional (1:30 k) regolith-landform map of the study area has been recently completed (Lau 2004), however, because this map contains minimal information about the regional distribution of RCAs, a regional RCA morphological map was produced here (Figure 2). A detailed regolith-landform map of approximately 2 km^2 was also produced at the Wilkins prospect. The regolith-landform units are given an abbreviated label, e.g. CHep$_2$, which provides information such as regolith type (represented by upper case abbreviations i.e. CH – sheet flow sediments) and landform (lower case abbreviations i.e. ep – an erosional plain). The modifier number signifies lesser regolith-landform differences (e.g. vegetation change or slight regolith lithological differences)(Figure 4a and Appendix 1).

Sampling and geochemical analytical methods

The sampling strategy involved a 3-tier approach that is equivalent to the typical scales of mineral exploration undertaken in a region:

- A regional RCA dataset of 166 samples, including reconnaissance samples, over an area of approximately 840 km^2, which encompasses four known mineralisation sites (Luxemburg, Wilkins, Green and Gold and White Dam) and the areas in between;

- Single line transects to follow-up regional geochemical anomalies with samples taken at about 50 m spacing over the 4 mineralisation sites, yielding a further 26 samples, with another 13 non-transect spot samples near mineralisation; and,

- A detailed, prospect-scale sampling array of 20 samples collected at a spacing of about 50 - 250 m in the area of the Wilkins prospect.

RCAs were collected from surface exposures within the study area. The preferred sites for sampling were rabbit warrens (Figure 4a, b). They were ideal sites because the RCAs were brought from depth to the surface when the rabbits dug their burrows, and the original morphology of the RCA sample could still be identified. Another advantage of sampling rabbit warrens is that they can be easily located in the field and on ortho-imagery, and therefore targeted in regional sampling programs. In some places, where there were few rabbit warrens, there were abundant RCAs transported across the land surface by shallow overland flow (sheet flow) and minor erosional gullies. These typically correspond with erosional (ep) and depositional (pd) plain landform settings. In addition, a profile of Willyama Supergroup saprock to soil was sampled in the old Radium Hill cutting.

Approximately 200 g of RCA fragments were collected at each site, in addition to a larger piece of ~7 cm diameter, which was to be kept aside for other analyses (e.g. thin

sections). Sampling was difficult in certain areas where the calcium carbonate content of the substrate was low, such as areas containing an abundance of quartz lag. Other attributes were also noted at each site, including: the morphology and lithology of RCAs, host regolith lithology, vegetation community and dominant species, and landform setting.

The samples were analysed using the IC3E/M and AA9 techniques at Amdel Laboratories, Thebarton, SA. The former involved a sub sample of 0.2 g of the analytical pulp being digested using an HF/multi acid digest. This was followed by the presentation of the solution to an inductively couple plasma mass spectrometer (ICP-MS) and an inductively couple plasma optical emission spectrometer (ICP-OES) for the quantification of the elements of interest. ICP-MS analysed elements included: Ag, As, Bi, Cd, Cs, Ce, Co, Cu, Ga, In, La, Mo, Ni, Pb, Rb, Sb, Se, Sr, Te, Th, Tl, U, W, Zn, Ce, La, Dy, Er, Eu, Gd, Ho, Lu, Nd, Pr, Sm, Tb, Tm, Yb, Y. ICP-OES analysed elements included: Ba, Ca, Cr, Fe, K, Mg, Mn, Na, P, Ti, V, S. The AA9 technique quantified the Au content, where a sub-sample of 40 g of the analytical pulp was digested with aqua-regia. The resulting Au in solution was extracted into di-iso butyl ketone (DIBK) and quantified by Graphite Furnace Atomic Absorption Spectrometer to a resolution of 1 ppb.

These assay values were then imported to Data Desk$^{©}$ for statistical analysis. After the below-detection limit values were allocated a numerical value (typically half of detection limit), a series of box and whisker plots were generated for each element, highlighting values that ranged between extremely high outliers, to extremely low

outliers. These plots are basically designed to define anomalous values (outliers), with respect to the bulk of the data (normally between the upper box to lower box range), somewhat like a histogram. These cut-off numbers were recorded and entered into ArcView GIS©, and a series of geochemical maps were plotted for each element.

The Philips XL30 FEGSEM was used to image selected RCA samples in backscatter mode, and to search for any visible Au. The CAMECA SX51 electron microprobe was used to compositionally search for Au in RCA samples. The machine was calibrated with the following package features: accelerating potential of 20 keV, sample beam current of 20 nA and beam diameter of 5 microns. Initial counting times of 30 seconds produced an analytical precision of 0.5 W% Au, and subsequent 300 second counting times reduced this detection limit to 0.03 W% nominally, and as low as 0.016 W%. Corrections made in the analysis included the rejection of Au values below detection limit, as they were related to instrumental noise, and the Au values where Zr was present in large quantities (as the Zr peak strongly overlaps with the Au Mα peak). Other elements analysed were O, Ca, Si, Mg, Na, Fe, As, Au, Pb and Zn.

MAPPING, GEOCHEMISTRY AND MICROANALYSIS RESULTS

Mapping

The RCA distribution map shows the presence or absence of RCAs, as well as the dominant morphological facies associated with different regolith-landform settings in the study area. This map serves as a "go-to map" for mineral explorers planning RCA

sampling programs. The dominant RCA morphology recorded was fragmented hardpan. The other major types were nodular, or a mixture of nodular and hardpan, along with rhizomorphic and powdery carbonates and minor carbonate coatings on detrital clasts (Figure 4c).

Regional-scale RCA assays

The regional-scale RCA assays are presented in appendix 2 and Figures 5 - 8. The Au assay results within the regional sample set were independent of the results for other elements, including pathfinder elements such as As, Sb, Mo, Bi, and W (Butt 1997) (Figure 5a, b). Elements such as Cr, As, Ga, Sc, V and possibly Au, have been reported to have an association with Fe-oxides in "lateritic" samples from previous studies (Butt 1997; Butt *et al*. 2000), however there were relatively poor correlations between these elements in the regional RCA sample assays (except for Cr and possibly V) (Figure 5c, d).

Strontium has a moderate correlation with Mg, whereas Ca poorly correlates with both of these elements (Figure 6a). No significant correlation was observed between Au and Ca or Mg on a regional scale (Figure 6b). For each of the landforms where RCAs occurred (erosional rises, erosional plains and depositional plains), Ca, Mg, Fe and Sr abundances were compared (Figure 7a, b). The following elements were plotted without any significant correlation: Ca/Mg vs. Fe (Figure 7a), as well Ca vs. Mg, Ca vs. Sr and Ca/Sr vs. Fe. A strong inversely proportional correlation was expressed in the

plot of (Ca/Mg)/Sr, and was consistent for all three landform settings examined (Figure 7b).

The regional geochemical maps produced in ArcView GIS© via Data Desk© were useful in displaying RCA elemental concentrations spatially (Figure 8 and Appendix 3). A similar technique has been used by Reimann *et al*. (1998).

RCA assays from Mineralisation transects

The transect-scale RCA assays are presented in Appendix 4 and Figure 9, and spot samples near mineralisation are in Appendix 5. Transects over mineralisation at the four prospects showed an increase in Au assay values from the RCAs closer to mineralisation. This trend was also expressed in other elements, including Zn, Pb, Fe, Cu, Bi, Co, Mo, V, W and Ni. The association between Au and certain pathfinder elements was also much stronger in the RCAs over mineralisation than in the regional samples (Figure 9a, b, c). Likewise, a similar trend was observed with the elements associated with Fe in the RCAs over mineralisation, where Ga and V were the dominant accumulative elements (Figure 9d, e, f). No significant correlation was observed between Au and Ca or Mg in the transect scale (Figure 9a, b, c), akin to the regional samples.

Prospect-scale RCA assays (Wilkins Prospect case study)

The prospect scale RCA assays are presented in appendix 6 and Figure 10. Another set of box and whisker plots were determined by using the local Wilkins prospect scale data, rather than the entire regional data set (e.g. Au in Figure 10). The Au values for the Wilkins box and whisker plots, for both the regional and Wilkins data, were fairly similar to the regional values in the non-anomalous cut off values (e.g. lower and upper box values), but the regional values were higher in the anomalous value cut off range. This was expected as the regional data includes the four transects over mineralisation, which had some very high Au assays. The ranges of results at both scales were similar, but the values for 'anomalous' elements increased when the sample locations were near the mineralisation.

Microanalysis

Based on thin section review, an average carbonate nodule (not including RCA coatings which contain a high lithic input) would include approximately 75% calcite and/or dolomite, 15% silica, 5% clay minerals and 5% detrital fragments including Fe $\pm$ Ti oxides, zircon, manganese nodules and lithic rock fragments. Samples GG01c (from Green & Gold), WK03c (from Wilkins) and LB08c (from Luxemburg) were targeted for microprobe analysis, as they yielded the highest bulk Au assays, but three other regional high Au samples (TBC025, TBC029 and TBC090) were also analysed. The Field Emission Gun Scanning Electron Microscope (FEGSEM) analysis showed that it

was not possible to identify visible Au at the resolution of analysis (3 μm), but identified various detrital phases, including the aforementioned in thin section review.

Given the well-documented association of Au with Fe-oxide material (e.g. Ferris *et al.* 2002), microprobe analysis was targeted at Fe-oxide detrital grains. Additionally, 15 lines of different size and varying point spacing (80 – 300 microns) for a total of 780 points were run across calcite grains to search for traces of Au within the carbonate material. Figure 11 shows typical areas where points and lines on the thin sections were microprobed. Gold was found at only 11 locations out of over 1000 probed points, and existed in various parts of the RCAs (Table 2). This included Au being finely and unevenly dispersed, both within the $CaCO_3$, as well as in various detrital phases including Fe oxides, Fe & Ti oxides (probably ilmenite), and Ti oxides (probably rutile).

DISCUSSION

RCA morphologies and mapping

RCAs most extensively occur in 'mid-slope' landscape settings, particularly along the upper margins of depositional plains and the lower parts of erosional plains and rises. This largely reflects an area where there is a suitable balance between: the destruction of RCAs due to dissolution (such as within valleys) and erosion (on rise crests) and, the accumulations of RCAs due to physical and chemical transport and precipitation.

The nodular RCAs tended to coexist with hardpan RCAs within plains, however, as relief increased there was a gradual dominance of hardpan RCAs (Figure 3). The reason for this may be due to erosion of hardpan RCAs in upslope settings and their downslope transport and deposition within plains. This may also partly explain the rounding of the carbonate-rich cores of many nodules, which then nucleate later carbonate overgrowths. Some hardpans have also reformed in low-lying depositional plains due to the nodular growth leading to coalescence and eventual hydromorphological 'plugging' of carbonate-rich zones within the regolith profile (Figure 4d).

The vertically extending profile upwards from Willyama Supergroup saprock to soil, sampled in the disused Radium Hill railway cutting, revealed that the RCA development was not laterally continuous. This observation suggests that local variations in the range of RCA formation factors such as Ca source (aeolian, bedrock etc.), carbonate source (vegetation respiration, meteoric water etc.), vegetation type, soil, groundwater etc. have a significant impact on RCA development. On such a small scale, other RCA formation factors such as landform and climate cannot affect the RCA distribution, as these affect more widespread areas.

The nodular RCAs generally overlie the fragmented hardpan or hardpan morphological facies (Figure 4e). The nodular RCAs may also have formed *in situ* by pedogenic accretion of calcium carbonate around grains of rock or other particles (ie. coated clasts). This seems feasible as nodular RCAs exhibited the concentric rings of calcium-carbonate accreted around rock fragments. These observations suggest a genetic model

that includes *in situ* accretion of the nodular RCAs followed by further accretion to eventually form hardpan RCAs. In contrast, the 'chronostratigraphic' RCA theory suggests that the RCAs are treated the same way as sedimentary layers, whereas in undeformed sequences the top of a profile is younger (e.g. Firman 1967). The evidence here does not support that theory, where instead the carbonate-rich zones have formed by overprinting. This interpretation is significant for understanding how trace metal assay results are monitored through dispersion pathways in the landscape, and it raises the potential for nodular morphologies to include geochemical signatures derived from broad areas of the scale of at least several hundred metres, compared to other morphologies that may form *in situ* and therefore have more localised dispersion pathways. This also increases the probability for nodular RCAs to host enlarged anomaly 'footprints' that translate to being larger area exploration targets (although in this case the 'anomaly' magnitude may not be as great).

Regional scale

The geochemical results from the regional data set provide a view of the background levels of Au and associated pathfinder elements in the region. The pathfinder element contents here are relatively low, but their poor association with Au is potentially overemphasised here because the Au assay concentrations were also low. Iron has some correlation with elements including V and Cr, which may mean its cumulative properties are relatively consistent at all scales. In addition, the regional geochemical maps showed that the values within a certain range in the box and whisker plots (e.g.

upper outliers) are independent of their spatial distribution, and it was possible for points a small distance away from each other to have completely different values.

The regional sampling program enables some assessment of associations between the RCA whole rock chemical assays with their morphology and landform settings. In general, the values of anomalously high element assays increased as the relief of the landscape decreased, and the fragmented hardpan RCAs generally showed higher trace metal assay values than the nodular morphological facies. There were, however, fewer nodular samples in the dataset, reducing the confidence of this suggestion. The regional samples also showed that sampling within drainage depressions, including very small ones, could have a major impact on the Au assay values. Site R028 showed assay values of 160 - 185 ppb in a small drainage depression, however further upslope and away from the drainage depressions the Au contents decreased to 59 ppb, and across slope to 29 ppb (Figure 4f). The anomalously high values in the drainage depression may relate to underlying mineralisation but this may also be due to lateral physical dispersion across the landscape.

The Au assay values in the regional samples were plotted according to the relative relief of the sample locations. The Au assays were generally lowest on the rises, increased as the relief decreased, and then declined again on the lowest relief landform (Figure 12). In contrast, a strong relationship between major element RCA geochemistry (e.g. Ca, Mg, Fe etc) and landform setting was not shown by this study. Figure 7 however, shows that there were high Mg assay values obtained on the erosional areas, and low Mg assay

values (<13000 ppm) from the depositional plains. This could be due to the mobility

properties of Mg, or simply a result of fewer depositional samples in the dataset.

The poor correlation of Au with both Ca and Mg in both the regional and transect

scales, suggests that the Au in this area is not reliant on the abundance of Ca or Mg to

exist as a component of the RCAs.

Mineralisation zone transect scale

When exploring for Au mineralisation using RCA samples, the best pathfinder indicator

element is Au, however, given the low absolute concentrations of Au in many samples,

the other pathfinder elements may also be useful. The close association between them

in certain cases may be significant, but it must be stressed that the correlations between

Au and all of its pathfinder elements in this study were not particularly strong, and they

should not be heavily relied upon as an indicator for mineralisation.

In the mineralised areas of the geochemical maps, certain elements such as Fe, Au and

Cu were shown as highly abundant outliers. With the linkage of the regional values and

the transect values from these maps, and their significant contrast, confidence can be

obtained in the determination of RCA Au anomaly definition in this area. In this study,

the box and whisker plots suggest that Au anomalies lay in the upper part of the range

of 4 - 12 ppb (i.e. >8 ppb) on the regional scale.

Prospect-scale

The box and whisker plots from the Wilkins prospect scale (figure 10) suggest that Au anomalies lay in the upper part of the range of 7 - 11 ppb (when using only the local data), i.e. >9 ppb. This is similar to the regional-scale anomaly definition, but is more tightly constrained. The Au assay values were particularly high near the mineralisation at Wilkins, but were also influenced by physical dispersion pathways up to a hundred metres away from the source. More steeply sloping landform settings directly influenced these pathways, where values obtained from up-slope settings reasonably close to the mineralisation were not very high, but further down-slope anomalously high values were recorded.

Microanalysis

It was expected that the anomalous Au in some of the RCAs would be found only in Fe-Ti oxides as detrital material, given the shallow sub-cropping to exposed bedrock in the prospect regions. Instead, the Au within the RCAs was also randomly dispersed throughout the calcite grains as well as within the Fe-Ti oxide grains. Importantly, the abundance of Au appears to be independent of Ca or Fe in the RCAs, although it has previously been linked with these elements in other studies (e.g. McQueen *et al*. 1999; Lintern 2002). The source of Ca in RCAs in the southern Curnamona Province has been investigated by Dart *et al.* (2004). Their work revealed a 96 to 100% atmospheric input of Ca, with a 4% input or less from bedrock. It is therefore proposed that the processes that are transporting Au from bedrock to sites in the RCAs are not the same

processes that are precipitating the RCAs. The RCAs are products of pedogenic systems, as they do not have a large, flat-lying, blocky structure typical of groundwater types. The existence of Au in the detrital Fe-Ti oxides is expected. However, the occurrence of Au situated randomly in the carbonate grains may be attributed to biological processes, allowing the Au to be highly soluble (e.g. Gray & Lintern 1997; Gray *et al*. 1997; Lintern & Butt 1998).

Regolith geochemical mapping

In order to evaluate the potential of RCA geochemistry as an indicator of the underlying basement geology, we compared the RCA 'whole rock' data with the interpreted solid geology maps and/or surface geology. Davy *et al*. (1999) have successfully used a similar technique in Western Australia to determine the extent or subdivision of bedrock units. The dominant lithologies in the study region include non-magnetic granitoids, variably magnetic mica-bearing granitoids, the Willyama Supergroup sequences and the various Adelaidean sediments as determined from mapping programs (Geological Survey of Primary Industries & Resources South Australia 2003). An important difference was noticed in the RCA geochemistry between the non-magnetic granitoids and the other variably magnetic biotite-muscovite granitoids, with the former plotting in distinct fields on a plot of Fe/Mg vs. K and Ca/Mg vs. Fe (Figure 13). This could possibly be attributed to the lack of magnetite, for example, in the non-magnetic granites, rather than an abundance of other Fe-bearing non-magnetic minerals. Additionally, some RCAs sampled over the known anomalous metallic occurrences of Bimba Formation showed:

- extreme upper outlier values for P;

- upper outlier values for Au, W, Mn, Cu, Pb; and,

- upper hinge values for As, Zn, Mo, U in the regional geochemical maps.

Also, some RCA assay values over mafic dykes showed upper outlier values for Ag, Cu, Pb, Zn, As, and upper hinge values for Au, Co. In contrast, some RCAs over Adelaidean sediments showed much lower anomalous concentrations of the same package of elements, compared to the Bimba Formation sites, with the values lying near the median (i.e. the upper box to lower box range in box and whisker plots).

CONCLUSIONS

The regolith geology and geochemistry of RCAs in this study contributes greatly to their application and interpretation for use in mineral exploration programs within the southern Curnamona Province. In particular it shows that an initial understanding of RCA morphology, distribution and landform setting is vital for the subsequent interpretations of exploration assay results across a region and within a prospect. Mineral explorers need to know where and what to sample and any anomalous element values need to be taken into the context of the landform setting. In addition, the sample spacing and quantity of data collected needs to be taken into account, as it may have a significant effect on anomalous value determination. As the tenement-scale sampling illustrated, it is also useful to include various other elements in the analysis package when analysing for Au in the RCAs, as the presence of certain minor elements, such as

some pathfinders, may also be useful indicators of mineralisation. The identifiable links between RCA major and trace element geochemical signatures in areas of shallow cover and the underlying bedrock lithologies may also provide insights for refining the interpreted geology maps in areas of shallow cover, and therefore aid further discoveries of mineralisation.

ACKNOWLEDGMENTS

REFERENCES

ALLEY N.F. 1998. Cainozoic stratigraphy, palaeoenvironments and geological evolution of the Lake Eyre Basin. *Palaeogeography, Palaeoclimatology, Palaeoecology* **144**, 239-263.

ANAND R.R., PHANG C., WILDMAN J.E. & LINTERN M.J. 1997. Genesis of some calcretes in the southern Yilgarn Craton, Western Australia: implications for mineral exploration. *Australian Journal of Earth Sciences* **44**, 87-103.

ASHLEY P.M., COOK N.D.J. & FANNING C.M. 1996. Geochemistry and age of metamorphosed felsic igneous rocks with A-type affinities in the Willyama Supergroup, Olary Block, South Australia, and implications for mineral exploration. *Lithos* **38**, 167-184.

BENTON R.Y. 1994. A petrological, geochemical and isotopic investigation of granitoids from the Olary Province of South Australia – implications for Proterozoic crustal growth. B.S.c. (Hons) thesis, University of Adelaide, Adelaide (unpubl.).

BIERLEIN F.P., ASHLEY P.M. & PLIMER I.R. 1995. Sulphide mineralisation in the Olary Block, South Australia: evidence for syn-tectonic to late-stage mobilisation. *Mineralium Deposita* **30**, 424-438.

BROWN A. & HILL S.M. 2003. White Dam – detailed regolith-landform mapping as a tool for refining the interpretation of surface geochemical results. *MESA Journal* **31**, 6-8.

BROWN A., LAU I.C., KERNICH A., SCHMIDT-MUMM A. & JAMES P.R. 2002. Preliminary results from geochemical dispersion investigations, Luxemburg workings, Curnamona Province, South Australia. *In:* PREISS V.P. ed. Geoscience 2002; expanding horizons; abstracts of the 16th Australian geological convention. Geological Society of Australia, Sydney.

BUSUTTIL S. & BARGMAN S. 2003. The geophysics of the White Dam deposit, near Olary, South Australia. *In*: DENTITH M. ed. *Geophysical signatures of South Australian mineral deposits*, pp. 127-134. Geology Department and Extension Service, University of Western Australia, Perth.

BUTT C.R.M. 1997. Geochemical dispersion and regolith evolution. Chemistry of gold in calcareous soils: field and laboratory studies and case histories. *In*: Calcrete geochemistry in gold exploration: AMF course notes 974/96. Australian Mineral Foundation, Adelaide.

BUTT C.R.M., LINTERN M.J. & ANAND R.R. 2000. Evolution of regoliths and landscapes in deeply weathered terrain – implications for geochemical exploration. *Ore Geology Reviews* **16**, 167-183.

CAMPANA B. & KING D. 1958. Regional geology and mineral resources of the Olary Province. *Geological Survey of South Australia* **34**.

CONOR C. & CROOKS A. 2003. Geology of the Olary Domain, Curnamona Province, S.A. Part 2 - Field guide and excursion stops.

COOKE A. 2003. White Dam – an exciting new gold project in the Curnamona Province. *MESA Journal* **31**, 4-5.

CORDON E.L. 1998. An investigation into the mineralisation of the White Dam prospect, Olary Block, South Australia. B.S.c. (Hons) thesis, University of Adelaide, Adelaide (unpubl.).

CROOKS A.F. 2002. Regolith mapping on the Mingary 1:100 000 map area, Curnamona Province. *MESA Journal* **25**, 42-45.

DART R.C., WITTWER P.D., BAROVICH K.M., CHITTLEBOROUGH D. & HILL S.M. 2004. Strontium isotopes as an indicator of the source of calcium for regolith carbonates. *CRC LEME regolith symposia 2004 abstracts* (in press).

DAVY R., PIRAJNO F., SANDERS A.J. & MORRIS P.A. 1999. Regolith geochemical mapping as an adjunct to geological mapping and exploration; examples from three contiguous Proterozoic basins in Western Australia. *Journal of Geochemical Exploration* **66**, 37-53.

DREW G.J. 1992. Goldfields of South Australia, report book **92/53**. Mines & Energy, South Australia.

FABRIS A. 2002. Northwestern Murray Basin; stratigraphy, sedimentology and geomorphology. *MESA Journal* **27**, 20-24.

FERRIS G.M., SCHWARZ M.P. & HEITHERSAY P. 2002. The geological framework distribution and controls of Fe-oxide Cu-Au mineralisation in the Gawler Craton, South Australia. *In*: PORTER T.M. ed. Hydrothermal iron oxide copper-gold and related deposits; a global perspective **2**, pp. 9-31. Australian Mineral Foundation, Adelaide.

FIRMAN J. B. 1967. Stratigraphy of late Cainozoic deposits in South Australia. *Transects of the Royal Society of South Australia* **91**, 167-178.

GEOLOGICAL SURVEY OF PRIMARY INDUSTRIES & RESOURCES SOUTH AUSTRALIA 2003. South Australia: mineral information pack. Department of Primary Industries and Resources South Australia (PIRSA), Adelaide.

GRAY D.J. & LINTERN M.J. 1997. Chemistry of gold in the weathering environment: simple carbonate soils. *In*: Calcrete geochemistry in gold exploration: AMF course notes 974/96. Australian Mineral Foundation, Adelaide.

GRAY D.J., LINTERN M.J. & BUTT C.R.M. 1997. Chemistry of gold in calcareous soils: Field and laboratory studies and case histories. *In*: Calcrete geochemistry in gold exploration: AMF course notes 974/96. Australian Mineral Foundation, Adelaide.

GREEN B. 1996. A study of the Wilkins and Green and Gold copper-gold prospects, Olary Block, South Australia with emphasis on petrology, geochemistry and ore mineralogy. B.S.c. (Hons) thesis, University of Adelaide, Adelaide (unpubl.).

HULME K.A. & HILL S.M. 2003. River red gums as a biogeochemical sampling medium in mineral exploration and environmental chemistry programs in the Curnamona Craton and adjacent regions of NSW and SA. *In:* ROACH I.C. ed. Advances in regolith; proceedings of the CRC LEME regional regolith symposia 2003. Cooperative Research Centre for Landscape Environments and Mineral Exploration. Bentley, W.A.

LAU I.C. 2004. Hyperspectral mineralogical investigation of regolith-dominated and basement terrains in the White Dam region, Olary Domain, South Australia. PhD thesis, University of Adelaide, Adelaide (unpubl.).

LINTERN M.J. 2001. Exploration for gold using calcrete - lessons from the Yilgarn Craton, Western Australia. *Geochemistry: Exploration, Environment, Analysis* **1**, 237-252.

LINTERN M.J. 2002. Calcrete sampling for mineral exploration. *In*: CHEN X.Y., LINTERN M.J. & ROACH I.C. eds. *Calcrete: characteristics, distribution and use in mineral exploration*, pp. 31-109. Instant Colour Press, Belconnen, ACT.

LINTERN M.J. & BUTT C.R.M. 1993. Pedogenic carbonate: an important sampling medium for gold exploration in semi-arid areas. *Exploration Research News* **7**, 7-11.

LINTERN M.J. & BUTT C.R.M. 1998. Gold exploration using pedogenic carbonate (calcrete). *Geological Society of Australia special publication* **20**, 200-208.

LINTERN M.J. & SHEARD M.J. 1999. Regolith geochemistry and stratigraphy of the Challenger gold deposit. *MESA Journal* **14**, 9-14.

McGEOUGH M. & ANDERSON J.A. 1998. Discovery of the White Dam Au-Cu mineralisation. *MIM exploration bulletin* **25**, 69-71.

McQUEEN K.M., HILL S.M. & FOSTER K.A. 1999. The nature and distribution of regolith carbonate accumulations in southeastern Australia and their potential as a sampling media in geochemical exploration. *Journal of Geochemical Exploration* **67**, 67-82.

REIMANN C., AYRAS M., CHEKUSHIN V., BOGATYREV I., BOYD R., CARITAT P.de., DUTTER R., FINNE T.E., HALLERAKER J.H., JAEGER O., KASHULINA G., LEHTO O., NISKAVAARA H., PAVLOV V., RAISANEN M.L., STRAND T. & VOLDEN T. 1998. Environmental geochemical atlas of the central Barents region. Grytting As, Norway.

SKIRROW R.G. & ASHLEY P.M. 2000. Proterozoic Cu-Au systems of the Curnamona Province - members of a global family? *MESA Journal* **19**, 48-50.

SKIRROW R.G., ASHLEY P.M., MCNAUGHTON N.J. & SUZUKI K. 2000. Time-space framework of Cu-Au(-Mo) and regional alteration systems in the Curnamona Province. *AGSO Record* **1998/25**, 104-108.

STEPHEN T. D., JAMES P. R. & HEINSON G. S. 2001. Insights into mineralisation of the Luxemburg Mine Area, Olary, South Australia, from geological mapping, strain and microstructural analysis, and geophysics. B.S.c. (Hons) paper, University of Adelaide, Adelaide (unpubl.).

WILLIAMS P.J. & SKIRROW R.G. 2000. Overview of iron oxide-copper-gold deposits in the Curnamona Province and Cloncurry District (eastern Mount Isa Block), Australia. *In:* PORTER T.M. ed. *Hydrothermal iron oxide copper-gold & related deposits: A Global perspective* **1**, 105-122. Australian Mineral Foundation, Adelaide.

FIGURE CAPTIONS

Figure 1

Map of the Curnamona Province, located in eastern South Australia and western New South Wales. The RCA sample locations are overlain onto the Olary 1:250 k geology map of the study area, highlighting the range of bedrock lithologies that do not extensively subcrop or outcrop in the area.

Figure 2

RCA distribution map highlighting the RCA occurrences. It shows the generally east-west trending alluvial drainage depressions, which incise through erosional landforms

and deposit sediment on low-lying plains. It also shows the various RCA morphologies found in the area including the dominant fragmented hardpan, nodular/nodular & hardpan, as well as minor carbonate coatings, rhizomorphic and powdery carbonates.

Figure 3

Catenary diagram showing the general observation of the morphological facies grading from fragmented hardpan style (FHP) on higher relief to nodular (Nod) RCAs on the plains. The downslope transition from pearl bluebush to black bluebush to bladder saltbush was also noticed over these landform changes.

Figure 4

Photo plate 1. (a) The subtle but important regolith and landform changes found in the area, and two vegetation types including black bluebush (BBB) and bladder saltbush (BSB). Photo from Wilkins catchment facing south at 0457357 E, 6437693 N. (b) The preferred sampling sites were intact rabbit warrens, shown for example near Wilkins at 0456591 E, 6437058 N. (c) Difficult sampling areas, where quartz or other lithic fragments were coated by $CaCO_3$, shown near White Dam at 0460104 E, 6450381 N. (d) Looking down a rabbit warren, where nodular RCAs were overlying fragmented hard pan, at 0456591 E, 6437058 N near Wilkins. (e) Cutting in a quarry at 0465657 E, 6433093 N on the old Radium Hill road, which revealed the cementation of hard pan RCAs around nodular morphologies. (f) A reconnaissance sample site, where the original sample recorded a Au assay of 160-185 ppb in a small channel near White Dam at 0460134 E, 6450379 N, and further samples were taken nearby, to evaluate the effect of a better range of landforms, morphologies and occurrences on the values. (All coordinates are in UTM Zone 54 S GDA-94)

Figure 5

Regional RCA geochemical results, highlighting the poor correlation between (i) Au and its pathfinder elements (a & b); and, (ii) Fe and the elements normally accumulated with it (c & d).

Figure 6

(a) Sr vs. Mg and Sr vs. Ca graphs in regional RCAs. (b) Au vs. Ca and Mg plots in regional RCAs.

Figure 7

The influence of three landforms on major element chemistry, including erosional rises, erosional plains, and depositional plains: (a) Ca/Mg vs. Fe plot; and (b) Ca/Sr vs. Mg plot.

Figure 8

Geochemical map of Au assay values over the study area, highlighting the contrast between regional Au values and the values over the mines.

Figure 9

Prospect scale RCA geochemistry on transects over the three known mineralisation sites: Luxemburg, Wilkins and Green and Gold. These show the direct linkage between Au and some of its pathfinder elements: (a) Au vs. W; (b) Au vs. Mo; and (c) Au vs. Bi; and Fe and its generally accumulated elements: (d), (e), (f) Fe vs. V, As, Ga. Plotted also are Au vs. Ca, Mg in (a), (b) and (c), highlighting their lack of correlation. It must be stressed that the lines between the values, on these graphs and others, are purely interpolative, and are not intended to reflect any trends. They are shown for viewing ease only.

Figure 10

Detailed regolith-landform map over the Wilkins Prospect, with overlain box plot Au values from Data desk, determined from only the Wilkins local data. This shows the influence of landform setting on physical dispersion geochemical pathways.

Figure 11

Field Emission Gun Scanning Electron Microscope (FEGSEM) back scattered electron images highlighting the major components of RCAs in thin section: (a) $CaCO_3$, $Fe/Fe\pm Ti$ oxides, and SiO_2; (b) $CaCO_3$, SiO_2, biotite and Fe oxides; and (c) Fe oxide and easily mistakeable remanent Sn from the thin section polishing process. Also shown are typical areas probed for composition information, in both selected point form (black circles on Fe oxides) and random lines of points (white circles).

Figure 12

Reconnaissance sample locations and the landform effect on their Au assays: (a) Three specific sites on a plot of Au vs. decreasing relief, highlighting Au value increase in erosional plain sites, rather than depositional; and b) Plot of all reconnaissance site Au assays vs. their relative relief setting.

Figure 13

Major element RCA chemistry investigation over underlying near-surface geology: (a) Fe/Mg vs. K; and (b) Ca/Mg vs. Fe, showing a distinct separation between circular non-magnetic S-type granites and S-type granites in both plots, with Adelaidean samples lying between them. (c) Plot of Ca/Mg vs. Fe, where the Adelaidean values appear separate from the Thackaringa Group, with the Thorndale composite gneiss appearing between them.

FIGURES

Study area

Olary 250 k map

Cover
- Alluvial fan sediments
- Pooraka Fm (clay, silt, carbonate, sand, with gravel lenses

Adelaidean sediments
- Wilypera Fm green siltstones

Willyama supergroup
- Bimba Fm calcsilicates
- Undifferentiated schist, gneiss, quartzite, migmatite
- Aplitic gneiss

Intrusives
- syn- to late tectonic granite to adamellite; pegmatoids

- Various sample style locations
- Station tracks
- Barrier highway
- White Dam deposit

Figure 1

Coordinates in GDA-94 datum, UTM UPS location format, zone 54 S

Kilometres

RCA distribution, morphology and associated landform map of the Tikalina-Bulloo Creek Station area
Compiled by P.D. Wittwer (2004)

Figure 2
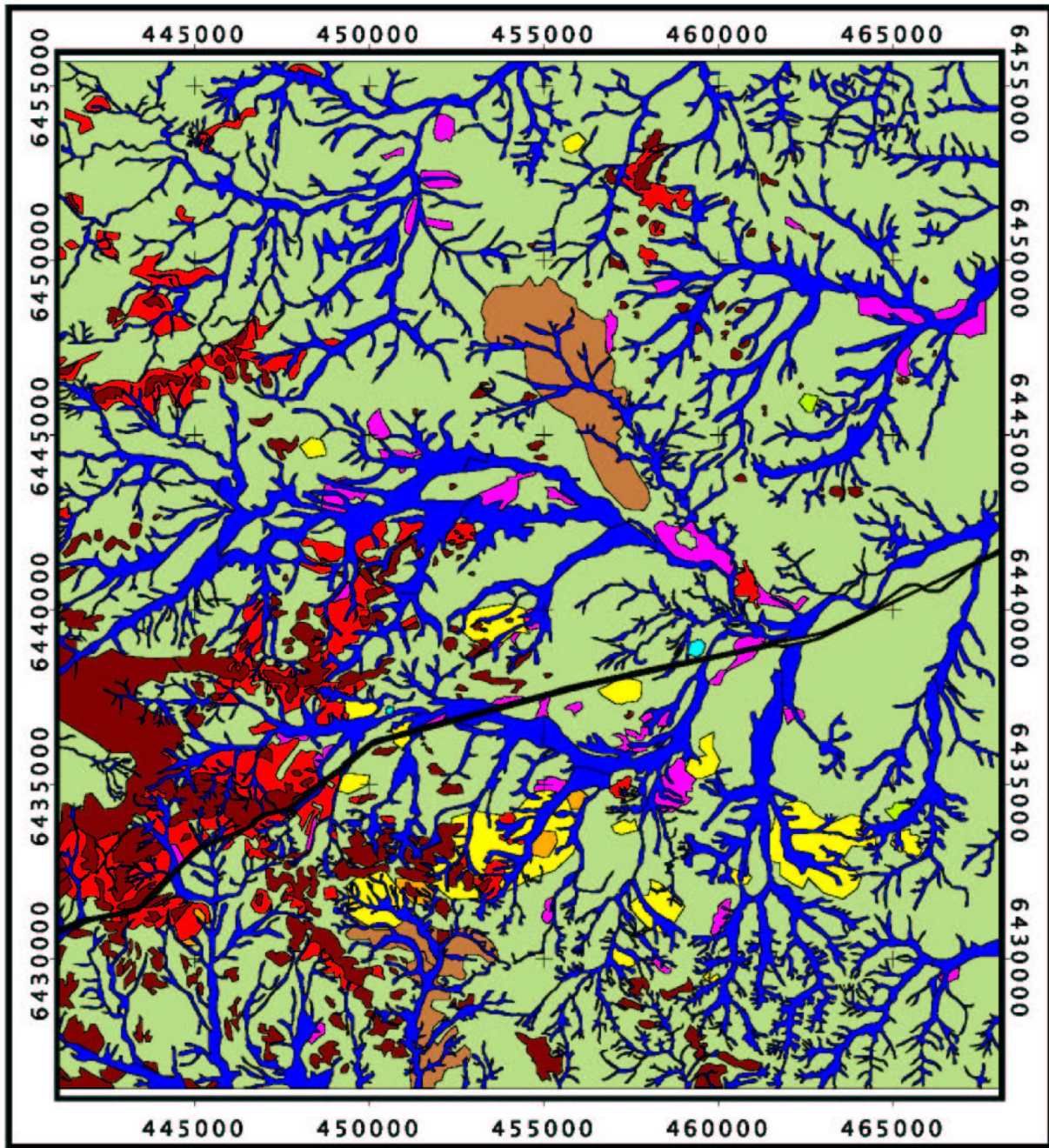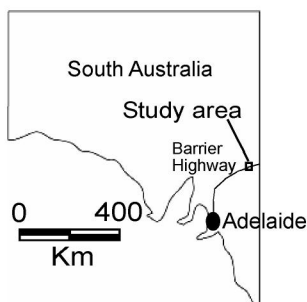
Coordinates in GDA-94 datum, UTM UPS location format, zone 54 S

- Fragmented hardpan - erosional rises/erosional plains
- Nodular/Nodular & hardpan - depositional plains/erosional plains
- Carbonate coating - rare occurrences
- Rhizomorphic - rare occurrences
- Powdery carbonate - rare occurrences
- Minor carbonate - clay regions near drainage depressions
- - alluvial drainage depressions
- Scarce carbonate - low lying plains
- - saprolite outcrop
- - subcrop basement

South Australia
Study area
Barrier Highway
Adelaide
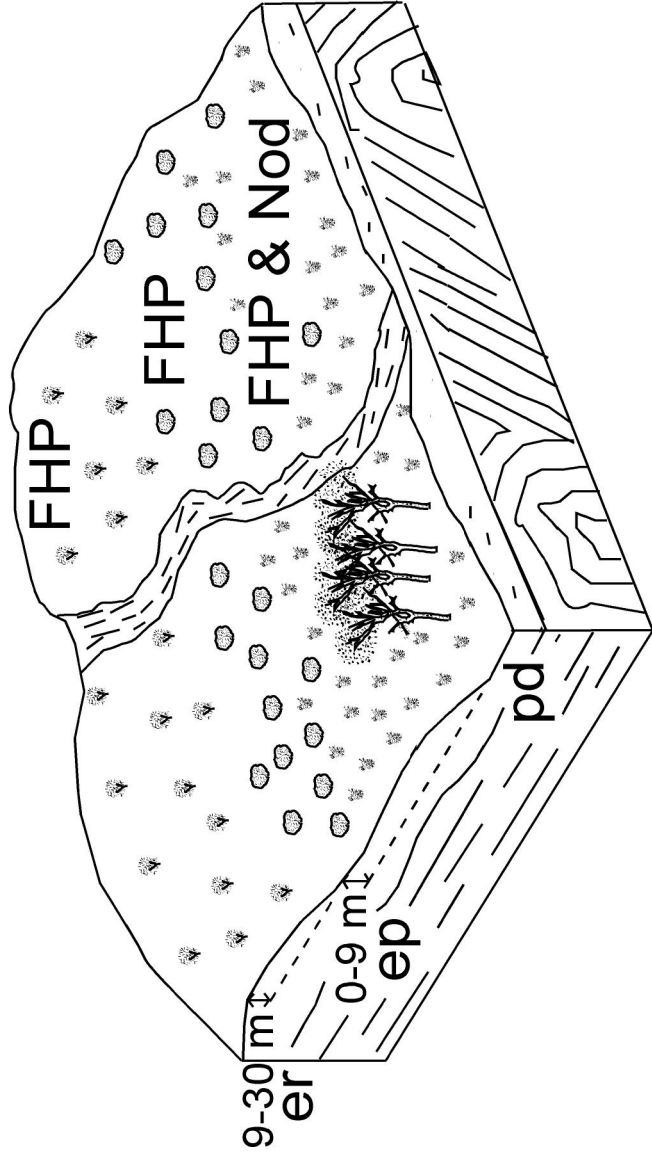
Figure 3

KEY

* pearl bluebush
* black bluebush
* bladder saltbush
* rosewoods

FHP

FHP

FHP & Nod

9-30 m

er

0-9 m

ep

pd
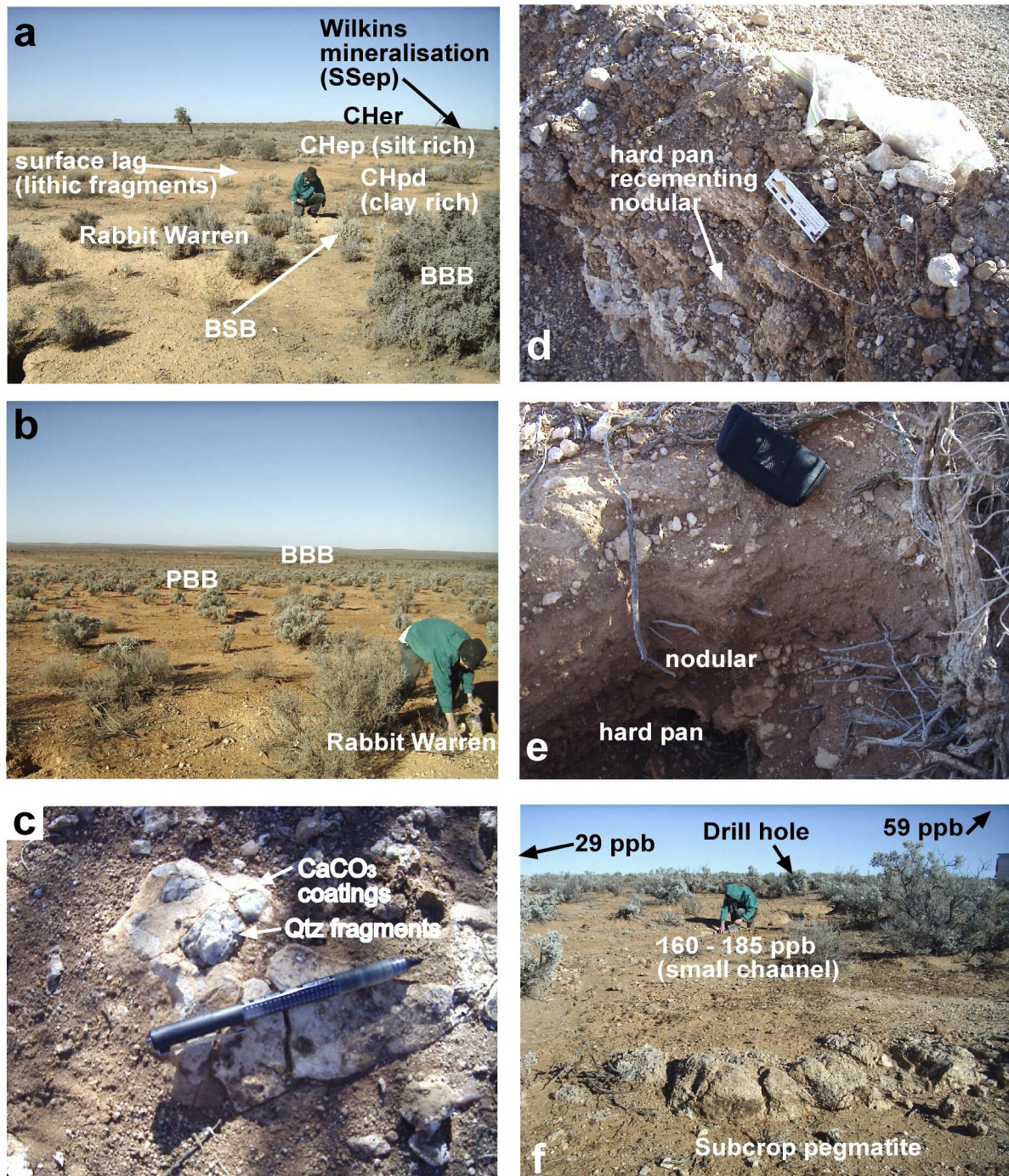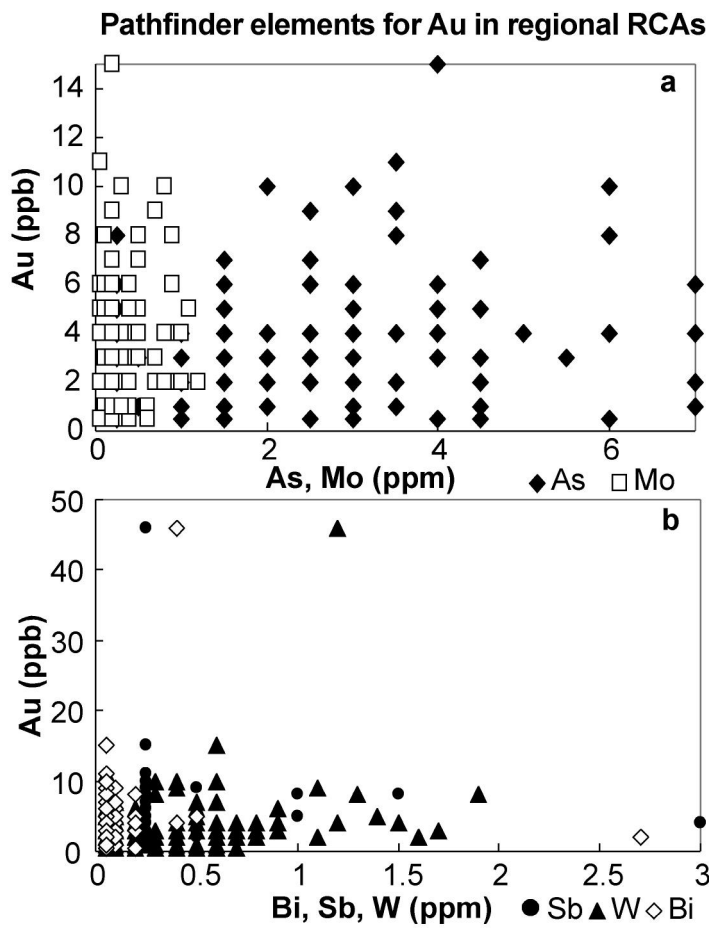
Figure 4

Figure 5

Regional RCAs
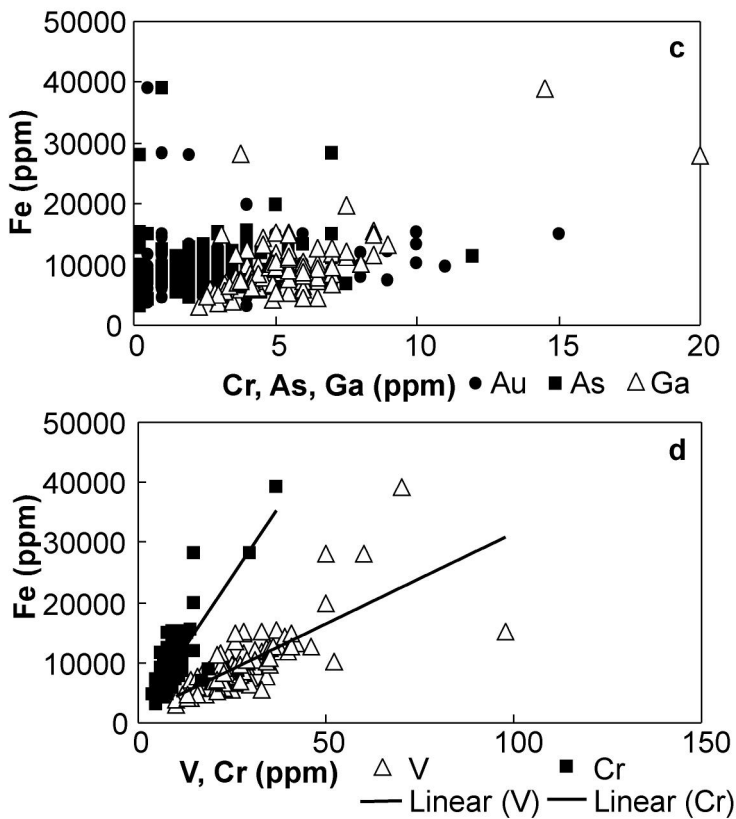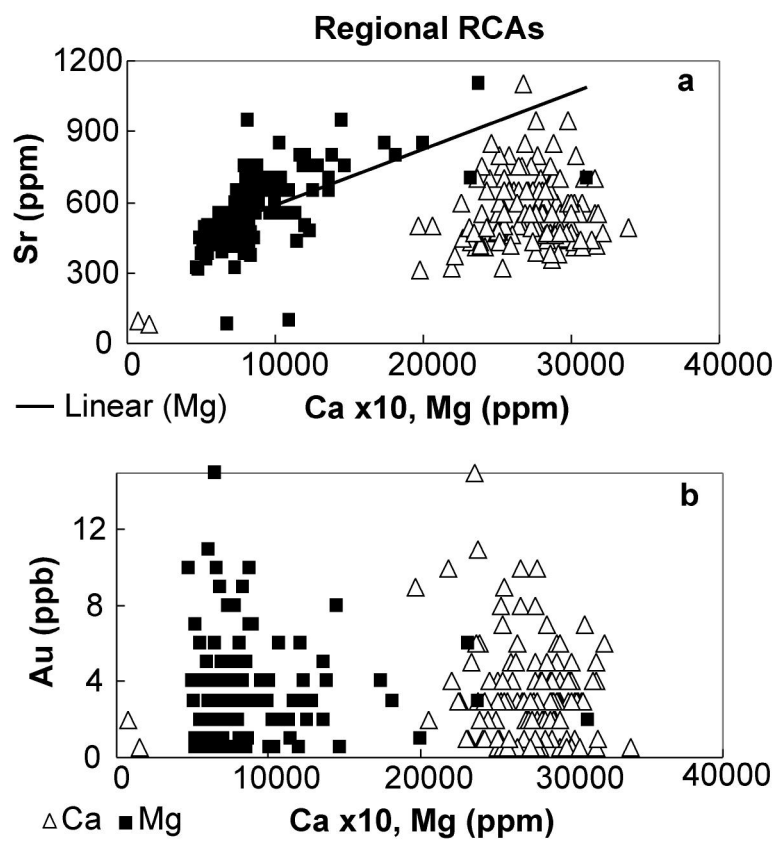
Figure 6

Figure 7

Figure 8

42
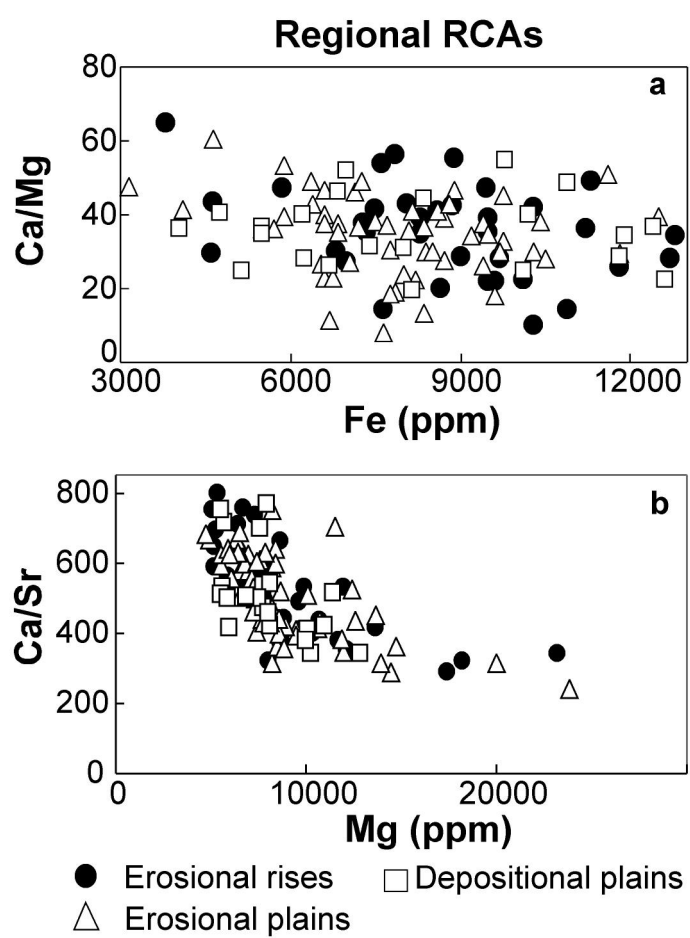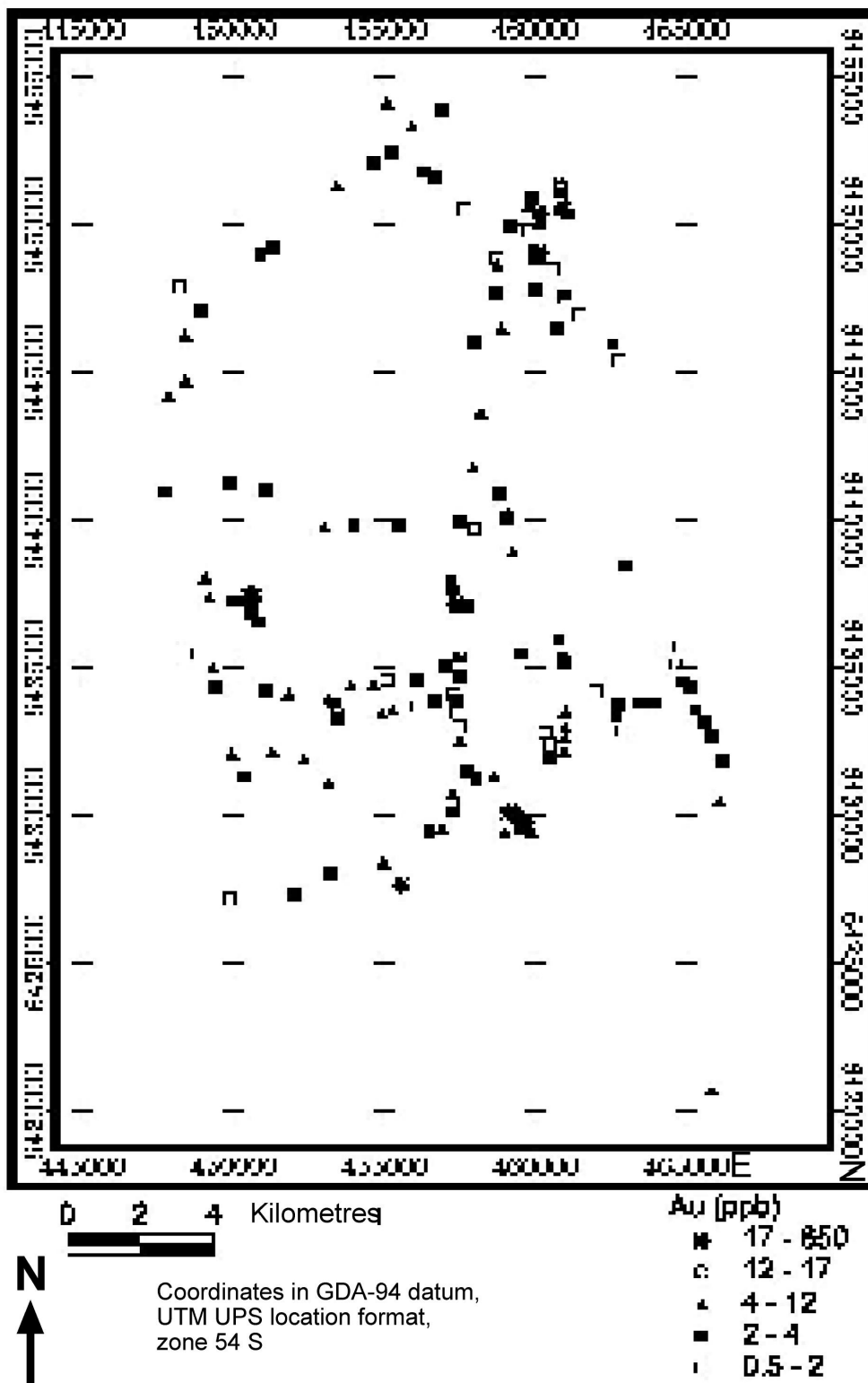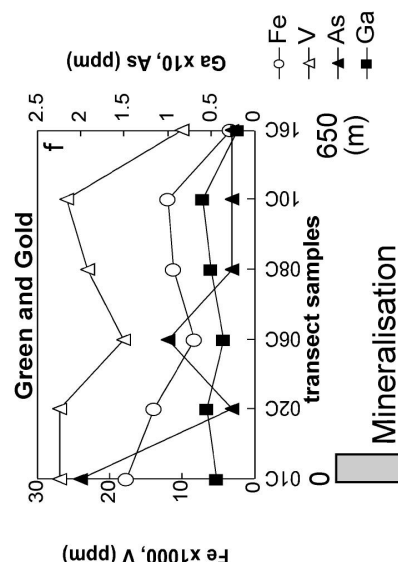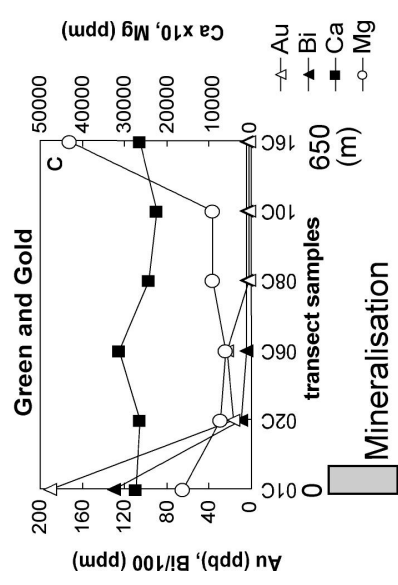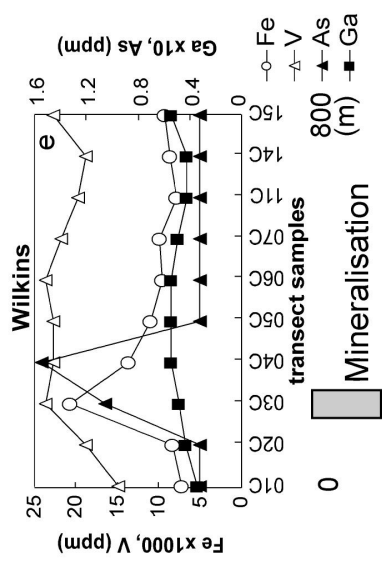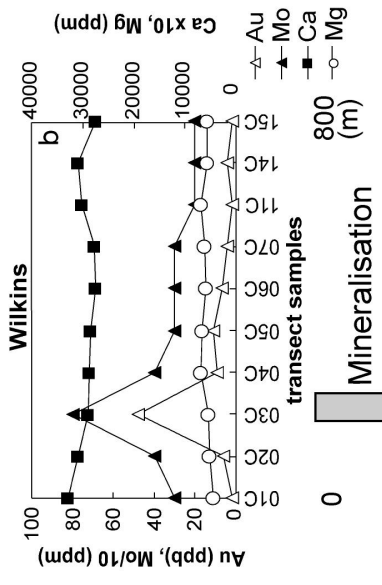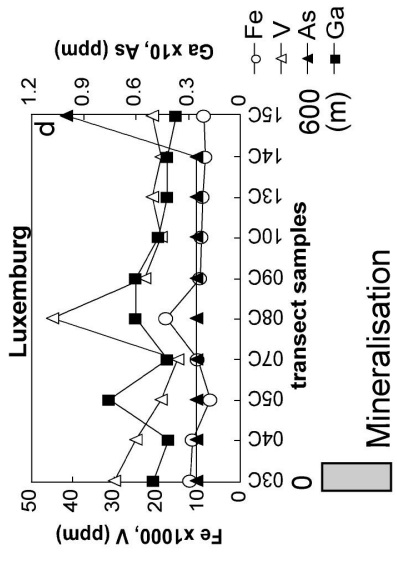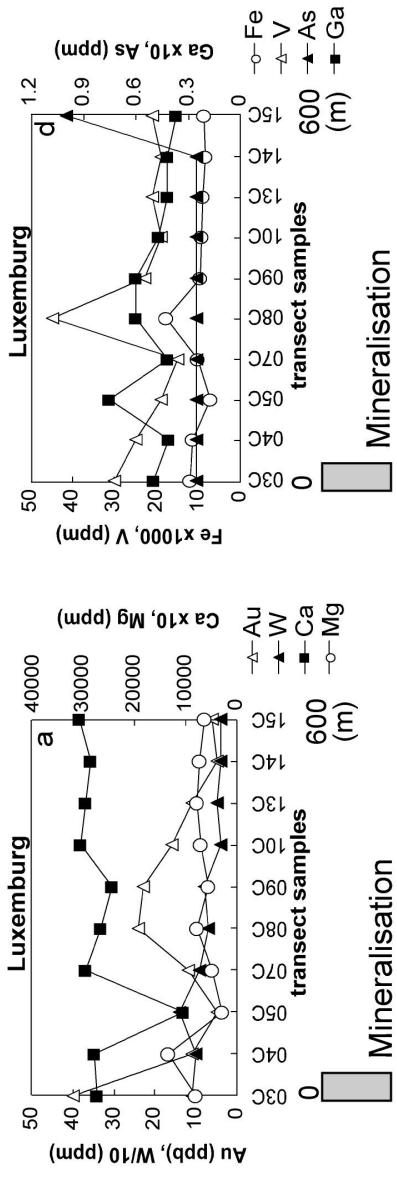
Figure 9

Regolith-landform and geochemical map of Wilkins

Compiled by P.D. Wittwer (2004)

Box & whisker plot

Extreme High Outliers	*******
Upper Outliers	
Upper Hinge	
Upper Box	
Lower Box	
Lower Hinge	
Lower Outliers	
Extreme Low Outliers	*******

Au (ppb)

- 🔴 17 - 47
- 🟠 11 - 17
- 🟡 7.5 - 11
- 🟢 4 - 7.5
- 🔵 0.5 - 4
- 🔵 N/A
- 🟣 N/A

Transported regolith

- Aed - Alluvial sediments in a drainage depression
- CHpd - Sheet flow material on a depositional plain
- CHep₁ - Sheet flow material on an erosional plain
- CHep₂ - Sheet flow material on an erosional plain
- CHer - Sheet flow material on an erosional rise
- Cer - Colluvial material on an erosional rise
- Fm - Anthropogenic impact

In-situ regolith

- SMer - Moderately weathered saprolite on an erosional rise
- SSep - Slightly weathered saprolite on an erosional plain

200   0   200

metres

N

Figure 10   Coordinates in GDA-94 datum, UTM UPS location format, zone 54 S; 1/2 detection limit for Au used for box & whisker plot

Figure 11

Specific reconnaissance sample locations

All reconnaissance sample locations
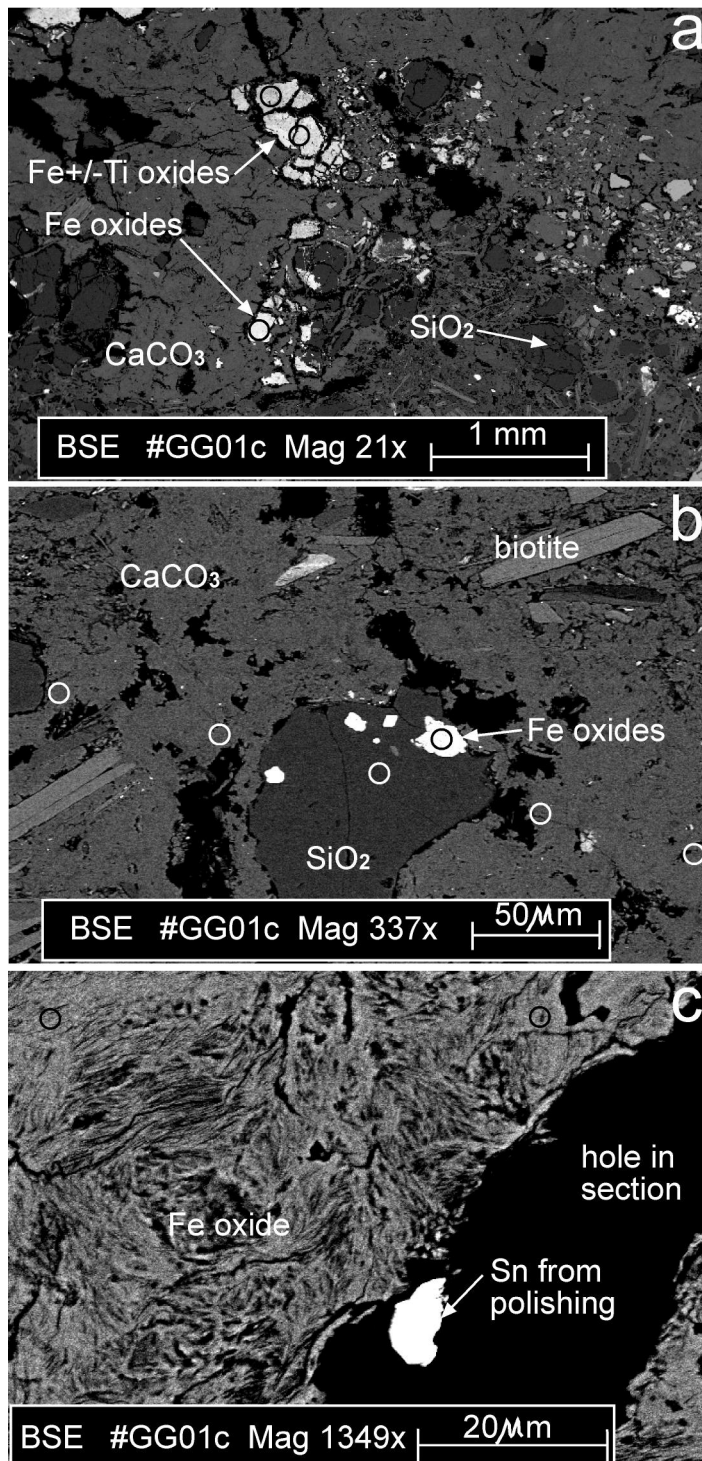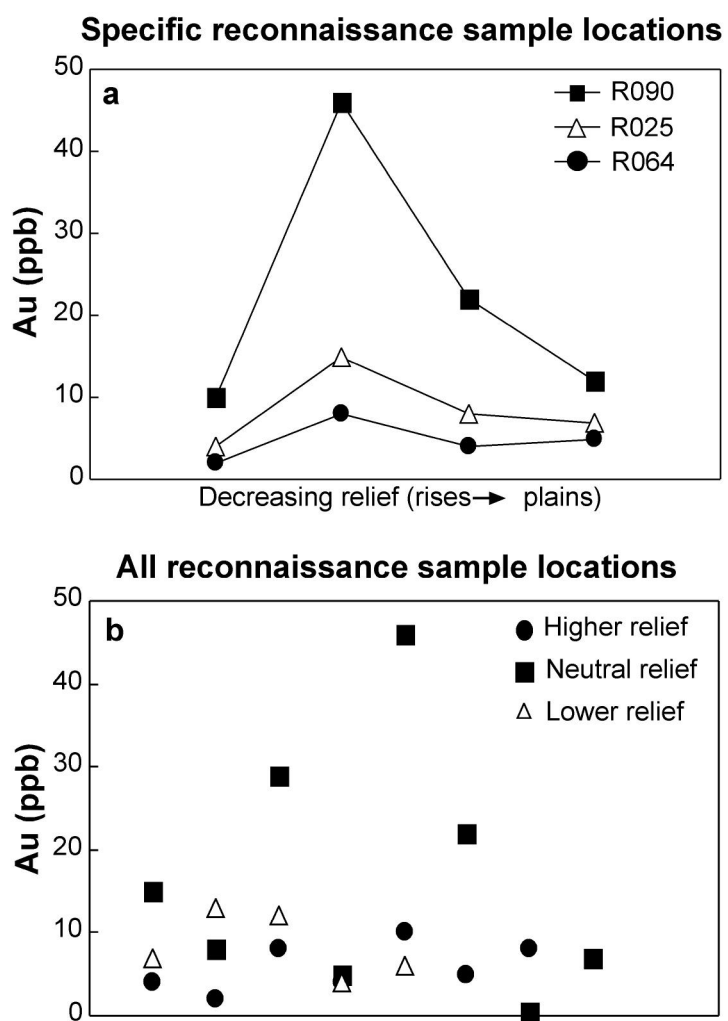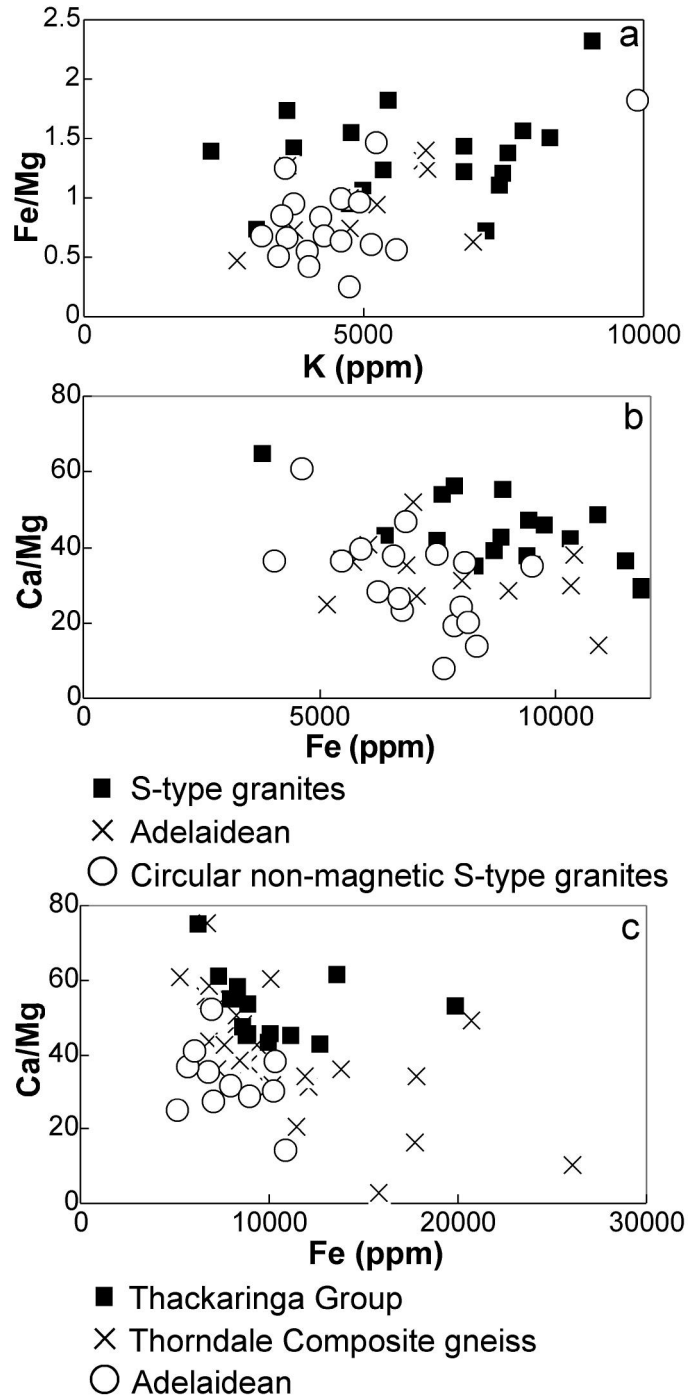
Figure 12

Figure 13

Table 1 – Local geology of the historical mines in the area.

Prospect & Features	Green & Gold	Luxemburg
Dominant Lithologies	Quartzo-feldspathic schists with disseminated sulfides, darker biotite-rich zones lighter quartz-plagioclase-muscovite-biotite zones (Green 1996)	Variable A-type Granite (Ashley et al. 1996) and metamorphic rocks, amphibolite (Campana & King 1958)
Deposit type	Epigenetic intrusive (Green 1996)	Shear zone (Stephen et al. 2001)
Host rocks	Massive haematite-quartz outcrops of banded iron formation (Campana & King 1958)	Parallel quartz-sulphide reefs (Campana & King 1958)
Alteration	Quartz-magnetite $\pm$ garnet $\pm$ chlorite $\pm$ amphibole, and probable Fe and Mn metasomatism (Green 1996)	Severe hydrothermal, shown by pure biotite/biotite schist halo around amphibolite and biotite close to mineralised quartz veins (Stephen et al. 2001)
Mineralisation introduced	Delamerian Orogeny (Green 1996)	D_1 and D_2 events of the Delamerian Orogeny (Stephen et al. 2001)
Occurrence and minerals	Veins - visible Au flakes, magnetite, chalcopyrite and malachite (Campana & King 1958)	Veins - Cu-Au mineralisation (Stephen et al. 2001)

Prospect & Features	White Dam	Wilkins
Dominant lithologies	Quartzofeldspathic gneiss of the Wiperaminga Subgroup (Williams & Skirrow 2000) and abundant syn- to post-deformational pegmatites (Cooke 2003)	Granites (correspond to the Bimbowrie Granite of Benton 1994), palaeoproterozoic migmatites, and psammitic psammopelitic gneisses (Green 1996)
Deposit type	Doesn't conform to the two models of sulphide mineralisation in the Olary Block of Bierlein et al. (1995): 1) strata-form; and 2) syn-tectonic to post-peak metamorphic replacement and veins; rather, within the oxidised region and transition to fresh rock zone (Cordon 1998)	Epigenetic intrusive (Green 1996). Anomalous metals concentrated in a sulphide halo surrounded by a barren oxide core (Conor & Crooks 2003)
Host rocks	Fe-oxide poor, biotite-quartzofeldspathic gneiss, of upper amphibolite facies metamorphism (Williams & Skirrow 2000)	Banded iron formation (Green 1996)
Alteration	Cloncurry-style alteration (McGeough & Anderson 1998) 1) early albitisation; 2) potassic alteration (biotite $\pm$ magnetite $\pm$ Au-Cu mineralisation); and 3) retrograde alteration (Cordon 1998)	Quartz-magnetite epigenetic $\pm$ sulphides $\pm$ Au $\pm$ chlorite $\pm$ amphibole (hornblende) $\pm$ garnet (Green 1996)
Mineralisation introduced	Tectonothermal events of the Olarian Orogeny (~1600 $\pm$ 20 Ma) (Skirrow et al. 2000)	Delamerian Orogeny (Green 1996)
Occurrence and minerals	Biotite-rich selvages to leucocratic bands and veins within the gneiss. Chalcopyrite-pyrite-molybdenite-Au mineralisation associated with alteration (Cordon 1998)	Associated with veins and quartz-magnetite epigenetic alteration. Narrow intersections of high grade Cu-Au within wide zones of low grade Cu-Au (Green 1996)

TABLES

Table 2 - Microprobe elements analysed and their precise W% values, corresponding detection limits, and beam current for the points that contained measurable Au. Note quantitative element values highlighted in bold, which represent the major elements in the points probed that contained Au.

Label	LB08c	TBC029	TBC090	TBC090	GG01c	GG01c	GG01c	GG01c	LB08c	LB08c	LB08c	TBC090
Location	Detrital	Detrital	Detrital	Detrital	Line 1	Line 1	Line 1	Line 3	Line 2	Line 4	Line1
Main elements	Si,Ti,Fe	Fe	Ti	Fe	Ca	Ca	Si	Ca	Ca	Ca	Ca
IDfix analysis	Ti	0	Ti,Mo,Ba	Ti	0	0	0	0	0	0	Si,Ti
W%(O)	30.3677	8.9726	0.4355	10.7199	17.6521	16.4044	16.5941	17.3091	17.1463	18.4315	53.4886
(O) Det. Limit (ppm)	0	0	0	0	0	0	0	0	0	0	0
W%(Na)	0.095	0.0517	0.0127	0.0414	0.0312	0.0598	0.0131	0.045	0.0188	0.026	0.0123
(Na) Det. Limit (ppm)	930.65	1675.93	59.98	1768.1	1031.27	2361.04	1708.94	1014.65	1055.17	1065.44	1502.44
W%(Mg)	1.6997	0.1235	0.0067	0.0003	3.8688	2.7912	0.0122	3.2509	0.9409	1.1312	0.0189
(Mg) Det. Limit (ppm)	63.403	94.758	40.255	1039.31	93.7	1886.23	1007.27	85.757	83.838	90.291	90.883
W%(Al)	**7.918**	0.5189	0.0521	0.0002	0.2768	0.0979	0.0242	0.0802	0.2043	0.1109	0.0272
(Al) Det. Limit (ppm)	613.1	768.53	284.06	790.48	441.65	926.64	605.78	458.12	379.1	433.41	740.66
W%(Si)	**17.7002**	1.119	0.156	0.0182	1.3393	0.5668	**14.4706**	0.6628	0.6725	0.3946	**46.8952**
(Si) Det. Limit (ppm)	541.29	480.82	286.52	537.21	375.45	790.15	917.26	370.07	343.81	367.07	1321.04
W%(S)	0.0529	0.0225	0.1026	0.0013	0.0264	0.0542	0.0002	0.0628	0.0444	0.0295	0.0132
(S) Det. Limit (ppm)	407.43	462.94	299.13	475.94	407.76	914.85	964.15	318.89	360.98	389.67	925.03
W%(Ca)	1.1558	0.8623	0.0958	0.0311	**32.8232**	**34.2239**	0.1274	**35.4921**	**38.6519**	**42.6819**	0.0001
(Ca) Det. Limit (ppm)	208.03	233.89	138.34	223.91	298.2	690.2	323.72	327.17	302.76	341.08	441.19
W%(Mn)	0.0476	0.0287	0.0082	3.5774	0.0001	0.0589	0.0001	0.0202	0.0001	0.0311	0.0001
(Mn) Det. Limit (ppm)	515.21	568.63	353.43	604.41	585.44	1398.56	1272.29	510.34	572.52	581.46	1136.32
W%(Fe)	**5.0116**	**23.5285**	0.0107	**31.6916**	0.556	0.1293	0.0033	0.1623	0.2693	0.1081	0.0026
(Fe) Det. Limit (ppm)	431.14	563.43	265.45	698.27	380.7	990.78	612.59	417.66	392.8	463.45	822.81
W%(Cu)	0.0429	0.0161	0.0026	0.0051	0.0877	0.0341	0.0697	0.0295	0.0001	0.0137	0.0001
(Cu) Det. Limit (ppm)	716.65	808.36	477.15	850.2	688.58	1646.57	933.33	708.11	773.78	749.71	1631.48
W%(Zn)	0.0314	0.0275	0.0469	0.0014	0.029	0.0001	0.0001	0.0001	0.0103	0.0188	0.1259
(Zn) Det. Limit (ppm)	809.81	1024.71	483.66	902.25	850.03	1839.83	1627.19	842.12	850.79	836.94	1395.28
W%(As)	0.0002	0.0003	0.011	0.0761	0.0002	0.0002	0.0002	0.0002	0.0002	0.0002	0.0002
(As) Det. Limit (ppm)	1723.63	1958.11	769.7	1846.78	2337.87	5177.45	2060.28	2087.15	1551.84	1854.62	1867.69
W%(Au)	0.0604	0.0508	0.0215	0.0861	0.1202	0.0831	0.0961	0.0267	0.0278	0.0256	0.076
(Au) Det. Limit (ppm)	292.72	388.97	173.19	237.99	159.06	711.05	886.72	255.57	243.89	259.98	694.68
W%(Pb)	0.0002	0.0253	0.0001	0.034	0.0001	0.0001	0.055	0.0418	0.0001	0.0001	0.0002
(Pb) Det. Limit (ppm)	1194.75	1305.78	800.83	1112.49	1031.75	2890.92	2586.66	891.32	990.32	1042.37	3029.76
Beam current (nA)	20.52	18.86	19.89	19.78	19.79	3.85	3.86	19.64	20.5	19.18	4.95

IDfix identification fix (qualitative element analysis program to identify elements not in microprobe analysis package); W%, weight percentage; nA, nano amperes; LB, Luxemburg transect samples; GG, Green and Gold transect samples; TBC, Tikalina-Bulloo Creek area (regional RCA sample set).

APPENDICES

APPENDICES
Appendix 1 - regolith-landform map units of the Wilkins Prospect

<u>Mapping unit description technique</u>
1) Regolith lithology   4) Dominant vegetation
2) Landform setting   5) Geohazards (if any)
3) Minor features

Transported regolith

ALLUVIAL SEDIMENTS

Aed –
> Clay rich sediments, sub rounded, moderately sorted, red-orange, in a low lying, broad drainage depression, with little sharp incision. Common lithic and quartzose fragments, with minor silts, sands and gravels. Minor RCA occurrences in either rabbit warrens or sheet wash. Chenopod shrubland dominanted by *Atriplex spp.* (bladder saltbush and pop salt bush). Geohazards: snakes, sunburn.

COLLUVIAL SEDIMENTS   *Sheet flow deposit*

CHpd –
> Clay rich red-orange sediments on a low lying depositional plain. Some moderately consolidated red-light brown, sub rounded silt. Minor RCA occurrences in sheet wash deposits, but sparse rabbit warrens bringing up fragmented hardpan and nodular RCAs. Chenopod shrubland dominated by *Atriplex spp.* (bladder saltbush and pop salt bush) and various grasses. Geohazards: snakes, sunburn.

$CHep_1$ –
> Silt sized, poorly sorted, unconsolidated red-brown sediments on slightly higher areas of relief (0 – 9 m) to adjacent depositional plains. Fragments of RCAs common from rabbit warrens, and occasional rounded fragmented hardpan RCAs. A few areas contain bare vegetation exposing red-brown clay/silt patches up to 30 m wide. Generally thick chenopod shrubland dominated by *Atriplex spp.* (bladder saltbush and pop salt bush), with minor *Maireana spp.* (black bluebush, but no pearl blue bush), and scattered trees of *Alectrylon* oleofolius (rosewood). Geohazards: snakes, rabbit warrens caving in, sunburn.

$CHep_2$ –
> Dominant silt sized sediments, with minor aeolian clay particles, deposited on areas slightly higher in relief than $CHep_1$, but still in the erosional plain relief range. Fragmented hardpan RCAs commonly found in rabbit warrens. Chenopod shrubland dominated by *Maireana spp.* (pearl bluebush and black bluebush), copper burr and various grasses. Geohazards: snakes, rabbit warrens caving in, sunburn.

CHer –

Red brown silts and fine to medium sand sized particles on erosional rises adjacent to CHep$_2$ units. Frequent fragmented hardpan RCAs found in rabbit warrens, minor RCA sheet flow occurrences from nearby rabbit warrens, and occasional laminar hardpan RCAs. Chenopod shrubland dominated by *Maireana spp.* (pearl bluebush and black bluebush), with minor copper burr and few grasses. Geohazards: snakes, rabbit warrens caving in, sunburn.

Colluvial sediments

Cer –

Rocky areas adjacent subcrop, with angular, poorly sorted lithic fragments of Willyama Supergroup saprock on erosional rises. No RCAs on this setting. Sparse chenopod shrubland, with only few occurrences of *Maireana spp.* (pearl bluebush and black bluebush). Geohazards: snakes, rocky terrain, sunburn.

FILL   *Fill*

Fm –

Wide area shaped for the Barrier Highway with road base added and adjacent railway cutting and built up area for the railway tracks. Common surficial lag and vegetation relatively unaffected immediately adjacent to the road and railway, and is a chenopod shrubland of *Maireana spp.* (black bluebush and pearl bluebush), with few *Casuarina* pauper (belah) next to the highway. Geohazards: snakes, sunburn, moving vehicles and trains.

In-situ regolith

SAPROLITH   *Saprock*

SMer –

Exposed outcrop of moderately surficially weathered Willyama Supergroup bedrock, containing undifferentiated schist, gneiss, migmatite, quartzite, and hornblende gneiss, on a moderate topographic relief of 30 – 90 m. Medium to coarse grained granitoids are also present, with a quartz-K-feldspar-plagioclase-biotite-muscovite-magnetite mineralogy. Common angular to subangular lithic and quartz fragments. No RCAs on this setting. Bare chenopod shrubland of *Maireana spp.* (pearl bluebush and black bluebush) around the outcrop. Geohazards: snakes, rocky terrain, sunburn.

SSep –

Exposed outcrop of the ferruginous banded formation known as the Wilkins mineralisation, occurring on an erosional plain of relief 0 – 9 m. Pits expose quartz magnetite alteration and secondary copper (crysocolla) staining. Some RCAs from rabbit warrens and sheet wash nearby the ironstone. Chenopod shrubland of *Maireana spp.* (pearl bluebush and black bluebush) around the ironstone, with some grasses. Geohazards: snakes, rocky terrain, sunburn.

Appendix 2 - Regional scale RCA assays

Element	Units	Analysis	TBC001	TBC002	TBC003	TBC004	TBC005	TBC006	TBC007	TBC008	TBC009	TBC010	TBC011	TBC012	TBC013	TBC014	TBC015	TBC016	TBC017	TBC018	TBC019	TBC020	TBC021	TBC022	TBC023
Sample #			TBC001	TBC002	TBC003	TBC004	TBC005	TBC006	TBC007	TBC008	TBC009	TBC010	TBC011	TBC012	TBC013	TBC014	TBC015	TBC016	TBC017	TBC018	TBC019	TBC020	TBC021	TBC022	TBC023
GDA-94 Eastings			460992	460964	460977	460931	459361	460738	459080	458768	457922	458169	458854	458688	458711	458712	458717	458710	459969	460557	460645	461472	462534	462738	461066
Northings			6433485	6432933	6432568	6432161	6430211	6435912	6440258	6440867	6441757	6443604	6446477	6447683	6447764	6448690	6448830	6448558	6447763	6447490	6446455	6446918	6445942	6445371	6450358
Au	ppb	AA9	8	5	8	4	9	2	6	3	4	4	4	3	10	4	1	4	3	<1	3	<1	2	<1	3
Au Dpt	ppb	AA9	–	–	–	–	–	–	–	–	–	–	–	–	13	–	1	–	–	–	–	–	–	–	–
Ba	ppm	IC3E	750	650	600	145	370	300	1050	1050	950	490	300	260	340	290	270	460	400	550	195	1150	280	300	460
Ca	ppm	IC3E	267000	290000	276000	299000	256000	250000	290000	293000	316000	293000	261000	302000	219000	280000	242000	286000	286000	300000	302000	317000	288000	293000	286000
Cr	ppm	IC3E	15	9	8	5	5	7	9	8	5	9	14	6	10	8	10	10	7	8	12	6	9	19	7
Fe	ppm	IC3E	11900	7500	7850	4650	7300	8350	15100	6600	3150	5900	15400	6600	13300	8700	11800	9400	6850	8300	8600	5850	8150	8900	7850
K	ppm	IC3E	5300	4600	4000	3750	6850	5000	2650	3600	1650	2400	6400	4900	3000	6800	6800	5350	3200	4050	3350	4450	5300	3900	4800
Mg	ppm	IC3E	7800	7600	14500	4950	6800	5650	5500	6250	6650	5500	7400	7550	4750	7200	8250	7650	7600	7650	7350	6700	7000	6300	5100
Mn	ppm	IC3E	88	52	52	64	56	72	62	72	42	64	72	170	78	125	130	320	70	70	84	1000	78	270	66
Na	ppm	IC3E	3750	3150	1500	1500	3700	7150	1150	2300	1950	1600	10100	3250	14400	3750	2550	5100	3650	5550	5600	3300	1950	6850	10800
P	ppm	IC3E	650	440	240	240	270	390	250	270	240	320	320	150	190	230	420	240	270	750	320	330	420	130	260
Ti	ppm	IC3E	1000	800	800	450	600	750	600	700	350	650	1350	700	1200	950	1150	900	700	750	1000	600	850	900	700
V	ppm	IC3E	34	30	34	12	14	24	98	22	10	19	37	20	42	25	38	31	23	17	25	22	22	20	18
S	ppm	IC3E	1400	1300	1200	850	550	750	1250	1300	1300	1050	700	800	450	700	750	800	850	1050	800	1150	1050	650	800
Ag	ppm	IC3M	0.4	<0.1	<0.1	<0.1	0.2	<0.1	<0.1	<0.1	<0.1	<0.1	<0.1	<0.1	<0.1	<0.1	<0.1	<0.1	<0.1	<0.1	<0.1	<0.1	<0.1	1.6	<0.1
As	ppm	IC3M	3.5	4.5	6	2	2.5	3	7	1.5	2.5	2.5	4	2.5	6	2	4.5	3	2	4	3.5	1.5	4	0.5	<0.1
Bi	ppm	IC3M	0.2	0.1	<0.1	<0.1	0.1	<0.1	<0.1	<0.1	<0.1	<0.1	<0.1	<0.1	<0.1	<0.1	<0.1	0.1	<0.1	0.1	0.1	<0.1	0.2	<0.1	<0.1
Cd	ppm	IC3M	0.1	0.1	0.6	0.5	0.8	0.8	0.5	0.8	<0.1	0.1	0.1	0.8	0.1	<0.1	0.1	0.1	<0.1	0.5	0.1	0.6	0.2	<0.1	0.6
Ce	ppm	IC3M	0.8	0.9	0.6	0.5	0.8	0.8	0.5	0.8	0.5	0.5	1.1	0.8	0.7	0.8	1.5	0.8	0.7	0.5	0.9	0.6	0.7	1.8	0.6
Cs	ppm	IC3M	25	28	23.5	18.5	58	42.5	19.5	20.5	10	13.5	50	24	50	30.5	32.5	31	22.5	32	36	43.5	33	23	30.5
Co	ppm	IC3M	6	5.5	6	6.5	5.5	6	4.1	5	9	4.7	10.5	6	5.5	10.5	6.5	17	6.5	15.5	7	7	5.5	4.8	30.5
Cu	ppm	IC3M	23	20	19.5	17	40	21.5	18	15	13	13	24	22.5	50	24	45.5	56	17	4.6	18.5	12	29	13.5	10.5
Ga	ppm	IC3M	5	4.4	4.4	3.1	6.5	6	3.1	4	2.3	2.7	8.5	4.7	9	6	7	6	4.3	4.6	6	4.2	4.7	5.5	6.5
In	ppm	IC3M	<0.05	<0.05	<0.05	<0.05	<0.05	<0.05	<0.05	<0.05	<0.05	<0.05	<0.05	<0.05	<0.05	<0.05	<0.05	<0.05	<0.05	<0.05	<0.05	<0.05	<0.05	<0.05	<0.05
La	ppm	IC3M	15	19.5	15.5	12	34.5	25	18.5	17	15	14.5	28.5	17.5	25	17.5	20	19	14	17.5	19.5	27.5	19.5	13.5	17.5
Mo	ppm	IC3M	0.9	0.5	0.5	0.4	0.7	0.9	0.9	0.5	0.5	0.5	0.4	0.4	0.8	0.3	0.6	0.9	0.3	0.2	0.2	0.2	0.9	0.3	0.2
Ni	ppm	IC3M	12	12	11	9	11	11	9	11	7	9	15	11	9	11	13	14	12	9	12	10	11	11	9
Pb	ppm	IC3M	7	5	5.5	5	11	4.5	6	5	3.5	4	8	3	4	5.5	9.5	5.5	4.5	3	3.5	18.5	4	5	4
Rb	ppm	IC3M	27.5	33	32.5	22.5	39.5	26	18.5	22	7.5	10	36	35	20	49.5	52	38.5	13.5	21	18	25	29	22	25
Sb	ppm	IC3M	1.5	1	1	3	0.5	0.5	0.5	0.5	0.5	0.5	0.5	0.5	0.5	0.5	0.5	0.5	0.5	0.5	0.5	0.5	0.5	0.5	0.5
Se	ppm	IC3M	0.5	1	0.5	<0.5	0.5	0.5	0.5	0.5	1	0.5	0.5	0.5	0.5	0.5	0.5	0.5	0.5	1	0.5	0.5	0.5	0.5	0.5
Sr	ppm	IC3M	500	600	950	450	470	470	490	550	550	470	650	600	320	550	410	650	470	500	410	420	460	440	380
Te	ppm	IC3M	0.3	0.3	0.3	0.2	0.2	<0.2	<0.2	<0.2	<0.2	<0.2	<0.2	<0.2	<0.2	<0.2	<0.2	<0.2	<0.2	<0.2	<0.2	<0.2	<0.2	<0.2	<0.2
Th	ppm	IC3M	2.5	3.1	2.9	3.1	9.5	3.6	3.6	2.3	1.1	1.65	6.5	3.4	5	4.6	4.4	4.6	3.2	3.7	3.9	2.9	4.1	2.6	<0.2
Tl	ppm	IC3M	0.1	0.1	<0.1	<0.1	0.2	0.1	<0.1	0.1	<0.1	<0.1	0.2	0.1	<0.1	0.3	0.4	0.2	<0.1	<0.1	0.1	<0.2	0.1	0.1	0.1
U	ppm	IC3M	2.4	2.3	2.5	0.88	1.1	1	1.7	1.15	1.4	0.84	1.05	1	1.95	1.45	1.9	1.7	0.99	0.85	0.93	1.1	0.97	3.5	1
W	ppm	IC3M	1.9	1.4	1.3	1.2	1.1	0.9	0.9	0.6	0.7	0.6	0.7	0.5	0.6	0.6	0.6	0.4	0.99	0.4	0.2	0.5	0.4	5.5	0.3
Y	ppm	IC3M	9	13	12	12.5	20	16	16	12.5	15.5	11	11	23.5	60	7.5	28.5	14.5	8.5	17.5	13.5	14	12.5	14	18.5
Zn	ppm	IC3M	22	12.5	9	9	11.5	13	11.5	12.5	5.5	2.3	14	11.5	12.5	31	37	23.5	12.5	11	13	12	14	14	12
Dy	ppm	IC3R	1.7	2.4	1.7	2.1	3.5	2.6	2.8	2.1	2.3	2.3	2.3	3.3	9.5	1.5	4.4	2.3	1.6	3	2.6	2.3	2.4	1.4	2.9
Er	ppm	IC3R	0.85	1.2	0.85	1.05	1.65	1.2	1.35	1.1	1.2	1.3	0.95	1.9	9.5	1.5	2.5	2.3	0.85	1.7	1.3	1.2	1.1	0.7	1.65
Eu	ppm	IC3R	0.66	0.89	0.64	0.49	1	1.05	1.05	0.88	0.9	0.77	0.99	0.84	1.7	0.53	1.15	0.67	0.56	0.8	0.75	0.98	0.77	0.53	0.76
Gd	ppm	IC3R	2.2	3.3	2.2	2.7	4.9	3.6	3.6	2.8	2.9	3	3.8	4	9	2.3	5.5	3.1	2.1	3.2	3.6	3.7	3.4	2	3.3
Ho	ppm	IC3R	0.29	0.41	0.29	0.34	0.57	0.41	0.47	0.37	0.4	0.42	0.36	0.63	1.75	0.24	0.83	0.41	0.27	0.52	0.43	0.42	0.38	0.25	0.55
Lu	ppm	IC3R	0.1	0.12	0.09	0.11	0.16	0.13	0.14	0.11	0.1	0.12	0.1	0.23	0.65	0.08	0.3	0.11	0.08	0.18	0.17	0.13	0.13	0.08	0.19
Nd	ppm	IC3R	13.5	19	13.5	13.5	30	22.5	19.5	16	15	16	26	16.5	31.5	15.5	20.5	17	12.5	18	20.5	25.5	21	12.5	17.5
Pr	ppm	IC3R	3.5	4.7	3.6	2.7	7.5	5.5	4.7	3.7	3.4	3.6	4.8	3.4	7	4.2	4.8	4.1	3	4.4	4.7	4.5	3.4	2.1	4.1
Sm	ppm	IC3R	2.3	3.5	2.5	3.6	5.5	4.5	3.7	2.6	2.5	3.6	4.8	3.4	8	2.8	5	3.2	2.2	3.6	4.1	4.5	4	2.1	3.5
Tb	ppm	IC3R	0.35	0.5	0.33	0.4	0.73	0.55	0.53	0.43	0.43	0.46	0.55	0.63	1.6	0.3	0.87	0.48	0.32	0.53	0.49	0.54	0.5	0.29	0.53
Tm	ppm	IC3R	0.1	0.15	0.1	0.15	0.2	0.15	0.15	0.1	0.15	0.15	0.1	0.25	0.75	0.1	0.3	0.15	0.1	0.2	0.15	0.15	0.15	0.05	0.2
Yb	ppm	IC3R	0.7	1	0.75	0.85	1.3	1.05	1.05	0.9	0.85	0.95	0.75	1.6	5	0.55	2.3	0.9	0.7	1.5	1.05	0.95	0.9	0.5	1.45

TBC - regional Tikalina-Bulloo Creek area, R - reconnaissance TBC samples

Appendix 2 -

Element	TBC024	TBC025	TBC026	TBC027	TBC028	TBC029	TBC030	TBC031	TBC032	TBC033	TBC034	TBC035	TBC036	TBC037	TBC038	TBC039	TBC040	TBC041	TBC042	TBC043	TBC044	TBC045	TBC046	TBC047	TBC048
	460775	460765	460776	460789	460131	459718	459343	459123	457654	456666	456274	455226	455878	456910	455070	454636	453396	451288	450843	448893	448179	448374	448387	447824	447726
	6451268	6451384	6450765	6450501	6450373	6450612	6449787	6449959	6450533	6451638	6451791	6452452	6453343	6453903	6454092	6452054	6451328	6449222	6448961	6447118	6447882	6446234	6444696	6444160	6440948
Au	1	15	1	7	160	10	1	2	2	<1	2	3	6	3	4	3	5	3	3	3	1	7	5	4	2
Au Dpt	–	6	–	–	–	–	–	–	–	–	–	–	4	–	–	–	–	–	–	–	–	7	5	–	–
Ba	240	850	600	360	650	300	380	440	260	270	1800	490	460	320	370	550	490	290	250	250	300	460	380	230	440
Ca	287000	236000	318000	284000	290000	277000	232000	278000	293000	339000	283000	292000	322000	298000	287000	307000	276000	305000	303000	268000	297000	309000	300000	314000	282000
Cr	7	12	7	10	11	9	10	2	7	5	6	8	6	6	9	7	5	11	10	8	11	10	9	9	9
Fe	7600	15000	9750	8900	10900	10300	11800	9500	6400	3800	5500	4600	6350	8600	8400	4100	11200	8800	11800	6700	12800	7350	10200	9800	10100
K	3750	9100	2300	3650	5450	7850	10200	7500	4750	3100	7200	5700	6400	7650	9100	5800	11100	8650	5950	6400	5950	4900	5300	3300	10400
Mg	5350	6500	7000	5150	6000	6600	8100	7900	6800	5250	7750	9900	6550	7300	9550	7450	7600	7150	11700	23800	8650	8800	7500	5750	11400
Mn	155	84	66	48	110	90	125	96	54	52	68	68	76	78	76	54	290	76	135	82	155	84	70	74	64
Na	8100	13700	4900	9450	4400	4300	3750	3200	7350	2900	1650	10000	3100	3600	4150	6100	4550	4150	4700	8300	5200	4900	5350	6550	8750
P	160	200	200	270	310	340	600	250	350	250	360	340	170	650	270	290	240	340	410	390	370	270	200	240	200
Ti	850	1150	700	900	1150	950	1200	1050	600	440	700	700	600	750	750	490	1000	950	1400	700	1850	700	950	650	1050
V	20	28	20	24	28	27	33	29	21	10	25	18	18	22	21	14	24	25	40	21	46	23	28	22	27
S	700	500	900	850	1000	850	800	950	1000	1000	1550	950	900	850	900	850	700	900	900	700	600	850	800	1050	700
Ag	<0.1	<0.1	0.4	<0.1	<0.1	0.2	<0.1	<0.1	<0.1	0.9	<0.1	<0.1	<0.1	<0.1	<0.1	<0.1	0.1	<0.1	<0.1	<0.1	<0.1	<0.1	<0.1	<0.1	<0.1
As	<0.1	4	2	2.5	3	2	3	3	3.5	3	4.5	2	1.5	5.5	2	0.5	12	4.5	<0.1	3	<0.1	3	<0.1	1.5	1.5
Bi	<0.1	<0.1	<0.1	<0.1	<0.1	<0.1	<0.1	<0.1	<0.1	<0.1	<0.1	<0.1	<0.1	<0.1	<0.1	<0.1	0.5	<0.1	<0.1	<0.1	<0.1	0.1	0.1	0.1	<0.1
Cd	<0.1	0.7	0.6	0.5	1.3	0.1	0.1	0.1	<0.1	0.2	<0.1	<0.1	<0.1	0.1	0.7	<0.1	0.5	<0.1	<0.1	0.3	<0.1	0.1	0.1	0.4	<0.1
Cs	0.5	0.7	0.6	1.3	1.3	1.1	1.6	1.4	0.6	0.2	1.1	2.2	0.7	1.2	0.7	0.7	2.7	1.3	1.1	1	1.4	0.8	0.7	0.4	1
Ce	27	36	41.5	64	40.5	29	44.5	32.5	31	20.5	56	21.5	25	27.5	30.5	19	32.5	36.5	21	31	21	30	27	24	31.5
Co	5	3.8	2.7	3.5	8	5.5	5.5	7	4.2	4.2	6	4.1	4.2	4.3	5.5	3.7	10	6	14	15.5	9.5	4	6.5	7.5	4.5
Cu	11	11.5	10.5	11.5	195	26	26	20	27	14.5	22	13.5	11	36	14	14.5	19.5	16.5	19	27.5	21	18.5	18.5	8.5	10
Ga	6	8.5	5	7	7	7.5	7.5	7	6	3	5.5	6.5	4.4	5	7	4.9	7.5	6	5.5	7	6.5	4.3	5	4	6
In	<0.05	<0.05	<0.05	<0.05	<0.05	<0.05	<0.05	<0.05	<0.05	<0.05	<0.05	<0.05	<0.05	<0.05	<0.05	<0.05	<0.05	<0.05	<0.05	<0.05	<0.05	<0.05	<0.05	<0.05	<0.05
La	18	18.5	22	26.5	26	17	25	18.5	18	12.5	22	13	24	16	19.5	11.5	19	21.5	12.5	18.5	12	22.5	19	15.5	20
Mo	0.2	0.2	0.1	0.2	1.2	0.8	0.6	0.4	0.7	0.2	0.1	0.2	<0.1	0.5	0.5	0.1	1.1	0.4	0.3	0.7	0.3	0.5	0.2	0.3	0.2
Ni	9	10	10	9	15	11	12	13	12	10	11	20	9	11	13	11	14	13	14	15	15	10	10	9	12
Pb	3.5	6	3.5	4	4.5	7.5	7.5	4.5	3.5	10	4.5	4	6	6	5	5.5	5	5.5	3.5	5	3	3.5	3	3	4
Rb	19	45	11	17.5	48.5	43	64	54	30	24	44.5	38.5	38.5	62	50	39	92	60	41	41.5	37.5	19	26.5	13.5	50
Sb	<0.5	<0.5	<0.5	<0.5	<0.5	<0.5	<0.5	<0.5	<0.5	<0.5	<0.5	<0.5	<0.5	<0.5	<0.5	<0.5	<0.5	<0.5	<0.5	<0.5	<0.5	<0.5	<0.5	<0.5	<0.5
Se	<0.5	<0.5	<0.5	<0.5	1	<0.5	<0.5	<0.5	<0.5	<0.5	1	<0.5	<0.5	<0.5	<0.5	<0.5	<0.5	<0.5	0.5	<0.5	<0.5	0.5	0.5	<0.5	<0.5
Sr	360	410	550	440	410	430	500	600	490	490	600	550	470	600	700	600	490	550	800	1100	450	700	600	440	550
Te	<0.2	<0.2	<0.2	<0.2	<0.2	<0.2	<0.2	<0.2	<0.2	<0.2	<0.2	<0.2	<0.2	<0.2	<0.2	<0.2	<0.2	<0.2	<0.2	<0.2	<0.2	<0.2	<0.2	<0.2	<0.2
Th	3.2	5.5	4.2	3.9	4.7	4.1	6.5	3.6	2.8	2.8	5.5	7	3.2	4.7	6	2.8	5	4.9	2.8	4.1	2.1	3.4	3.6	3.6	6.5
Tl	<0.1	0.2	<0.1	0.1	0.3	0.2	0.3	0.3	0.1	<0.1	0.2	0.1	0.1	0.3	0.2	0.2	0.6	0.3	0.2	0.2	0.2	0.1	0.1	<0.1	0.2
U	1.4	0.92	0.95	1.8	1.9	1.4	2.3	<0.1	2.5	0.81	1.85	1.25	1.5	0.3	1.75	1.1	2.3	1.8	2.2	2.5	1.2	0.88	0.74	1.1	1.1
W	0.3	0.6	0.1	0.1	0.2	0.3	0.3	<0.1	0.1	<0.1	<0.1	0.1	<0.1	0.3	0.1	0.1	4.8	1.7	0.8	0.7	0.5	0.1	0.5	0.3	0.3
Y	19	11	16.5	21	8.5	17.5	17.5	10.5	10	8	19	7	29	7	9.5	6	7	12.5	18.5	6.5	12.5	13.5	18	9.5	12
Zn	13	13.5	12.5	13	18.5	25.5	18	16.5	11.5	13	13	13	10.5	17.5	14	13.5	22	14.5	18.5	15	19.5	13.5	10.5	6.5	7
Dy	2.8	2.2	2.9	4.2	1.65	3.5	1.55	2.1	1.8	1.5	3.7	1.25	3.6	1.5	1.8	1.15	1.5	2.4	2.7	1.4	2.3	2.7	10.5	6.5	10
Er	1.65	1.1	1.55	2.2	0.7	1.55	1.55	0.9	0.85	0.65	1.65	0.6	2.4	0.6	0.85	0.5	0.6	1.1	1.75	0.6	1.2	1.25	2.7	1.65	0.7
Eu	0.62	0.83	0.91	1.35	0.74	1.15	1.15	0.75	0.5	0.5	1.3	0.47	0.89	0.51	0.55	0.48	0.62	0.82	0.69	0.55	0.74	0.89	1.55	0.9	0.63
Gd	3	2.9	5	5	2.7	4.9	4.9	2.9	2.5	2.2	5	1.7	4.1	2.1	2.4	1.6	2.4	3.8	3	2.2	2.7	3.1	3.1	2.2	2.4
Ho	0.52	0.35	0.5	0.72	0.26	0.54	0.54	0.32	0.28	0.25	0.59	0.21	0.76	0.23	0.3	0.18	0.23	0.39	0.53	0.22	0.41	0.44	0.51	0.26	0.25
Lu	0.18	0.12	0.17	0.23	0.07	0.16	0.16	0.09	0.08	0.06	0.18	0.08	0.28	0.06	0.08	0.06	0.05	0.11	0.21	0.06	0.14	0.13	0.18	0.1	0.09
Nd	16	18.5	22.5	33.5	18.5	26.5	26.5	18	15.5	12	29	11	20.5	14	16	10.5	16.5	21	13	15.5	13	21.5	17	13	16.5
Pr	3.9	4.6	5.5	7.5	4.9	6.5	6.5	4.3	4.2	2.9	6.5	2.8	4.9	3.6	3.9	2.5	4.1	4.3	2.9	3.8	2.9	5.5	4.3	3.6	4.5
Sm	3	3.3	4	6.5	2.9	5.5	3.2	3.2	3	2.3	5.5	1.85	3.8	2.5	2.9	1.8	2.9	4.3	2.8	2.6	2.7	4.3	3.3	2.7	3.1
Tb	0.52	0.42	0.56	0.84	0.36	0.7	0.42	0.3	0.35	0.3	0.79	0.25	0.7	0.31	0.38	0.23	0.35	0.54	0.52	0.3	0.43	0.57	0.51	0.3	0.36
Tm	0.2	0.15	0.2	0.25	0.05	0.15	0.1	0.1	0.1	0.05	0.2	0.05	0.3	0.05	0.1	0.05	0.05	0.1	0.2	0.05	0.15	0.15	0.2	0.1	0.1
Yb	1.5	0.95	1.4	1.85	0.55	1.25	0.75	0.75	0.7	0.6	1.4	0.6	2.1	0.55	0.7	0.45	0.45	0.9	1.6	0.45	1.05	1	1.25	0.75	0.7

Appendix 2

Element	TBC049	TBC050	TBC051	TBC052	TBC053	TBC054	TBC055	TBC056	TBC057	TBC058	TBC059	TBC060	TBC061	TBC062	TBC062	TBC062	TBC062	TBC062	TBC062	TBC063	TBC064	TBC065	TBC066	TBC067	TBC068
	460085	459991	460974	448398	450823	450170	449970	449139	449051	462998	464349	464628	464858	465128	465128	465128	465128	465128	465128	465281	465596	465835	466155	466074	463947
	6450008	6450889	6450528	6434466	6436538	6437232	6437235	6437358	6438036	6438410	6435698	6434095	6434490	6434348	6434348	6434348	6434348	6434348	6434348	6433557	6433134	6432666	6431865	6430451	6433782
Au	4	3	1	1	3	5	3	4	4	3	<1	<1	3	9	2	5	11	8	<1	2	2	3	3	4	3
Au Dpt	—	—	—	—	—	—	—	—	—	—	—	—	—	—	—	—	—	—	—	—	—	—	—	—	—
Ba	420	430	800	185	260	150	320	210	240	1100	340	400	220	650	650	650	440	220	260	200	200	190	260	175	270
Ca	276000	275000	283000	302000	291000	316000	308000	276000	281000	239000	265000	300000	265000	197000	7150	260000	239000	254000	15300	271000	245000	300000	227000	221000	252000
Cr	8	9	6	12	10	7	11	7	8	8	<1	6	10	11	30	11	10	9	37	8	8	11	10	9	12
Fe	9450	11500	7500	14300	12400	6600	7700	8050	8700	12500	8350	11600	9600	12200	28100	9450	9650	9850	39100	8650	7650	8100	9500	9400	15200
K	12800	8350	7450	3350	4900	3800	4550	4800	6900	2950	3900	2750	6500	10700	31800	5300	6300	5400	14400	4850	4750	4950	5250	4850	5700
Mg	5850	7650	6800	11500	7950	13700	8250	6450	10100	6050	7250	5900	12000	8300	11000	5950	6050	7350	6800	13700	31100	8400	6500	8400	7550
Mn	80	105	110	80	72	110	86	90	82	58	60	46	74	40	105	48	40	66	210	80	60	64	58	80	60
Na	4900	3400	6950	6250	6850	1750	3800	6000	4500	1800	3950	2550	5000	16300	33900	6750	6650	4600	19400	4500	3200	2800	17500	12400	6200
P	430	190	550	390	220	220	220	250	320	270	230	155	260	160	270	110	100	175	260	300	220	180	220	430	220
Ti	1250	700	1100	150	750	600	850	850	750	650	850	650	950	1350	3000	1050	950	1050	3700	750	700	800	1150	900	1050
V	28	20	39	39	34	19	21	19	20	35	24	22	28	31	60	27	25	25	70	22	16	22	28	27	33
S	900	1250	800	800	750	900	850	550	650	1050	700	950	600	600	100	700	700	700	100	800	550	950	600	550	750
Ag	<0.1	<0.1	<0.1	<0.1	<0.1	<0.1	<0.1	<0.1	<0.1	<0.1	<0.1	<0.1	<0.1	<0.1	<0.1	<0.1	<0.1	0.8	<0.1	<0.1	<0.1	<0.1	<0.1	<0.1	<0.1
As	1.5	2	<0.5	<0.5	<0.1	1.5	1.5	3.5	2	5.5	2.5	2.5	1	3.5	4	4	3.5	<0.5	3.5	<0.1	<0.5	<0.5	<0.5	1.5	<0.1
Bi	<0.1	<0.1	<0.1	<0.1	<0.1	<0.1	<0.1	<0.1	<0.1	<0.1	<0.1	<0.1	<0.1	<0.1	<0.1	<0.1	<0.1	<0.1	<0.1	<0.1	<0.1	0.1	0.1	<0.1	<0.1
Cd	0.2	<0.1	0.1	0.1	0.1	0.2	0.2	0.1	<0.1	0.1	0.1	0.1	0.1	0.1	<0.1	<0.1	<0.1	<0.1	<0.1	0.2	0.2	0.1	0.1	0.1	0.1
Cs	1.3	0.7	0.7	0.7	0.8	0.7	0.8	0.8	0.1	0.6	0.5	0.5	0.8	1	3.9	0.9	0.9	0.9	1.9	0.9	0.7	0.8	0.8	0.7	0.9
Ce	26.5	21.5	19	24.5	34.5	18	19	34.5	35.5	26	28	22	23.5	50	74	42	32	23.5	98	24.5	38.5	21.5	38	42	29
Co	7.5	3.5	6.5	5.5	6	12.5	5.5	7.5	9	4.5	4.5	4.4	15	6	12	12.5	5	7	7.5	5.5	4.1	5	5	5.5	5
Cu	18	12	8.5	8.5	12.5	6	11.5	12.5	19	15	15	15.5	15	15.5	4.5	12.5	11	11.5	12.5	11.5	8.5	9.5	11	16	13.5
Ga	8.5	5.5	4.6	5.5	3.3	4.5	4.2	5	4	5.5	5.5	3.6	5.5	7.5	20	4.9	5	4.8	14.5	4.6	3.6	4.3	7	6.5	5.5
In	<0.05	<0.05	<0.05	<0.05	<0.05	<0.05	<0.05	<0.05	<0.05	<0.05	<0.05	<0.05	<0.05	<0.05	0.05	<0.05	<0.05	<0.05	<0.05	<0.05	<0.05	<0.05	<0.05	<0.05	<0.05
La	20	13.5	15	17	21.5	12.5	21.5	23.5	21.5	17.5	16.5	19	13.5	31	43	26	20	15	56	15	23.5	15.5	24.5	28.5	20.5
Mo	16.5	0.2	0.2	0.2	0.1	3.3	0.1	0.2	0.5	0.5	0.4	0.6	0.2	0.2	0.2	0.1	0.1	0.1	0.4	0.1	0.1	0.2	0.2	0.3	0.1
Ni	13	13	14	13	13	14	10	10	11	12	12	10	12	12	23	13	14	12	15	11	9	11	11	12	12
Pb	4.5	4.5	3	4.5	4.5	4.5	4.5	6.5	3.5	4.5	3.5	3	5.5	4	6.5	3	3.5	3	10	3.5	3.5	4.5	4.5	3.5	4
Rb	52	54	24	16	23	13.5	17	23.5	12	12	19	12.5	23.5	31.5	105	22	25	24.5	54	19.5	24.5	22	24	23.5	27.5
Sb	<0.5	<0.5	<0.5	<0.5	<0.5	<0.5	<0.5	<0.5	<0.5	<0.5	<0.5	<0.5	<0.5	<0.5	<0.5	<0.5	<0.5	<0.5	<0.5	<0.5	<0.5	<0.5	<0.5	<0.5	<0.5
Se	<0.5	0.5	<0.5	<0.5	<0.5	0.5	<0.5	<0.5	<0.5	<0.5	<0.5	1	<0.5	0.5	1	<0.5	<0.5	<0.5	<0.5	0.5	<0.5	<0.5	<0.5	<0.5	<0.5
Sr	490	650	460	430	380	700	410	390	550	430	500	470	500	500	94	460	420	320	84	650	700	470	450	370	480
Te	<0.2	<0.2	<0.2	<0.2	<0.2	<0.2	<0.2	<0.2	<0.2	<0.2	<0.2	<0.2	<0.2	<0.2	<0.2	<0.2	<0.2	<0.2	<0.2	<0.2	<0.2	<0.2	<0.2	<0.2	<0.2
Th	5.5	4.6	10.5	4.8	3.1	2.4	3.1	5.5	3.8	3.8	5.5	3.3	4.5	9	13	6	5	4.1	5	3.9	6	3.7	6.5	6.5	4.5
Tl	0.4	0.1	<0.1	0.1	<0.1	<0.1	<0.1	0.2	<0.1	<0.1	<0.1	<0.1	0.1	0.2	0.7	0.1	0.1	0.1	0.3	0.1	<0.1	0.1	0.1	0.1	0.1
U	1.5	2.1	2.1	0.72	0.1	1.5	0.65	0.83	1.2	0.65	0.64	0.73	0.64	0.76	0.56	0.7	0.56	0.48	1.25	0.56	1.6	0.68	0.62	1.5	0.73
W	0.5	0.6	0.6	0.3	0.1	<0.1	0.5	1.5	0.8	0.6	0.4	0.4	0.4	0.4	0.8	0.1	<0.1	0.3	0.6	<0.1	<0.1	0.2	0.2	0.1	<0.1
Y	10	11.5	11	12	9	11	17	10	6.5	9	6.5	11.5	7	8.5	7.5	7	5.5	5.5	12.5	11.5	9.5	10	10	10	11.5
Zn	16	11.5	11.5	9	11	9	9.5	10	6.5	10	9.5	8	6.5	6.5	19.5	8	6	11	30.5	6	9	8	13	10.5	10
Dy	2.6	2	2	2.1	1.65	2	3	1.55	1.8	1.8	1.4	2.1	1.95	1.95	2.4	1.65	1.35	1.45	3.5	2.2	2.1	1.75	1.95	2.1	2.1
Er	1.05	1.8	1.2	1.15	0.85	1.1	1.5	0.65	1	0.87	0.65	1.05	0.8	0.8	0.75	0.6	0.75	0.6	1.3	0.9	0.85	0.95	0.72	1	1.05
Eu	1.25	0.85	0.7	0.55	0.6	0.6	0.97	0.79	0.65	0.87	0.57	0.73	0.57	0.94	1.05	0.74	0.58	0.54	1.45	0.62	0.67	0.57	0.72	0.67	0.73
Gd	3.9	2.5	2.3	2.4	2.4	2.3	3.8	2.4	2.5	2.5	1.95	2.8	1.95	3.3	3.9	2.8	2.1	1.95	6	2.5	2.9	2.2	2.9	3.1	2.8
Ho	0.37	0.3	0.36	0.34	0.27	0.36	0.48	0.33	0.22	0.29	0.22	0.34	0.22	0.28	0.29	0.24	0.21	0.24	0.47	0.35	0.33	0.28	0.32	0.34	0.37
Lu	0.1	0.1	0.17	0.14	0.09	0.11	0.15	0.11	0.06	0.09	0.08	0.12	0.08	0.08	0.08	0.08	0.06	0.08	0.16	0.11	0.08	0.1	0.1	0.09	0.11
Nd	26.5	15	13	13	14.5	13	19.5	18.5	17	16	13.5	17.5	13.5	24	34	21	15.5	12.5	47	15	20	13	18.5	21	17.5
Pr	6	3.9	3.4	3.8	3.8	3.3	5	4.9	5	4.3	3.6	4.5	3.6	6.5	9.5	5.5	4.3	3.4	13	3.8	5	3.4	3.7	6	4.5
Sm	6	2.9	2.5	2.7	2.7	2.7	4	3.4	2.8	2.8	2.6	3.5	2.6	4.1	6	3.8	2.9	2.5	8.5	3	3.7	2.5	3.7	4	3.5
Tb	0.58	0.39	0.36	0.37	0.32	0.37	0.56	0.45	0.31	0.37	0.44	0.3	0.29	0.45	0.54	0.37	0.31	0.29	0.8	0.42	0.43	0.32	0.42	0.44	0.42
Tm	0.1	0.1	0.15	0.15	0.15	0.2	0.2	0.1	0.1	0.1	0.1	0.15	0.1	0.1	0.15	0.1	0.1	0.1	0.15	0.15	0.1	0.1	0.1	0.1	0.15
Yb	0.85	0.7	1.2	1	0.75	0.85	1.15	0.9	0.55	0.75	0.6	0.85	0.6	0.65	0.6	0.6	0.7	0.7	1.25	0.9	0.75	0.7	0.8	0.75	0.9

Appendix 2 -

Element	TBC069	TBC070	TBC071	TBC072	TBC073	TBC074	TBC075	TBC076	TBC077	TBC078	TBC079	TBC080	TBC081	TBC082	TBC083	TBC084	TBC085	TBC086	TBC087	TBC088	TBC089	TBC090	TBC091	TBC092	TBC093
	1463433	462732	462647	462903	461963	460835	460466	460312	460438	458631	457991	457721	457487	457439	457411	457326	457228	457202	457249	456877	456463	455522	454955	453205	451969
	6433783	6433741	6433318	6432832	6434160	6432277	6433386	6432778	6431952	6431311	6431186	6431448	6432476	6432988	6433475	6433881	6430748	6430464	6430085	6429522	6429427	6427609	6428371	6427962	6427321
Au	3	2	1	1	<1	<1	<1	<1	2	4	3	3	4	1	1	3	6	1	3	4	2	46	5	3	2
Au Dpt	-	-	-	-	-	-	-	-	-	-	-	-	-	-	-	-	-	-	-	-	-	-	-	-	-
Ba	330	240	420	950	2200	1750	1650	950	1000	380	400	270	1200	250	380	450	340	360	300	320	1650	310	750	550	700
Ca	287000	289000	282000	269000	280000	277000	265000	255000	288000	300000	288000	286000	298000	231000	253000	258000	293000	276000	254000	251000	281000	198000	234000	256000	274000
Cr	10	8	8	-	7	7	6	6	7	9	10	10	7	13	7	11	5	7	8	15	7	5	9	8	8
Fe	9750	7200	8200	8350	7000	6750	6700	6850	6250	6600	7750	8000	5500	15000	7400	7650	4050	5900	8150	19900	5700	6050	10300	7050	5150
K	4450	3650	4650	4050	4900	5600	3650	3600	5150	4250	4850	4300	3200	9900	8550	3450	3500	3550	4600	4000	3750	6150	6050	4750	2750
Mg	8700	7900	12600	20000	10400	12000	10100	5500	10300	8000	9450	11900	8200	8250	8100	18200	8100	7000	12900	12400	7750	4850	7800	9450	11000
Mn	74	60	78	150	60	100	64	62	64	62	60	82	62	82	64	100	54	60	76	125	74	78	160	82	72
Na	4050	3150	2500	2950	1700	1450	2400	2300	2150	2500	2750	2750	2300	10200	5900	2700	1650	2950	2950	6100	2000	6200	3500	2900	950
P	160	260	185	185	185	200	220	190	320	390	330	260	155	340	300	200	300	180	210	600	260	185	230	210	92
Ti	850	650	800	800	650	600	700	700	750	700	800	850	550	1200	650	850	330	750	750	1350	650	750	1050	850	650
V	25	21	24	25	19	27	22	21	30	22	24	24	22	41	25	24	13	19	28	50	23	21	52	23	21
S	800	1150	1000	1250	1600	1500	1500	1250	1550	1150	1200	950	1550	1000	1350	1150	1650	1200	950	700	1850	500	850	800	1300
Ag	<0.1	<0.1	<0.1	<0.1	<0.1	<0.1	<0.1	<0.1	<0.1	<0.1	<0.1	<0.1	<0.1	<0.1	<0.1	0.6	0.2	<0.1	<0.1	0.1	<0.1	<0.1	<0.1	<0.1	<0.1
As	<0.5	<0.1	1	<0.1	<0.5	4.5	<0.1	1.5	7	2	1	<0.1	1.5	0.5	3.5	2.5	0.2	<0.5	0.1	5	2	2.5	4	2.5	2
Bi	0.1	0.1	0.1	0.1	<0.1	<0.1	0.1	<0.1	2.7	0.4	0.2	0.2	<0.1	<0.1	<0.1	0.2	0.1	0.1	0.1	0.4	0.1	0.4	0.1	0.1	<0.1
Cd	0.1	0.1	0.7	0.1	0.1	0.1	0.2	0.1	0.1	0.2	0.1	0.1	0.2	0.1	0.1	0.2	0.1	0.2	0.1	0.4	0.3	0.3	0.2	0.5	<0.1
Cs	0.8	0.7	0.8	0.7	0.8	0.6	0.7	0.6	0.6	0.7	0.7	0.8	0.5	1	0.7	0.9	0.6	0.8	0.9	1.4	1	2.1	1.9	1.2	0.9
Ce	32.5	25	34.5	34.5	19	39	22	29.5	29.5	19.5	19.5	21.5	21	36	17.5	35	19.5	24	28	240	21	29	24.5	23.5	15
Co	4.4	4.3	5	5	3.6	5.5	3.8	4.3	5.5	4.2	4	6	4.2	6	4.6	6	2.9	3.1	6	9.5	4.8	8	7.5	5.5	5
Cu	9	14	8.5	8.5	9.5	14.5	22	11.5	24.5	15	12.5	14.5	12	13	12.5	17.5	19.5	13	14	10.5	14	15	15.5	12	11.5
Ga	4.4	3.8	4.2	4.1	3.3	4.1	3.7	3.2	4.2	3.6	3.7	3.6	2.9	8.5	6	4.2	3.5	3.8	4.8	7.5	3.2	6	6	4.2	3
In	<0.05	<0.05	<0.05	<0.05	<0.05	<0.05	<0.05	<0.05	<0.05	<0.05	<0.05	<0.05	<0.05	<0.05	<0.05	<0.05	<0.05	<0.05	<0.05	<0.05	<0.05	<0.05	<0.05	<0.05	<0.05
La	21	17.5	19	17	20	23.5	21	17	17	15.5	14	20.5	15.5	22	20.5	20.5	11.5	18.5	18.5	145	23.5	20.5	22	23	16
Mo	0.1	0.4	0.2	0.3	0.2	0.2	0.2	0.3	0.8	0.2	0.3	0.2	0.2	0.2	0.3	0.5	0.4	0.3	0.3	0.2	0.3	0.4	0.4	0.2	0.1
Ni	11	12	11	11	10	10	11	13	11	11	11	11	10	13	9	12	9	10	11	18	11	12	16	12	11
Pb	4	11	3.5	3.5	4.5	4.5	11	11	12.5	6.5	5.5	6	4.5	4.5	4.5	4.5	3.5	4.5	10.5	17.5	6	12	6	4.5	4
Rb	20.5	17.5	23.5	15	24	29.5	16.5	14.5	25	16	21.5	22	13	45.5	37.5	25	20.5	19.5	24.5	24.5	23	33.5	25	26	17.5
Sb	<0.5	<0.5	<0.5	<0.5	<0.5	<0.5	<0.5	<0.5	<0.5	<0.5	<0.5	<0.5	<0.5	<0.5	<0.5	0.5	0.5	<0.5	<0.5	<0.5	<0.5	<0.5	<0.5	<0.5	<0.5
Se	0.5	<0.5	<0.5	<0.5	0.5	0.5	<0.5	1	<0.5	0.5	0.5	0.5	1.5	0.5	0.5	1.5	1	<0.5	<0.5	<0.5	1.5	<0.5	<0.5	<0.5	1.5
Sr	550	460	650	850	700	800	650	500	850	550	700	750	950	490	600	800	700	550	750	480	650	310	470	650	650
Te	<0.2	<0.2	<0.2	<0.2	<0.2	<0.2	<0.2	<0.2	<0.2	<0.2	<0.2	<0.2	<0.2	<0.2	<0.2	<0.2	<0.2	<0.2	<0.2	<0.2	<0.2	<0.2	<0.2	<0.2	<0.2
Th	6	2.7	3.3	3.6	3	5.5	4.6	3.1	5	3.2	3.3	3.5	3.2	6.5	2.8	5.5	4.7	4.9	6	60	7.5	7.5	5.5	4.7	3
Tl	<0.1	<0.1	<0.1	<0.1	<0.1	<0.1	<0.1	<0.1	<0.1	0.3	0.2	0.2	<0.1	0.2	0.2	0.1	<0.1	<0.1	0.2	0.2	0.1	0.1	0.1	0.1	<0.1
U	0.89	1.1	2.1	2.1	0.61	1.8	1.95	1.65	1.2	0.84	0.93	1.15	1.55	3.4	2.8	2	2.1	0.3	0.86	0.93	0.1	0.3	1.45	0.79	0.72
W	<0.1	0.4	<0.1	0.2	0.2	0.2	0.1	<0.1	1.6	0.6	0.4	0.3	0.1	0.3	0.2	0.9	<0.1	0.3	0.5	0.5	1.25	1.25	0.5	0.5	0.4
Y	13	12.5	10.5	8.5	16.5	25.5	16	9.5	7.5	13	10	11	10	10.5	8.5	12.5	8	13	11	30	14	20	15	13	13.5
Zn	10.5	10.5	16	16	13	8	11	10	12.5	11	10	11	10.5	10.5	9.5	10	8.5	8.5	10.5	20	11.5	14	18.5	12.5	10
Dy	2.7	2.3	1.95	1.8	3.1	5	2.8	1.8	1.65	2.2	1.85	2	1.9	2.2	1.75	3	1.6	2.6	2.4	9.5	2.8	2.9	2.9	2.5	2.4
Er	1.25	1.15	1.05	0.85	1.5	2.4	1.4	0.9	1.6	1.15	0.95	1.05	0.9	0.9	0.9	1.3	0.85	1.3	1.15	2.6	1.35	1.5	1.6	1.25	1.25
Eu	0.92	0.64	0.73	0.8	1.45	1.4	1.2	0.7	0.75	0.65	0.58	0.6	0.83	0.83	0.56	1.3	0.47	0.78	0.72	3.7	1.1	0.81	0.9	0.82	0.77
Gd	3.4	2.6	2.6	2.3	3.9	6	3.7	2.2	2.2	2.6	2.2	2.4	3.1	3.1	1.95	3.6	1.7	2.9	2.7	15.5	3.2	3.1	3.1	2.9	2.5
Ho	0.42	0.36	0.35	0.27	0.51	0.83	0.47	0.67	0.25	0.37	0.3	0.35	0.34	0.34	0.29	0.47	0.27	0.41	0.38	0.45	0.45	0.47	0.53	0.44	0.41
Lu	0.12	0.13	0.11	0.09	0.16	0.31	0.16	0.22	0.1	0.14	0.11	0.13	0.1	0.1	0.1	0.16	0.11	0.14	0.13	0.2	0.16	0.19	0.2	0.13	0.15
Nd	19.5	14.5	16.5	16.5	21.5	26.5	20.5	13	14.5	14	12	12.5	19.5	5	10.5	22.5	11	18	17.5	135	20	20	19	20	15
Pr	4.9	3.8	4.2	4.2	3.7	6.5	5.5	3.3	3.8	3.6	3.2	3.3	5	3.9	2.3	5.5	2.8	4.4	4.3	34.5	2.8	3.2	4.8	2.9	3.6
Sm	4	2.8	3	2.8	3.7	5.5	3.6	2.2	2.5	2.8	2.5	2.6	3.9	3.9	4	5	1.7	2.9	2.8	20	2.8	3.2	3	2.9	2.2
Tb	0.54	0.38	0.4	0.35	0.59	1	0.57	0.33	0.31	0.4	0.35	0.39	0.47	0.47	0.57	0.57	0.26	0.46	0.41	2.1	0.5	0.53	0.53	0.47	0.42
Tm	0.15	0.15	0.1	0.1	0.2	0.35	0.15	0.1	0.1	0.15	0.15	0.15	0.1	0.1	0.2	0.2	0.1	0.15	0.15	0.25	0.15	0.2	0.2	0.15	0.15
Yb	1.1	0.95	0.7	0.7	1.2	2.1	1.15	0.8	0.7	1	0.8	0.95	0.85	0.85	0.85	1.15	0.75	1.15	1.05	1.5	1.15	1.4	1.45	1.05	1.1

Appendix 2 -

Element	TBC094	TBC095	TBC096	TBC097	TBC098	TBC099	TBC100	TBC101	TBC102	TBC103	TBC104	TBC105	TBC106	TBC107	TBC108	TBC109	TBC110	TBC111	TBC112	TBC113	TBC114	TBC115	TBC116	TBC117	TBC118
	449860	457286	456677	455669	455241	454904	457447	457474	457014	456050	455037	454627	453855	453299	453418	453457	453161	451798	451069	449397	449300	451272	452339	453127	449917
	6427159	6434049	6433884	6433650	6433513	6433427	6434701	6435323	6435059	6434550	6434561	6434459	6434350	6433810	6433449	6433222	6433919	6434093	6434208	6434347	6434957	6432102	6431882	6431060	6432075
Au	<1	<1	3	<1	6	5	3	<1	–	–	<1	10	6	2	<1	2	5	6	3	3	4	5	7	4	4
Au Dpl	–	–	–	–	–	–	–	–	–	–	–	10	5	–	–	–	–	3	–	–	–	–	8	–	–
Ba	350	650	490	310	320	500	550	400	750	300	200	600	195	230	300	490	250	195	165	240	270	340	420	460	480
Ca	251000	255000	252000	258000	240000	276000	278000	297000	240000	243000	273000	267000	265000	270000	306000	283000	263000	237000	226000	269000	252000	284000	255000	246000	255000
Cr	10	10	12	9	8	6	8	9	17	11	<1	9	8	9	4	5	8	8	12	7	9	8	6	9	6
Fe	8000	8500	10500	9700	10100	6200	9200	7150	6800	12700	7750	15300	9500	13400	4750	6550	15000	10300	12600	9700	9600	10400	9000	10900	6850
K	4750	3800	6100	4050	8200	3400	5550	2800	4100	7550	3650	3850	5250	4700	1800	2850	5700	3300	5800	5300	6400	6100	4600	6950	5250
Mg	8050	8500	8950	8600	10700	6900	8100	6450	8000	8700	14700	8800	12100	10600	7550	10700	8600	23200	10000	9650	13900	7450	8950	17400	7250
Mn	92	64	74	86	74	54	70	82	66	54	110	80	60	84	50	68	72	115	78	60	68	185	88	115	60
Na	2200	2800	4800	5750	6650	5000	2500	2200	2450	7100	1700	2900	4250	2550	1900	2600	3500	8450	9150	4950	3750	3000	7450	3900	4850
P	220	220	230	320	220	250	250	220	150	210	190	140	230	200	175	250	350	310	120	165	105	210	140	195	170
Ti	950	800	1050	1100	1050	650	1000	650	650	1200	700	800	800	900	500	700	950	1250	1250	800	1050	1050	700	1150	750
V	27	28	31	35	29	16	26	22	23	41	20	28	26	26	16	23	26	34	36	34	27	29	23	35	20
S	1050	1550	1200	1300	600	1200	1400	1350	1550	1300	850	1150	1200	950	1200	1050	1050	700	700	900	900	1100	950	700	700
Ag	<0.1	<0.1	<0.1	<0.1	<0.1	<0.1	<0.1	<0.1	0.65	<0.1	0.2	<0.1	<0.1	<0.1	<0.1	<0.1	<0.1	<0.1	<0.1	<0.1	<0.1	<0.1	<0.1	<0.1	<0.1
As	6	1.5	3	–	4	<0.5	<0.1	<0.5	7.5	4	1.5	3	2.5	2.5	<0.5	2.5	3	3	2	<0.5	<0.1	1.5	4.5	7	2.5
Bi	0.2	<0.1	<0.1	<0.1	<0.1	<0.1	<0.1	<0.1	0.1	<0.1	<0.1	<0.1	<0.1	<0.1	<0.1	<0.1	<0.1	<0.1	<0.1	<0.1	0.1	0.2	0.1	0.2	0.2
Cd	0.5	0.1	0.1	0.1	<0.1	0.2	0.1	0.1	0.7	<0.1	0.2	<0.1	<0.1	0.2	0.3	0.6	0.1	0.1	<0.1	<0.1	0.1	0.6	0.5	0.3	0.2
Cs	1.4	1	1	1.3	1	0.7	1.3	0.8	0.7	1.2	0.8	0.8	0.8	0.9	0.5	0.6	0.9	1	1.1	0.8	1.2	2	0.9	1.8	1.1
Ce	27.5	25.5	36.5	24	34	19.5	31	18	15	28.5	32.5	39	25.5	25	17	16.5	21.5	25	26	26	29.5	38	19	27.5	20
Co	6.5	6.5	10	7	8.5	3.4	7	5.5	5	7	5.5	9	5.5	6	2.9	3.8	6	5.5	4.7	6.5	7	12	5.5	7.5	6
Cu	14	20.5	20	14.5	17	9.5	14.5	11	31.5	16.5	11	72	15.5	13	9.5	11.5	13.5	13.5	11	10.5	14	21	26	17	13.5
Ga	4.6	4.4	6	5.5	8	4.2	5	3.7	3.7	7	3.8	5	4.8	4.6	2.6	3.4	5.5	4.9	7	5	6	5	5.5	5.5	4.9
In	<0.05	<0.05	<0.05	<0.05	<0.05	<0.05	<0.05	<0.05	0.65	<0.05	<0.05	<0.05	<0.05	<0.05	<0.05	<0.05	<0.05	<0.05	<0.05	<0.05	<0.05	<0.05	<0.05	<0.05	<0.05
La	21	16	23.5	15.5	20.5	12	20.5	16	11.5	18	23	32.5	19.5	19.5	34.5	17	13.5	18	22.5	22.5	20	29.5	13.5	23.5	15
Mo	0.2	0.3	0.2	0.1	0.2	0.2	0.3	<0.1	1	0.2	0.2	0.3	0.1	0.1	0.4	0.2	0.2	0.2	0.3	0.2	<0.1	0.2	0.2	0.2	0.2
Ni	12	12	14	14	13	10	14	12	18	15	12	12	12	13	10	12	13	11	12	13	13	16	10	13	11
Pb	6.5	4	3.5	4	2.5	16	3	3.5	25	3.5	4	3.5	3.5	3.5	3.5	3.5	13	2.5	4.5	3.5	4.5	7.5	36.5	21.5	6
Rb	24	20.5	30	20	35	16	31.5	13	19.5	33.5	20	21.5	26.5	23.5	10.5	9	21.5	14	24	22.5	33	35	21.5	40.5	27
Sb	<0.5	<0.5	<0.5	<0.5	<0.5	<0.5	<0.5	<0.5	0.5	<0.5	<0.5	<0.5	<0.5	<0.5	<0.5	<0.5	<0.5	<0.5	<0.5	<0.5	<0.5	<0.5	<0.5	<0.5	<0.5
Se	1	1.5	0.5	0.5	1	1.5	1	<0.5	1.5	1	1	1	0.5	1	2	2	2	2	0.5	0.5	<0.5	0.5	1	0.5	0.5
Sr	550	700	600	650	550	550	650	470	750	650	750	750	750	650	440	650	600	700	600	550	800	470	650	850	550
Te	<0.2	<0.2	<0.2	<0.2	<0.2	<0.2	<0.2	<0.2	<0.2	<0.2	<0.2	<0.2	<0.2	<0.2	<0.2	<0.2	<0.2	<0.2	<0.2	<0.2	<0.2	<0.2	<0.2	<0.2	<0.2
Th	5	4.2	7.5	4.8	4.8	4.5	6	2.9	2.8	4.2	3.9	4.4	5.5	4.5	2.4	2.6	3.8	4.4	5.5	4.6	6	5	4.6	6.5	3.9
Tl	0.1	0.1	0.1	0.1	0.2	<0.1	0.2	<0.1	<0.1	0.2	<0.1	<0.1	0.1	<0.1	<0.1	<0.1	<0.1	<0.1	<0.1	<0.1	0.1	0.2	0.1	0.2	0.1
U	0.85	1.05	1.05	1	0.84	0.89	1.25	0.91	0.97	1.6	1.15	0.92	1	0.78	0.59	0.73	0.54	0.73	0.52	0.63	0.99	1.15	0.85	1.15	0.79
W	0.7	0.3	0.1	0.2	0.2	0.1	<0.1	<0.1	<0.1	0.2	<0.1	0.4	0.2	0.3	0.4	0.2	0.1	0.5	0.2	0.2	0.2	0.5	0.5	0.9	0.9
Y	11.5	8.5	10.5	10.5	8	17.5	8.5	12.5	9.5	9	19.5	22	11	14	31.5	14	11	14.5	9	10	8.5	14.5	11	20.5	11
Zn	15.5	10	17	15	18	8.5	10.5	8.5	68	9	9.5	11.5	8	10	7	9	9.5	10	13	18	11.5	18.5	15.5	30	9
Dy	2.4	1.95	2.4	2.1	1.85	3.1	1.95	2.5	1.65	1.9	4	4.2	2.5	2.6	5.5	2.6	1.95	3	2	3.3	1.85	2.8	2.1	3.3	1.8
Er	1.15	0.85	1.05	1.15	0.75	1.55	0.9	1.2	0.85	0.75	1.95	1.65	1.2	1.35	2.8	1.25	0.95	1.65	0.9	1.6	0.8	1.35	1.05	1.7	0.9
Eu	0.75	0.79	0.82	0.7	0.68	1.1	0.86	0.84	0.64	0.7	1.2	1.2	0.75	0.76	1.75	0.93	0.67	0.85	0.64	1.05	0.68	0.89	0.62	0.89	0.62
Gd	2.7	2.3	3	2.4	2.4	3.7	2.5	2.7	1.9	2.4	4.7	6	2.9	2.9	6.5	2.9	2.3	3.1	2.3	4.1	2.5	3.5	2.2	3.5	2
Ho	0.4	0.29	0.38	0.38	0.26	0.52	0.29	0.38	0.27	0.27	0.69	0.68	0.38	0.45	0.99	0.45	0.32	0.52	0.31	0.55	0.27	0.47	0.35	0.57	0.3
Lu	0.13	0.1	0.11	0.13	0.06	0.16	0.09	0.12	0.08	0.08	0.21	0.23	0.1	0.16	0.27	0.14	0.1	0.21	0.11	0.2	0.09	0.16	0.14	0.2	0.11
Nd	19	16.5	21	15	18	22.5	19.5	16	11.5	17	25.5	37.5	18	17	36.5	17	14	18	16	22	17	25	13.5	21	14.5
Pr	4.8	4	5.5	3.7	4.8	5.5	4.9	3.8	2.7	4.2	6	8.5	4.5	4.2	8.5	4.2	3.3	4.4	2.5	5	4.4	6	3.2	5	3.6
Sm	2.8	2.5	3.2	2.4	2.8	3.6	2.9	2.6	1.8	2.6	4.8	6.5	2.9	2.9	6	2.7	2.4	3.2	2.5	3.7	2.7	3.8	2.2	3.4	2.2
Tb	0.45	0.36	0.47	0.39	0.38	0.55	0.39	0.44	0.27	0.35	0.74	0.84	0.46	0.46	1	0.49	0.38	0.52	0.35	0.63	0.38	0.54	0.34	0.57	0.31
Tm	0.15	0.1	0.15	0.15	0.1	0.15	0.1	0.15	0.1	0.1	0.25	0.25	0.15	0.15	0.3	0.15	0.1	0.2	0.1	0.2	0.1	0.15	0.15	0.2	0.1
Yb	1	0.75	0.9	0.9	0.6	1.2	0.7	1.05	0.7	0.6	1.7	1.65	0.85	1.15	2	1	0.85	1.55	0.9	1.4	0.7	1.15	1	1.4	0.85

Appendix 2 -

Element	TBC119	TBC120	TBC121	TBC122	TBC123	TBC124	TBC125	TBC126	TBC127	TBC128	TBC129	TBC130	TBC131	TBC132	TBC133	TBC134	TBC135	TBC136	TBC137	TBC138	TBC139	RCA01	RCA02	RS01C	RS02C
	450326	457673	459531	460861	460940	458676	457976	460909	460531	460131	448374	443387	461472	454636	459531	454627	457326	457474	465596	465281	459219	458983	457961	457439	
	6431288	6437066	6435466	6435298	6435174	6447680	6445990	6447626	6448477	6450373	6446234	6444696	6446918	6452054	6435466	6434459	6433881	6435323	6433134	6433557	6438883	6440066	6439695	6439919	
Au	2	3	2	2	1	2	2	1	1	140	10	4	<1	7	3	3	5	4	4	4	4	4	2	1	3
Au Dp1	–	–	–	–	–	–	–	–	–	155	17	–	–	–	–	–	–	–	–	–	–	–	–	–	–
Ba	370	440	370	340	1300	310	500	950	370	600	290	260	650	800	1150	400	430	650	450	240	220	190	800	250	280
Ca	286000	273000	293000	206000	243000	272000	274000	252000	259000	292000	318000	302000	317000	291000	295000	315000	306000	294000	321000	183000	273000	236000	301000	296000	303000
Cr	7	8	10	8	15	7	7	7	5	14	8	6	6	8	8	10	12	13	9	16	13	11	5	5	6
Fe	7000	9500	7250	5500	28300	8300	8850	11300	4650	10900	5600	7700	6100	4050	6900	7150	12100	8050	7050	18400	11600	12100	5250	6700	6650
K	3650	6500	3250	2450	1950	5000	7600	4850	3500	5100	4250	3900	5950	4750	4200	3750	3900	3900	2950	9250	5550	5150	2200	3450	3650
Mg	5500	7000	6000	5950	5900	7850	6450	5150	6000	6550	7250	3900	5950	9000	5450	7050	8900	14100	6350	11200	8200	7500	4950	5400	5450
Mn	96	74	54	4	70	170	180	72	185	105	70	66	270	52	66	68	72	70	76	78	78	78	52	76	62
Na	1750	4100	1850	2050	1100	4950	5250	13200	10600	4450	4950	4800	4350	7850	10200	2150	3150	2850	3150	9250	7650	4200	1350	2100	2000
P	170	160	240	260	600	150	390	250	140	320	230	230	195	250	330	270	100	210	260	280	350	470	280	200	170
Ti	850	850	750	4000	750	900	950	900	550	1000	550	750	600	490	600	700	750	800	600	1400	1050	1200	480	700	700
V	27	22	21	33	50	23	19	21	13	27	19	25	16	16	15	24	28	26	22	36	29	29	16	19	21
S	1000	1150	950	650	1450	800	1100	1200	700	1000	700	750	1000	850	1100	600	800	800	1050	<50	550	1650	1300	1000	1100
Ag	<0.1	<0.1	0.2	0.3	0.2	<0.1	<0.1	<0.1	0.1	<0.1	<0.1	0.1	<0.1	<0.1	<0.1	<0.05	<0.1	<0.1	<0.1	<0.1	<0.1	0.3	0.1	0.1	0.05
As	1.5	1.5	1.5	2.5	7	<0.1	1.5	1.5	0.1	2	<0.5	3.5	2.5	4.5	2.5	3.5	5	<0.5	2	1	2.5	0.25	0.25	0.25	2.5
Bi	<0.1	<0.1	0.1	0.1	<0.1	<0.1	<0.1	<0.1	<0.1	<0.1	<0.1	0.3	<0.1	<0.5	<0.1	<0.1	<0.1	<0.1	<0.1	<0.1	0.2	0.2	0.05	0.05	0.05
Cd	0.2	<0.1	0.2	<0.5	0.5	<0.1	<0.1	<0.1	0.5	<0.1	0.1	0.2	0.1	0.2	0.4	0.8	<0.1	0.2	<0.1	<0.1	0.4	1.2	0.5	0.2	0.2
Cs	1.5	0.8	0.9	0.5	0.5	1	1.3	0.5	1.4	0.8	0.8	0.7	0.7	0.8	0.8	0.7	0.7	0.8	1	1.1	1	1.2	0.5	0.6	0.5
Ce	17.5	29	25.5	14.5	52	26	27	32	43	30.5	25	35.5	30.5	21	32.5	34.5	39	23.5	21.5	60	45.5	29.5	16.5	26.5	25
Co	4.6	7	4.5	4	5.5	6	9.5	29	3.9	3.9	3.9	5	4.4	3.7	2.9	4	7.5	5.5	4.8	6	7	9.5	16.5	12	11
Cu	10.5	15.5	12.5	16	31.5	27.5	23.5	13.5	32.5	17.5	17.5	19	14.5	14.5	12	12.5	45.5	16.5	10	12	14.5	11.5	9.5	12.5	11
Ga	3.7	6	3.8	5	3.8	6	6	5.5	6	4.3	4.3	5	4.8	5.5	5	4.1	5	4.6	4.2	8	6	7	2.7	3.7	3.4
In	<0.05	<0.05	<0.05	<0.05	<0.05	<0.05	<0.05	<0.05	<0.05	<0.05	<0.05	<0.05	<0.05	<0.05	<0.05	<0.05	<0.05	<0.05	<0.05	<0.05	<0.05	0.025	0.025	0.025	0.025
La	17.5	18	12.5	19.5	19.5	18	16	18	21.5	29	23	22	21.5	12.5	17.5	26	31.5	14	17.5	35.5	26.5	34	23.5	17.5	17.5
Mo	<0.1	0.2	0.4	1.2	0.4	0.2	0.4	0.2	0.3	0.4	0.4	1.3	0.4	3.3	0.9	0.5	0.4	0.4	0.3	0.3	0.2	0.7	0.5	0.2	0.2
Ni	12	13	11	9	18	13	13	9	11	11	11	10	10	11	9	11	11	11	11	11	12	17	13	16	16
Pb	4.5	3	4.5	6	23.5	3.5	4.5	2.5	8	3.5	3.5	3.5	5	8	4	4	4	3.5	3.5	5.5	3.5	27	7	4	3.5
Rb	17	31.5	16	8	9.5	31.5	43.5	15.5	54	25.5	25.5	20.5	35	33	17	22	23	27.5	14.5	52	29	13.5	2.8	7	7.5
Sb	<0.5	<0.5	<0.5	<0.5	<0.5	<0.5	<0.5	<0.5	<0.5	<0.5	<0.5	<0.5	<0.5	<0.5	<0.5	<0.5	<0.5	<0.5	<0.5	<0.5	<0.5	1	0.5	0.25	0.25
Se	1	<0.5	<0.5	1.5	1.5	<0.5	1	<0.5	0.5	0.5	0.5	0.5	0.5	0.5	0.5	0.5	0.5	0.5	0.5	0.5	0.5	4.5	4.5	0.25	3
Sr	380	490	470	500	490	550	430	430	420	420	600	750	440	650	500	550	800	900	500	440	600	850	490	550	550
Te	<0.2	<0.2	<0.2	<0.2	<0.2	<0.2	<0.2	<0.2	<0.2	<0.2	<0.2	<0.2	<0.2	<0.2	<0.2	<0.2	<0.2	<0.2	<0.2	<0.2	<0.2	0.2	0.1	0.1	0.1
Th	3	7.5	3.8	3.8	4.2	5.5	6.5	7.5	5	3.9	3.1	3.8	3.9	3.1	4.5	4.5	3.3	2.9	2.4	7.5	5.5	5.5	2.3	3.9	3.5
Tl	<0.1	0.1	0.2	0.2	<0.1	0.3	0.3	0.1	0.4	0.1	0.1	<0.1	0.1	0.5	0.2	0.2	<0.1	0.1	<0.1	0.2	0.7	0.2	0.5	0.1	0.1
U	0.69	0.97	0.58	1.6	1.85	0.96	1.35	0.4	1.6	0.81	0.97	0.96	0.97	1	0.9	0.63	0.85	1.2	0.87	0.98	0.85	2	1.85	1.25	1.2
W	0.3	0.3	0.7	0.3	0.3	0.2	0.3	0.1	0.3	0.2	0.5	0.3	0.5	0.7	0.5	0.2	0.3	0.2	0.3	0.3	0.3	1.4	0.9	0.3	0.2
Y	12.5	6.5	14	10.5	19	16	6.5	13.5	8	15.5	14.5	15	14.5	4.5	13	14.5	18	9.5	12.5	8.5	8.5	41.5	24	11	10.5
Zn	12	8	9.5	10.5	24	10.5	15.5	6.5	17.5	8	8	8.5	7	11	10	11	18	9.5	9.5	17	10.5	220	15	9.5	10
Dy	2.2	1.45	2.9	2.9	4	2.9	2.7	2.7	1.75	2.9	2.9	2.6	2.6	3.6	2.7	2.5	3.6	2.3	2.3	2.2	2.1	5.5	3.9	1.9	1.8
Er	1.15	0.65	1.3	1.35	2.1	1.5	1.45	1.45	1.4	1.4	1.4	1.45	1.4	1.4	1.4	1.4	1.75	1.1	1.15	0.8	0.9	3.1	2.1	0.95	0.95
Eu	0.69	0.58	0.97	0.44	1.3	0.76	0.92	0.92	0.76	0.89	0.81	0.8	0.84	0.52	0.84	0.84	1.25	0.74	0.75	0.87	0.77	1.7	1.65	0.82	0.95
Gd	2.4	2.1	3.4	1.3	4	2.9	2.8	2.8	2.7	4.1	4.1	3.4	3.2	1.45	2.7	2.9	5.5	2.9	2.9	3.7	5.5	5.5	4.7	2.5	2.4
Ho	0.38	0.21	0.14	0.22	0.67	0.48	0.47	0.47	0.41	0.32	0.52	0.52	0.52	0.15	0.5	0.4	0.63	0.4	0.43	0.34	0.36	0.36	0.82	0.38	0.34
Lu	0.15	0.07	0.07	0.1	0.25	0.19	0.19	0.19	0.19	0.11	0.18	0.21	0.2	0.06	0.21	0.18	0.25	0.17	0.16	0.11	0.13	0.36	0.24	0.09	0.08
Nd	15	16	21.5	9.5	22	17	15	18	19	17.5	16.5	18	14	9	14	14	29	13	14.5	20	20	30.5	25	16	15
Pr	3.6	4	4.8	2.6	5	4.1	3.7	4.6	4.7	4.7	4.2	4.4	4.8	2.3	3.5	5	6.5	3.1	3.4	5	5	8.5	7	4.7	4.4
Sm	2.4	2.4	3.6	1.4	3.5	2.8	2.1	4.6	3.6	3	4.8	3.9	3.4	1.7	2.8	4.8	6.5	3.1	3.1	5.5	4.1	0.92	6	4.7	3.2
Tb	0.39	0.28	0.53	0.21	0.68	0.29	0.29	0.49	0.78	0.37	0.57	0.49	0.45	0.19	0.45	0.59	0.7	0.45	0.43	0.47	0.41	0.92	0.74	0.38	0.35
Tm	0.15	0.05	0.15	0.1	0.25	0.2	0.05	0.2	0.4	0.1	0.15	0.2	0.15	<0.05	0.2	0.15	0.25	0.15	0.15	0.1	0.1	0.4	0.3	0.1	0.1
Yb	1.1	0.6	1.15	0.85	1.95	1.3	0.6	1.4	3	0.6	0.95	1.15	1.15	0.35	1.25	1.1	1.35	0.95	0.95	0.7	0.65	2.5	1.7	0.85	0.8

Appendix 2 -

Element	RS03C	RS04C	RS05C	RS05C	RS06C	RS07C	1008	3083	6193	R013	R013a	R013b	R025	R025a	R025b	R028	R028a	R028b	R064HP	R064N	R064a	R064b	R090	R090a	R090b	R102
	1455404	453962	452991	451052	449813					458711	458607	458567	460765	460829	460820	460131	460104	460156	465605	465602	465601	465657	455522	455488	455519	457014
	6439812	6439771	6439731	6440970	6441234	?	?	?	?	6447764	6447698	6447722	6451384	6451378	6451299	6450373	6450381	6450316	6433137	6433137	6433063	6433093	6427609	6427638	6427571	6435059
Au	2	2	4	3	3	3	8	5	1	21	23	41	8	4	7	185	59	29	8	4	5	13	22	12	10	<1
Au Dp1																180	51									
Ba	135	650	310	125	430	550	850	500	330	390	390	330	1350	1700	600	850	480	470	300	290	330	250	430	1650	410	1750
Ca	301000	278000	292000	308000	296000	316000	299000	232000	228000	261000	195000	219000	185000	272000	274000	250000	288000	195000	275000	278000	240000	204000	186000	264000	305000	
Cr	6	8	5	4	6	4	6	11	11	6	9	9	11	7	6	11	19	12	14	4	5	6	7	9	8	7
Fe	6750	10200	7650	6800	6700	3600	7400	10200	11400	6600	7950	17200	10000	6600	11200	14400	10100	18900	6000	8300	8000	10000	18800	9800	8150	
K	3350	4550	3150	2000	3950	2400	2950	11900	3400	7450	6700	7250	23100	7600	5750	10100	6900	8300	3450	5300	4600	9200	10100	6550	4250	
Mg	4000	8800	6850	5250	11200	6300	7900	4650	4950	4100	5000	6300	4200	6400	5900	7500	7700	9700	41300	10900	40000	5050	5550	6250	7950	
Mn	86	64	135	48	120	74	44	72	82	96	58	120	98	84	105	125	175	72	58	54	78	110	110	110	66	
Na	2000	2200	1850	2650	1800	1450	1950	7850	10100	5350	22600	16100	11500	11200	5050	4950	3450	8200	2200	2950	2950	9900	11000	2450	3100	
P	330	330	260	150	270	155	92	460	230	230	320	210	280	290	360	330	330	340	250	310	180	380	600	290	1200	230
Ti	650	850	700	650	650	410	600	1100	950	650	750	1200	750	600	1050	1400	950	1550	600	750	750	1200	900	850	27
V	14	25	21	20	20	9	16	27	39	18	34	30	17	15	28	37	25	36	14	19	18	34	29	27	27	
S	750	1100	700	850	900	450	650	600	450	600	400	550	500	700	850	950	950	300	550	650	400	450	950	850	1400	
Ag	0.1	0.05	0.05	0.1	0.2	0.05	0.05	0.05	0.05	<0.1	<0.1	<0.1	<0.1	<0.1	<0.1	0.2	<0.1	<0.1	<0.1	<0.5	<0.1	<0.1	<0.1	<0.1	<0.1	<0.1
As	0.25	1	0.05	0.25	1	2	2.5	5	4.5	2	2	3.5	3.5	3.5	3	2.5	2.5	<0.1	<0.1	<0.5	1.5	3	0.4	0.3	3.5	0.5
Bi	0.05	0.05	0.05	0.05	0.2	0.05	0.05	0.2	0.05	<0.1	<0.1	<0.1	<0.1	<0.1	<0.1	<0.1	<0.1	<0.1	<0.1	<0.5	0.1	0.6	0.4	0.3	0.2	<0.1
Cd	0.2	0.3	0.3	0.2	0.2	0.7	0.2	0.2	<0.1	0.1	<0.1	<0.1	<0.1	<0.1	0.1	<0.1	<0.1	<0.1	<0.1	<0.1	0.1	0.6	0.4	0.3	0.2	0.5
Cs	0.5	0.9	0.7	0.6	0.6	0.6	0.6	1.1	0.8	0.7	1.1	0.6	1.1	1.2	1.7	1.3	1.1	1.1	0.6	0.9	0.9	2.5	2.4	2.1	0.7	
Ce	18	24	20.5	17.5	17	17	25	56	60	21.5	100	44	27	30	48	49	31.5	64	24	37	28	42.5	38.5	37.5	30.5	
Co	11.5	8.5	9.5	9.5	9.5	4	4.3	25	7	7	6	44	4.1	9.5	7	9.5	9.5	6.5	6.5	4.6	24	6.5	9.5	9.5	6
Cu	15	16.5	18	8.5	11.5	17	4.3	14	44	6	54	11	27	4.1	44	49	165	39.5	64	11	78	20.5	60	21.5	14
Ga	3.6	4.4	3.4	3.3	3.5	2.4	4.3	7	4.6	42.5	11	9.5	16	37	16.5	14.5	16	12	13.5	11	16	16.5	9.5	35.5	13.5	14
In	0.025	0.025	0.025	0.025	0.025	0.025	0.025	0.05	<0.05	<0.05	<0.05	<0.05	<0.05	<0.05	<0.05	<0.05	<0.05	<0.05	<0.05	<0.05	<0.05	<0.05	<0.05	<0.05	<0.05	36.5
La	11	15.5	23.5	23.5	15.5	17	26.5	30	27	11	60	15.5	21.5	15.5	31	26.5	26.5	35	14	20.5	14.5	23.5	23.5	22	21	<0.05
Mo	0.2	0.3	0.2	0.2	0.2	0.2	0.1	0.6	0.1	0.4	3.6	0.4	0.4	0.4	2.2	1.3	1.3	1.1	0.2	3.7	0.6	0.2	0.3	1.3	1.3	21
Ni	16	15	16	16	16	4	7	16	11	12	14	7	9	10	15	14	14	15	12	10	12	5	14	19	13	13
Pb	3.5	5.5	9.5	9.5	5	4	2.5	54	4.5	37.5	7	4.2	10.5	5	4	3	4.5	6	6	3	5	4	8.5	9.5	5.5	3
Rb	9.5	13	9	6	14	12	15	25	21	37.5	100	40	40.5	120	35.5	45	78	50	42.5	20.5	30.5	30	54	56	44	30.5
Sb	0.25	0.25	0.25	0.25	0.25	0.25	0.25	0.25	0.25	<0.5	<0.5	<0.5	<0.5	<0.5	<0.5	<0.5	<0.5	<0.5	<0.5	<0.5	<0.5	<0.5	<0.5	<0.5	<0.5	<0.5
Se	2.5	2	6	5.5	3.5	2.4	4.3	3	3	1.5	4	1.5	1.5	1.5	0.5	1	1	1	0.5	0.5	0.5	0.5	0.5	0.5	0.5	1
Sr	360	650	600	390	600	550	700	330	350	330	300	350	360	330	380	450	450	390	390	600	420	650	290	400	350	850
Te	0.1	0.2	0.1	0.1	0.1	0.1	0.1	0.1	<0.2	<0.2	<0.2	<0.2	<0.2	<0.2	<0.2	<0.2	<0.2	<0.2	<0.2	<0.2	<0.2	<0.2	<0.2	<0.2	<0.2	<0.1
Th	3.2	4.4	3.4	2.1	3.1	2.3	3.1	8	6	4.1	11.5	11.5	7.5	5.5	6.5	6.5	9.5	7	10.5	3.7	8	5	8.5	8	11	19
Tl	0.05	0.2	0.2	0.05	0.3	0.1	0.1	0.1	0.3	0.2	0.2	0.2	0.2	0.2	0.2	0.2	0.2	0.2	0.2	0.1	0.3	0.7	0.4	0.23	0.15	0.15
U	0.81	1	0.68	0.81	1.05	1.15	0.97	2.9	2.8	1.7	1.4	2.7	0.96	2.1	2.4	0.72	0.58	0.92	0.53	3.1	0.97	0.76	0.88	1.15	0.72	1.1
W	0.2	0.3	0.2	0.3	0.3	0.1	0.2	0.1	0.4	0.27	0.18	0.56	0.44	0.29	0.35	0.32	0.35	0.36	0.36	0.1	0.39	0.25	0.6	0.55	0.43	0.53
Y	8.5	11	18	23	14	13	29	28	120	10	40	18.5	14	14.5	18	21.5	21.5	14	27	12.5	19	13	22.5	15.5	18.5	19
Zn	12	18	17	9.5	11	20.5	21	29	14	11.5	14	11.5	12.5	11	15	23.5	8	7	16	9	16	30	42	44	18.5	10.5
Dy	1.35	1.95	2.8	4.2	2.1	2.9	4.5	4.5	18.5	1.75	3.2	3.2	2.3	1.55	1.65	1.9	1.9	2.1	2.1	1.55	2	1.4	2.9	2.9	2.3	3.4
Er	0.75	1.1	1.55	2.3	1.15	1.55	2.4	2.4	11.5	0.7	1.4	1.4	2.3	0.75	0.7	0.7	0.7	0.85	0.85	0.75	1.8	0.7	1.45	1.45	2.3	3
Eu	0.54	0.9	0.97	1.25	0.79	0.73	1.55	1.55	2.8	0.49	1.3	1.3	0.63	0.65	0.58	0.65	0.7	0.92	0.92	0.53	2	0.62	1.15	1.15	1.05	1.35
Gd	1.7	2.3	3.1	4.6	2.4	2.7	4.7	4.7	16.5	1.7	5	2.8	2.7	0.63	2.4	2.4	2.1	3.5	3.5	2	1.65	0.7	3.6	3.7	1.05	1.1
Ho	0.26	0.41	0.6	0.86	0.43	0.49	0.74	0.74	4.2	0.27	0.56	0.56	0.54	0.22	0.25	0.3	0.3	0.36	0.36	0.36	0.3	0.12	0.55	0.55	0.6	3.6
Lu	0.07	0.13	0.17	0.22	0.12	0.16	0.26	0.26	1.45	0.09	0.18	0.18	0.22	0.54	0.09	0.09	0.11	0.11	0.11	0.1	0.39	0.13	0.6	0.19	0.23	0.16
Nd	10	15	19	23	14	13	28	28	38.5	10	40	40	13.5	20	18	18	21.5	27	27	18	2	12.5	21	23	20	19
Pr	2.9	4.2	5.5	6	4	6.5	6.5	6.5	8	2.5	11.5	11.5	8	13.5	6	7.5	6	5.5	27	3.2	7.5	5	5.5	5	4	4.8
Sm	2.2	3.1	4	5.5	3.1	4.7	6	6	10.5	1.75	6.5	6.5	3.7	3.3	3.7	3.4	3.4	4.6	4.6	2.2	3.3	3.5	3.8	3.4	3	0.52
Tb	0.25	0.36	0.5	0.73	0.39	0.51	0.81	0.81	4.7	0.27	0.72	0.72	0.45	0.45	0.88	0.4	0.4	0.47	0.47	0.3	0.45	0.31	0.57	0.55	0.43	0.52
Tm	0.1	0.15	0.2	0.3	0.15	0.15	0.3	0.3	1.6	0.1	0.2	0.2	0.25	0.25	0.1	0.1	0.1	0.1	0.1	0.1	0.2	0.15	0.25	0.2	0.15	0.15
Yb	0.65	1	1.3	1.8	0.95	1.2	1.9	1.9	11	0.65	1.3	1.3	1.6	1.05	1.6	0.6	0.6	0.7	0.7	0.7	0.95	0.65	1.65	1.4	1.05	1.1

Appendix 2

Element	R102a 1457072 6435025	R102b 456940 6435017	R117 453127 6431060	R117a 453284 6431039	R117b 452962 6430978
Au	5	4	7	8	6
Au Dp1	–	–	–	–	–
Ba	1000	1750	600	340	550
Ca	281000	316000	215000	244000	277000
Cr	9	9	8	8	7
Fe	10700	7700	9100	11100	7800
K	7500	3500	6000	7550	3750
Mg	6900	7000	11900	6400	10500
Mn	78	62	88	175	88
Na	4350	2350	6450	3400	1600
P	260	290	230	200	185
Ti	1000	700	950	1150	950
V	26	21	29	36	28
S	1050	1450	500	400	600
Ag	<0.1	<0.1	<0.1	0.2	<0.1
As	1	0.5	5	13	4.5
Bi	<0.1	<0.1	0.2	0.4	<0.1
Cd	0.2	0.2	0.3	1.1	0.2
Cs	1.1	0.7	1.4	1.5	1.1
Ce	30.5	33.5	38	31.5	21.5
Co	7	5	6	12.5	7.5
Cu	15.5	13	16	20	12
Ga	23.5	36.5	17	12.5	14.5
In	<0.05	<0.05	<0.05	<0.05	<0.05
La	19	23.5	26.5	20	16.5
Mo	0.1	0.3	0.2	0.6	0.2
Ni	13	14	12	18	14
Pb	4.5	3.5	20.5	29.5	5.5
Rb	41.5	18	38.5	48.5	21
Sb	<0.5	<0.5	<0.5	0.5	<0.5
Se	1.5	1.5	<0.5	<0.5	1
Sr	400	460	650	470	500
Te	<0.2	<0.2	<0.2	<0.2	<0.2
Th	5.5	3.7	6	5	3.2
Tl	0.2	<0.1	0.2	0.2	0.1
U	0.86	1.3	1.15	1	0.75
W	0.2	0.1	0.7	2.3	0.7
Y	12	16.5	17	12	16
Zn	11	11	25.5	32.5	17
Dy	2.3	2.9	2.8	2.2	2.5
Er	1.1	1.4	1.45	1.2	1.4
Eu	0.9	1.25	0.96	0.68	0.75
Gd	3.1	3.9	3.8	2.8	2.9
Ho	0.44	0.55	0.56	0.44	0.53
Lu	0.14	0.18	0.18	0.17	0.18
Nd	17	20	22.5	16.5	14.5
Pr	4.3	5	6	4.4	3.7
Sm	2.9	3.4	3.9	3	2.7
Tb	0.46	0.57	0.55	0.44	0.45
Tm	0.15	0.2	0.2	0.15	0.2
Yb	1	1.3	1.25	1.25	1.25

Appendix 3 - Regional RCA assay geochemical maps

Au values over magnetics

Au (ppb)
- 17 - 650
- 12 - 17
- 4 - 12
- 2 - 4
- 0.5 - 2

0   2   4   Kilometres

N

Coordinates in GDA-94 datum, UTM UPS location format, zone 54 S
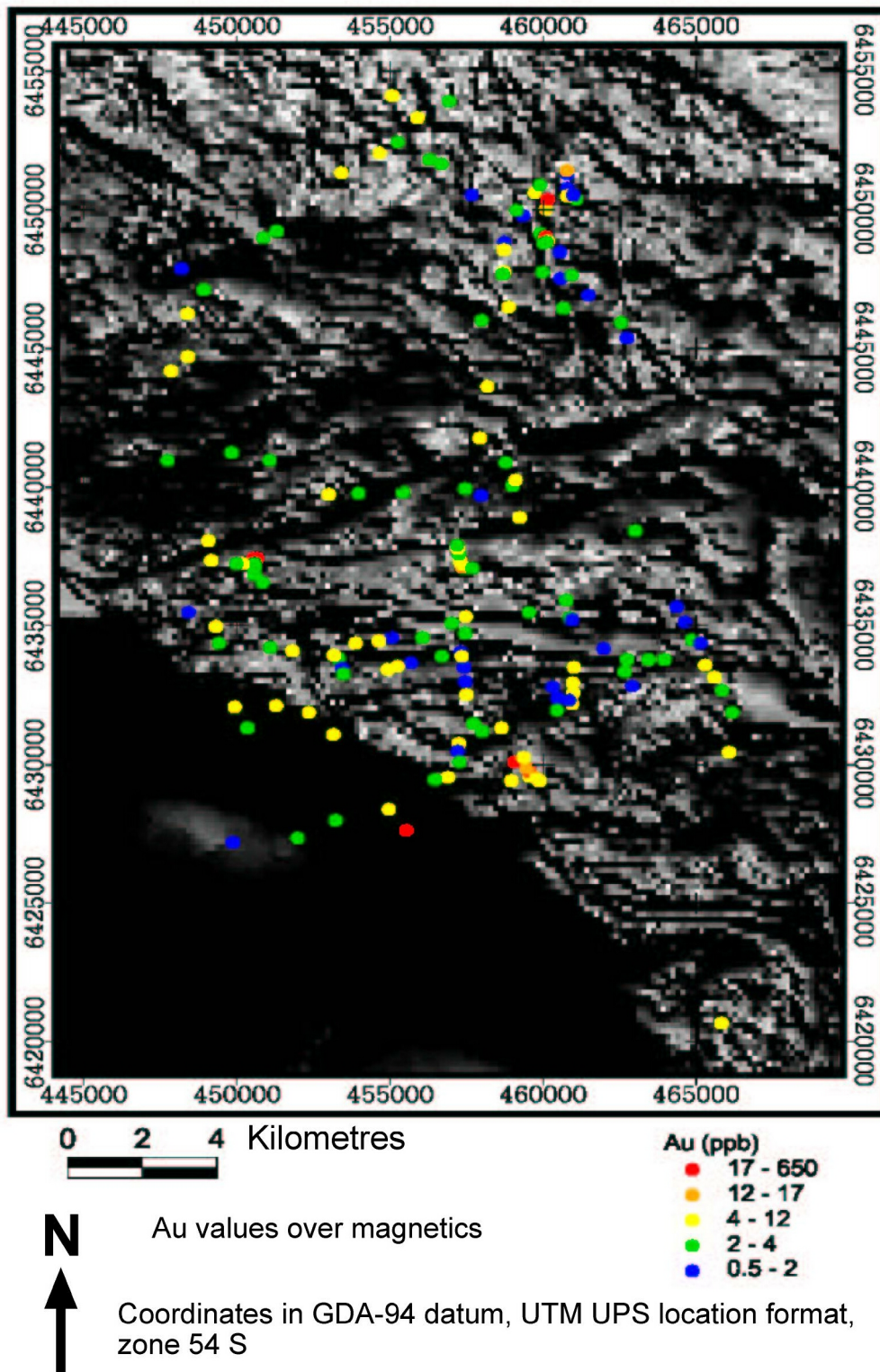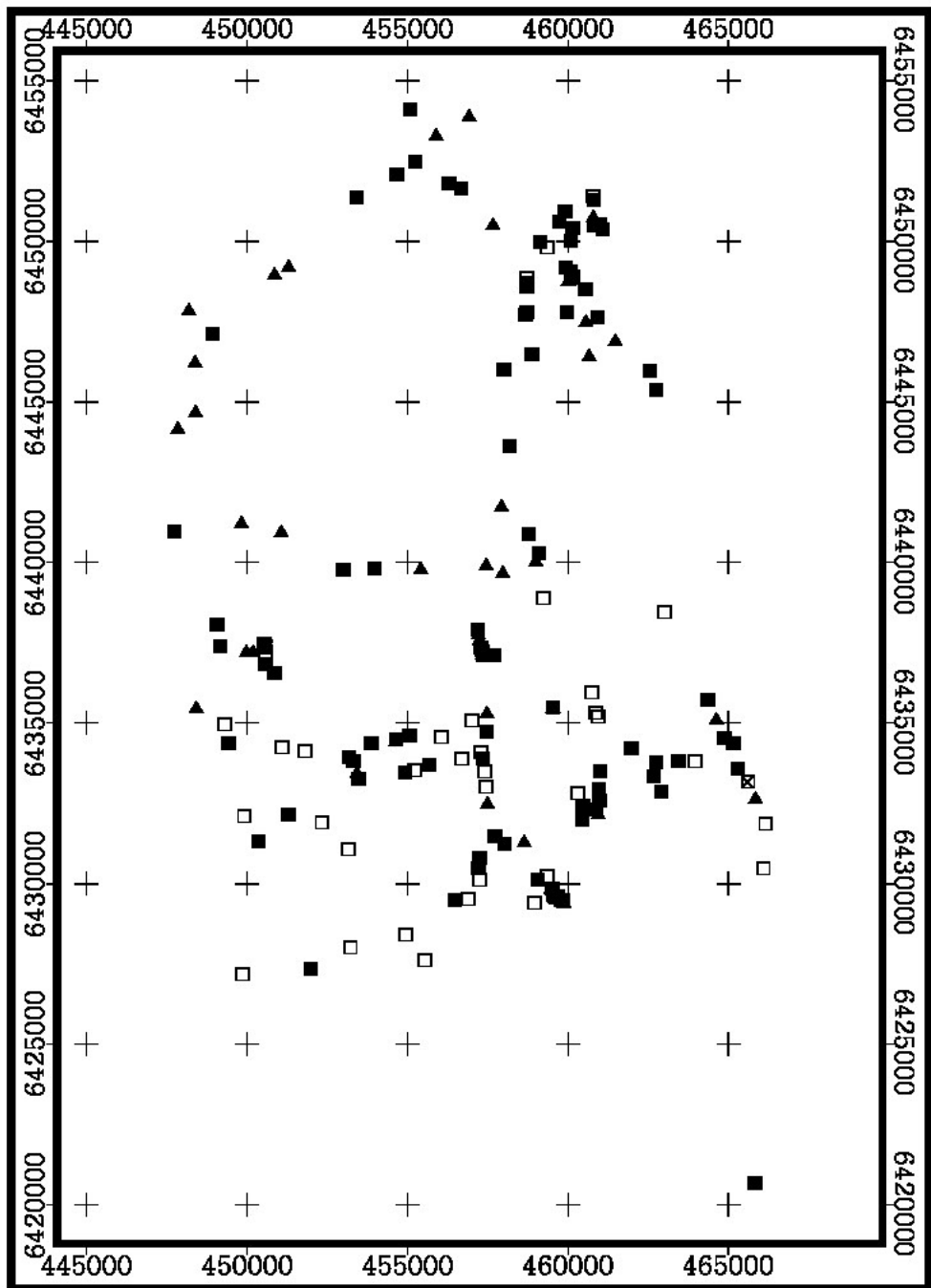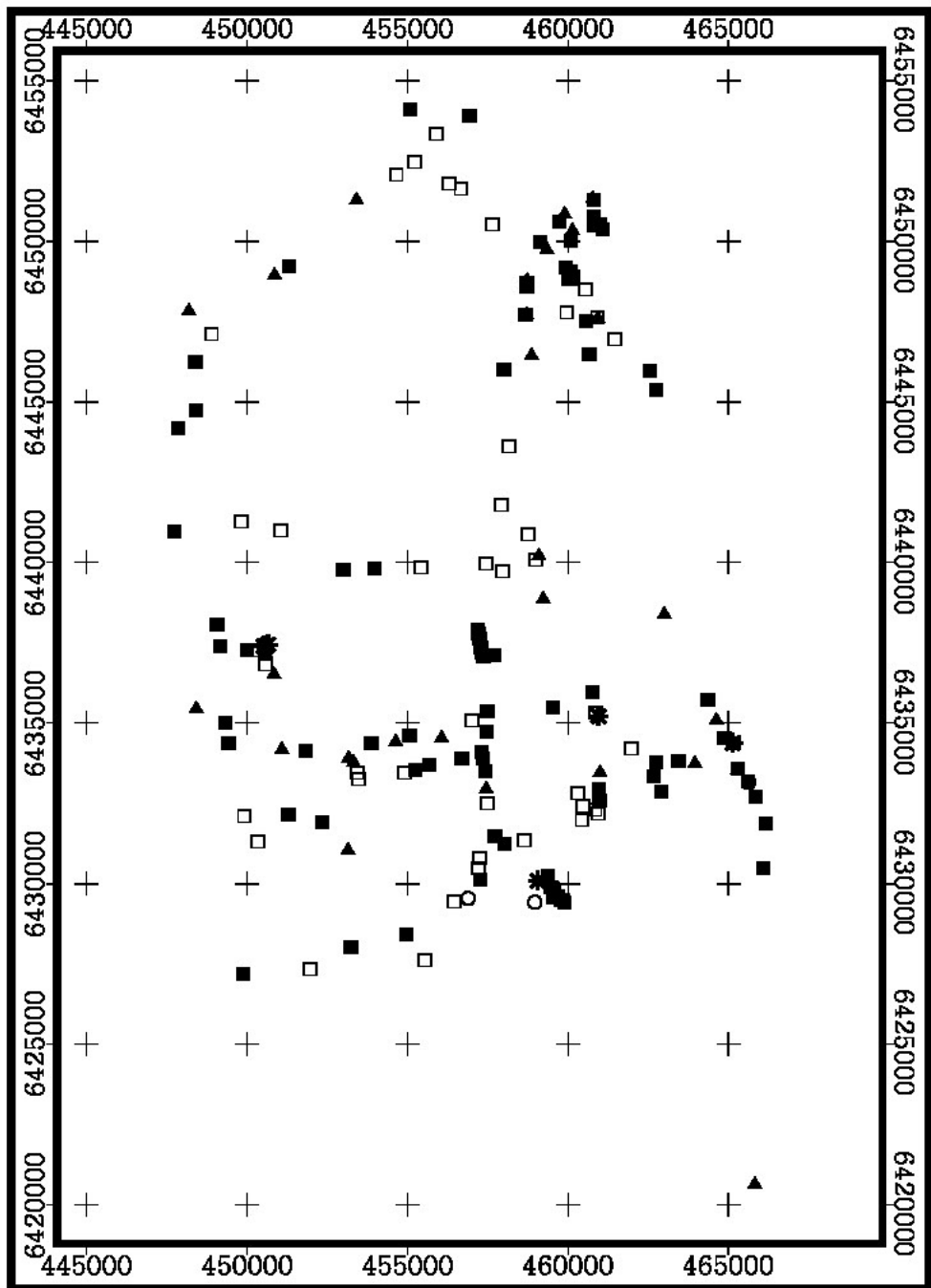
0   2   4   Kilometers

Ca (ppm)
▲   296000 - 339000
■   258000 - 296000
□   198000 - 258000
×   181000 - 198000
●   7150 - 181000
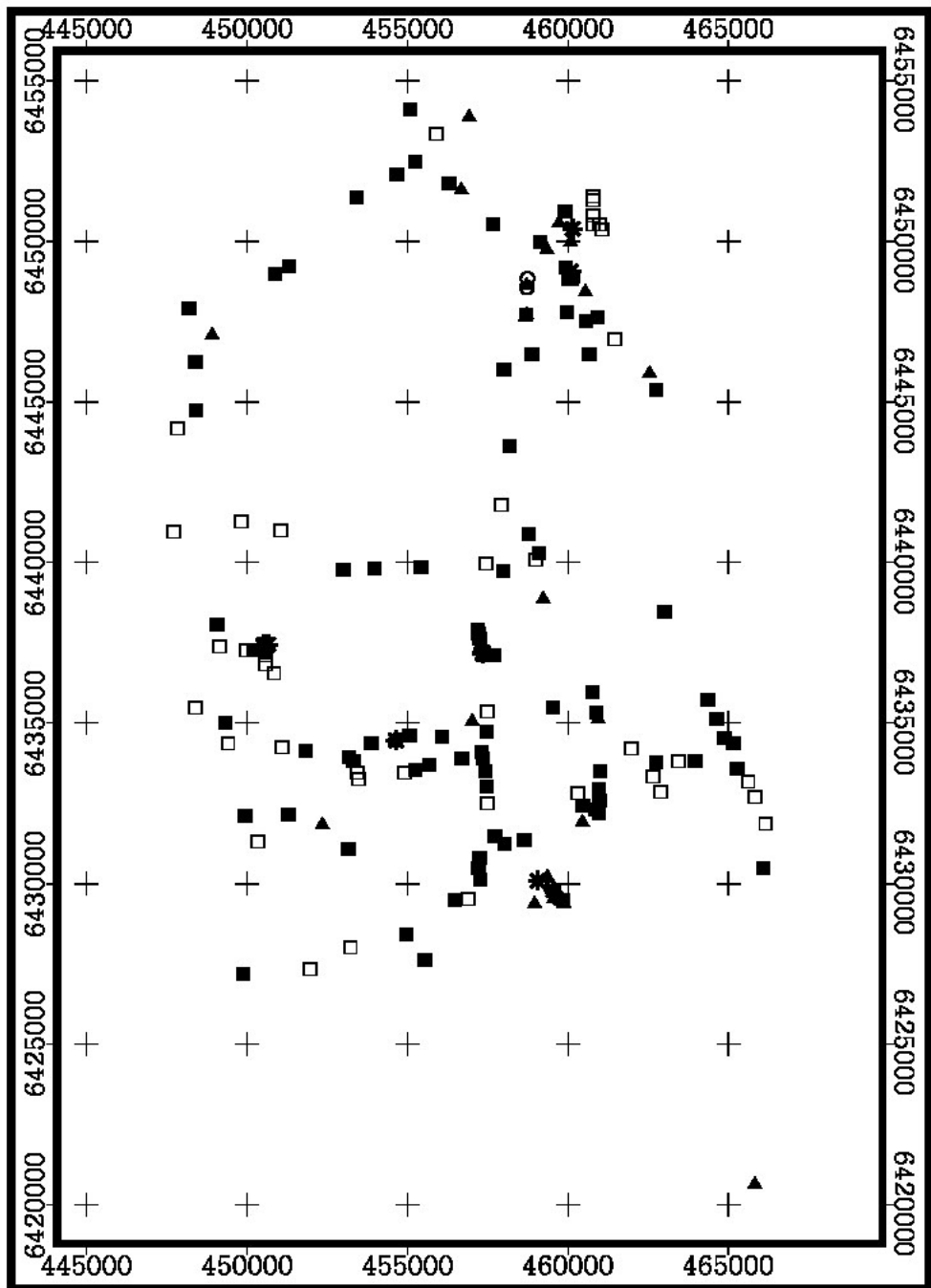
Fe (ppm)
* 20700 - 67500
○ 15800 - 20700
▲ 10900 - 15800
■ 7050 - 10900
□ 3150 - 7050
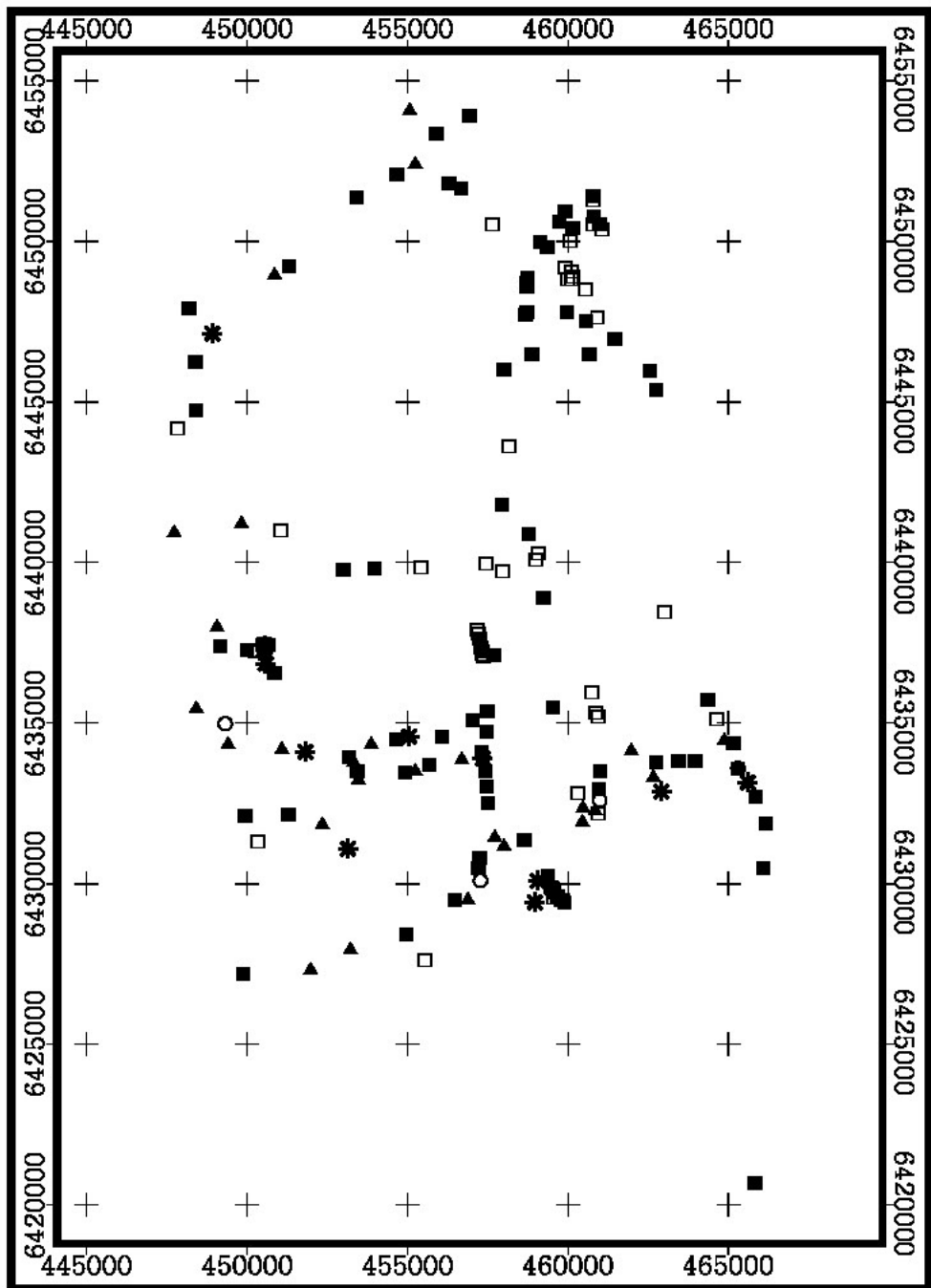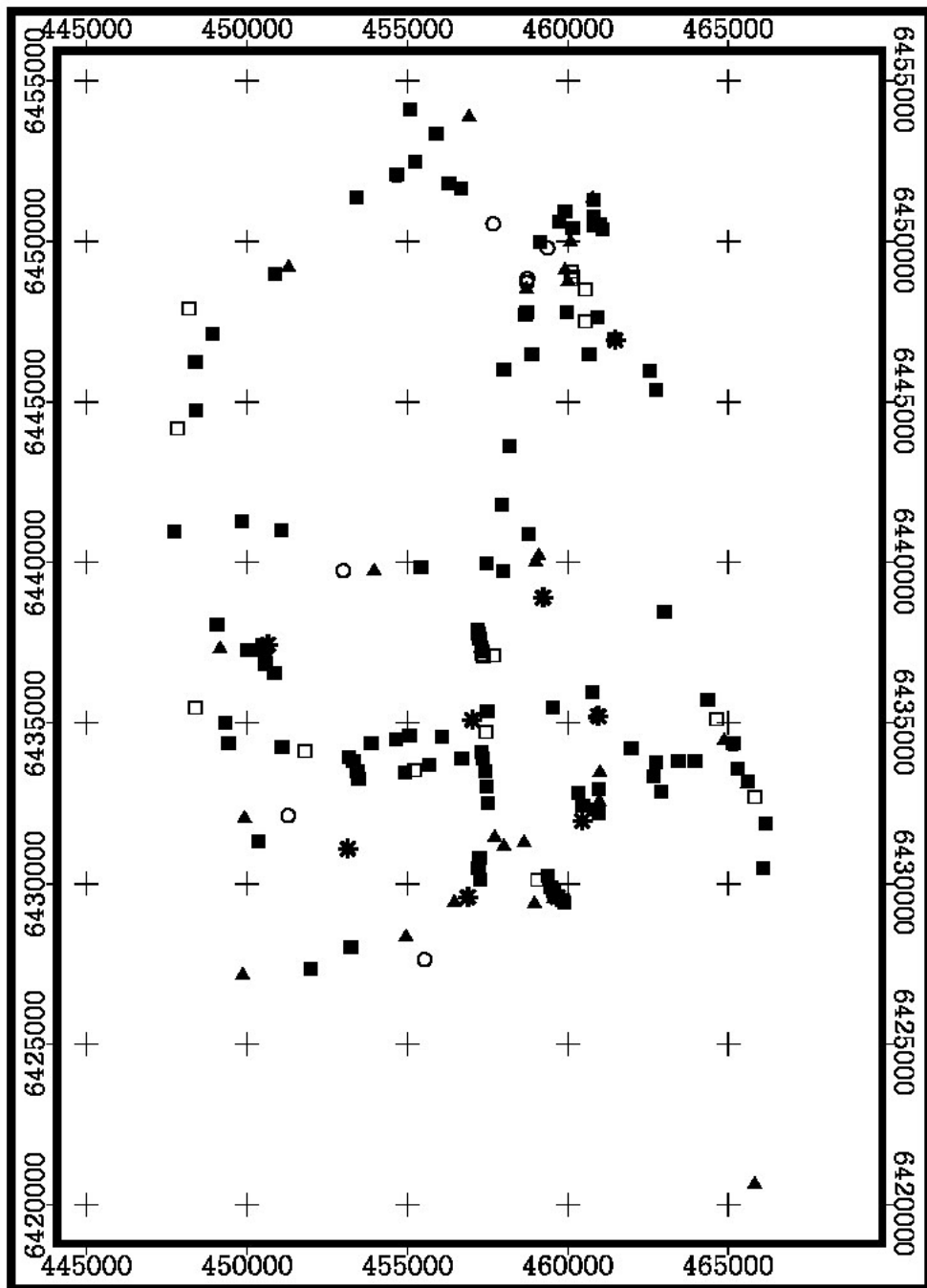
0   2   4   Kilometers

Pb (ppm)

✳	11.5 - 36.5
○	8 - 11.5
▲	5.5 - 8
■	3.5 - 5.5
□	2.5 - 3.5
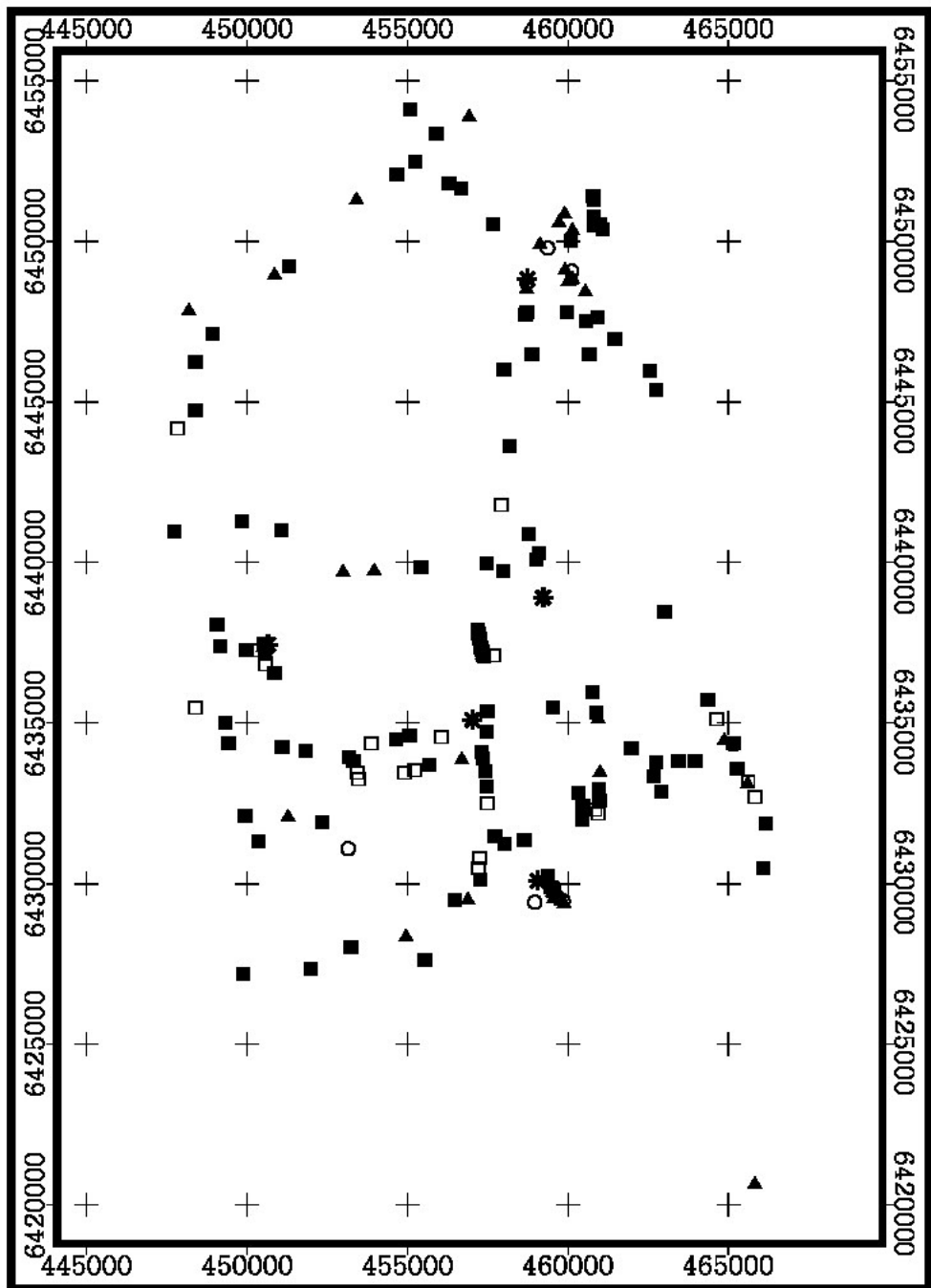
Appendix 4 - Transect scale RCA assays over mineralisation

Element	Units	Analysis	LB03C	LB04C	LB05C	LB07C	LB08C	LB09C	LB10C	LB13C	LB14C	LB15C	WK01C	WK02C	WK03C	WK04C	WK05C	WK06C	WK07C	WK11C	WK14C	WK15C	GG01C	GG02C	GG06C	GG08C	GG10C	GG16C
Sample # (GDA-94)			LB03C	LB04C	LB05C	LB07C	LB08C	LB09C	LB10C	LB13C	LB14C	LB15C	WK01C	WK02C	WK03C	WK04C	WK05C	WK06C	WK07C	WK11C	WK14C	WK15C	GG01C	GG02C	GG06C	GG08C	GG10C	GG16C
Eastings			459667	459627	459540	459538	459499	459511	459458	459782	459630	459874	457370	457351	457325	457325	457295	457296	457269	457244	457201	457187	450531	450518	450559	450565	450557	450567
Northings			6429551	6429592	6429542	6429714	6429760	6429809	6429834	6429476	6429435	6429380	6437046	6437095	6437138	6437200	6437254	6437304	6437335	6437594	6437770	6437878	6437387	6437431	6437320	6437208	6437112	6436813
Au	ppb	AA9	40	11	5	12	24	23	16	11	5	6	2	6	48	9	11	7	4	2	4	2	190	17	23	2	3	2
Au Dp1	ppb	AA9	-	-	-	-	-	-	-	-	-	-	-	-	-	-	-	-	-	-	-	-	-	-	-	-	-	-
Ba	ppm	IC3E	400	200	270	180	250	270	195	330	240	220	460	270	550	260	230	700	220	700	600	230	600	1350	420	340	380	105
Ca	ppm	IC3E	273000	278000	105000	296000	267000	244000	306000	295000	285000	308000	329000	308000	289000	288000	285000	275000	278000	301000	310000	274000	272000	263000	312000	243000	224000	264000
Cr	ppm	IC3E	13	32	16	7	10	8	10	13	12	7	-	6	5	7	8	8	8	6	6	7	6	8	4	8	8	<2
Fe	ppm	IC3E	11900	11500	7300	10100	17800	9750	9350	8900	8450	8600	6250	7400	19900	12700	10000	8650	8850	6850	7700	8300	17700	13800	8250	11100	12000	3300
K	ppm	IC3E	5300	4800	15000	4250	7850	9300	6100	4500	4650	3050	3100	4500	3800	6050	5400	4650	4400	4050	3800	3800	4650	9750	5650	5350	6000	1600
Mg	ppm	IC3E	8000	13500	2900	4900	7800	5700	7150	7900	7400	6400	4400	5050	5450	6800	6650	5800	6200	6900	5550	5700	16400	7300	6150	9150	9350	43000
Mn	ppm	IC3E	62	130	64	76	135	68	98	94	88	100	74	84	310	105	82	66	92	46	70	64	240	200	145	105	115	92
Na	ppm	IC3E	1800	1550	18900	1250	3150	11100	2200	2300	3550	2600	1250	1600	1700	2450	2950	3700	2350	1600	1800	5700	1750	3400	1850	5050	5200	2250
P	ppm	IC3E	220	310	200	145	550	280	200	340	175	290	290	260	330	480	320	330	440	320	310	210	270	200	360	440	550	210
Ti	ppm	IC3E	800	850	1000	550	1600	900	850	750	650	650	550	700	700	850	850	800	800	650	700	800	600	850	600	1000	1100	320
V	ppm	IC3E	30	25	19	15	45	23	19	21	19	21	14	18	23	22	22	23	21	19	18	22	27	27	18	23	26	10
S	ppm	IC3E	850	750	<50	850	550	500	850	850	650	800	1300	1050	1050	750	950	1250	1000	1450	1350	800	1300	1200	1250	900	950	650
Ag	ppm	IC3M	0.1	0.2	0.2	0.1	0.1	0.1	0.1	0.1	0.2	0.1	<0.1	0.1	<0.1	0.2	0.1	0.1	<0.1	<0.1	0.2	<0.1	0.1	0.1	<0.1	0.1	0.1	<0.1
As	ppm	IC3M	<0.5	<0.5	<0.5	<0.5	<0.5	<0.5	<0.5	<0.5	<0.5	0.1	<0.5	<0.5	1	1.5	<0.5	<0.5	<0.5	<0.5	<0.5	<0.5	2	0.1	1	<0.5	0.1	<0.5
Bi	ppm	IC3M	<0.1	0.3	<0.1	0.1	<0.1	0.1	0.2	0.1	0.5	0.7	0.1	0.2	0.2	0.1	0.1	0.1	0.2	0.2	0.2	0.1	0.5	0.2	0.2	<0.1	<0.1	<0.1
Cd	ppm	IC3M	0.2	0.2	0.1	0.2	0.1	0.2	0.2	0.4	0.7	0.8	0.6	0.6	1.5	0.2	0.1	0.7	0.7	0.6	0.7	0.7	0.8	0.9	0.9	0.3	0.3	0.1
Cs	ppm	IC3M	0.9	0.9	1	0.7	1.1	0.8	0.9	0.8	0.8	0.8	0.6	0.6	0.2	0.9	0.8	0.1	0.2	0.2	0.2	0.1	0.5	0.9	0.9	1	1.1	0.3
Ce	ppm	IC3M	66	34	48.5	47	34.5	39.5	37	25	20.5	25	20	17.5	24	27.5	32.5	62	31	24	25.5	27	26	50	24.5	20.5	23.5	23.5
Co	ppm	IC3M	12.5	14.5	6	13.5	16.5	10.5	12	11	11.5	13	11.5	18	54	13.5	11	9.5	11	9	10.5	11.5	19	12.5	12.5	9	9	11
Cu	ppm	IC3M	39	36.5	28.5	19	25.5	39.5	42.5	25	21	31	30	42.5	1800	9.8	60	36.5	32	13	17.5	4.8	440	64	38	14	12	8
Ga	ppm	IC3M	5	4.1	7.5	4.2	6	6	4.7	4.2	4.2	3.7	2.8	3.7	4.2	4.8	4.8	4.8	4.3	3.6	3.6	<0.05	4.3	5.5	3.5	5	3.5	9
In	ppm	IC3M	<0.05	<0.05	0.05	<0.05	<0.05	<0.05	<0.05	<0.05	<0.05	<0.05	<0.05	<0.05	0.15	<0.05	<0.05	<0.05	<0.05	<0.05	<0.05	<0.05	0.1	<0.05	<0.05	<0.05	<0.05	1.9
La	ppm	IC3M	35.5	31.5	33	37	22.5	24.5	24.5	19.5	19	22	13.5	10.5	16.5	16	19.5	60	17	15	21	17.5	17.5	23.5	20.5	15.5	22.5	<0.05
Mo	ppm	IC3M	0.5	0.3	0.6	0.3	0.6	0.3	0.3	0.3	0.3	0.6	0.3	0.4	0.8	0.4	0.3	0.3	0.3	0.2	0.2	0.2	0.7	0.6	0.3	0.3	0.2	7.5
Ni	ppm	IC3M	18	31	15	17	21	16	18	17	17	18	18	19	28	18	16	16	16	15	16	16	16	17	17	16	15	0.3
Pb	ppm	IC3M	11.5	3.5	6.5	3.5	4.5	5.5	24	10	4.5	4.5	2.5	3	2.5	3	11.5	7.5	5.5	4.5	4.5	7.5	7.5	6.5	4	6	6.5	12
Rb	ppm	IC3M	12.5	12	36.5	17.5	34	21.5	14.5	8.5	9.5	4.9	9	19	19	16	11.5	8.5	8.5	10	9	5.5	5.5	29.5	18	13	15	3.5
Sb	ppm	IC3M	<0.5	<0.5	<0.5	2.5	2.5	4.5	<0.5	<0.5	<0.5	<0.5	<0.5	3	<0.5	<0.5	<0.5	<0.5	<0.5	<0.5	<0.5	<0.5	<0.5	<0.5	<0.5	<0.5	<0.5	<0.1
Se	ppm	IC3M	2.5	4	4.5	4.5	4.5	4.5	3	3	2.5	1	2	12	2.5	1.5	2	2	2	2.5	1.5	2.5	2.5	<0.5	1.5	1.5	1.5	0.5
Sr	ppm	IC3M	750	850	240	380	450	500	550	650	600	550	370	470	380	550	650	550	500	650	500	500	1000	650	500	700	700	650
Te	ppm	IC3M	<0.2	<0.2	<0.2	<0.2	<0.2	<0.2	<0.2	<0.2	<0.2	<0.2	<0.2	<0.2	<0.2	<0.2	<0.2	<0.2	<0.2	<0.2	<0.2	<0.2	<0.2	<0.2	<0.2	<0.2	<0.2	<0.2
Th	ppm	IC3M	5.5	4.8	9	7	5.5	6.5	6.5	5.5	4.3	3.5	3.2	3.2	3.1	4.3	5	3.8	4	3.5	3.6	5	3.5	5.5	3.8	3.8	4.3	1.45
Tl	ppm	IC3M	1.7	0.2	0.2	0.2	0.3	0.2	0.2	0.1	0.1	0.1	0.1	0.1	0.3	0.2	0.2	0.1	0.1	0.1	0.1	0.1	0.2	0.3	0.2	0.1	0.1	<0.1
U	ppm	IC3M	1.1	1.2	0.93	0.97	1.2	1.05	0.89	0.74	0.68	0.93	0.93	0.86	2.9	1	0.86	1.4	0.66	1.3	0.84	0.88	3.5	1.85	1.35	1.8	1.9	1.9
W	ppm	IC3M	26	1	1.4	0.9	0.7	0.8	0.4	0.5	0.4	0.4	0.3	0.3	0.5	0.5	0.4	0.3	0.4	0.2	0.3	0.2	0.2	0.6	0.6	0.4	0.5	0.2
Y	ppm	IC3M	19	21	12.5	19.5	18	14.5	17.5	16.5	17	16.5	6.5	8	18	9.5	11	14.5	11	14.5	15.5	13	18	10	11	10.5	15.5	7
Zn	ppm	IC3M	4.4	26	17.5	14.5	22.5	15	14.5	22	25.5	22.5	15.5	12	15.5	12	11.5	12	16	10.5	12.5	12	13	13.5	10.5	18	19.5	8.5
Dy	ppm	IC3R	2.5	3.3	2.4	3.2	3.3	2.6	2.9	2.5	2.4	2.5	1.25	1.3	3.7	1.75	2.8	3.1	2.5	2.5	2.6	2.1	3	0.9	1.75	1.6	2.4	1.2
Er	ppm	IC3R	1.55	1.8	1.15	1.7	1.7	1.4	1.55	1.45	1.4	1.4	0.55	0.7	1.5	0.85	1	1.3	1	1.2	1.3	1.1	1.55	1.25	0.95	0.95	1.35	0.65
Eu	ppm	IC3R	4.9	1	1.1	1.1	1.1	0.97	0.86	0.88	0.81	0.87	0.62	0.57	1.5	0.85	0.92	4.6	0.78	1.3	1.3	0.92	1.25	2.7	0.75	0.65	0.89	0.38
Gd	ppm	IC3R	0.92	3.6	3.2	4	3.5	3	3.3	3	2.7	2.9	1.8	1.6	4.2	0.79	2.8	0.54	2.5	3.4	3.5	2.9	3.1	2.1	2.1	1.9	2.8	1.3
Ho	ppm	IC3R	0.32	0.69	0.46	0.64	0.66	0.54	0.59	0.54	0.52	0.53	0.22	0.26	0.63	0.33	0.38	0.54	0.38	0.49	0.52	0.42	0.61	0.35	0.37	0.33	0.5	0.24
Lu	ppm	IC3R	0.34	0.21	0.16	0.2	0.2	0.18	0.18	0.18	0.16	0.16	0.06	0.07	0.15	0.09	0.11	0.14	0.11	0.11	0.14	0.1	0.14	0.12	0.09	0.1	0.17	0.07
Nd	ppm	IC3R	10	22.5	25	27.5	19	20.5	19	17	16	17	12.5	9.5	16	14	18.5	30	15.5	21	20.5	16.5	14.5	19	14.5	12	17.5	7
Pr	ppm	IC3R	7.5	7	8	8.5	5.5	6	5.5	4.8	4.6	5	3.6	2.7	4.3	4.1	5	8	4.5	6	5.5	4.2	4.2	5.5	4.3	3.6	5	1.95
Sm	ppm	IC3R	0.8	4.8	5	6	4.5	4.4	4.3	3.7	3.5	3.8	2.6	2.1	4.3	3.2	5	7	3.5	4.5	4.6	3.7	3.4	3.4	2.8	2.5	3.5	1.6
Tb	ppm	IC3R	0.35	0.59	0.48	0.61	0.6	0.49	0.53	0.47	0.43	0.44	0.26	0.25	0.73	0.35	0.41	0.37	0.37	0.49	0.5	0.41	0.55	0.4	0.33	0.29	0.43	0.21
Tm	ppm	IC3R	2.4	0.25	0.15	0.25	0.25	0.2	0.2	0.2	0.2	0.2	0.05	0.1	0.2	0.1	0.15	0.15	0.15	0.15	0.15	0.15	0.2	0.1	0.1	0.1	0.2	0.1
Yb	ppm	IC3R		1.55	1.05	1.4	1.5	1.3	1.35	1.3	1.2	1.25	0.5	0.6	1.25	0.75	0.85	1.1	0.9	0.95	1.1	0.95	1.3	0.8	0.75	0.9	1.25	0.65

WK - Wilkins, GG - Green & Gold, LB - Luxemburg

Appendix 5 - Spot RCA assays near mineralisation

Element	Units	Analysis	WD RCA1	WD RCA2	WD RCA3	WD RCA4	WD RCA5	WK RCA	RH RCA	G&G1	G&G2	LB RCA1	LB RCA2	LB RCA3	LB RCA4
GDA-94		Eastings	459911	460086	460139	460096	459999	457336	465820	450634	450502	459040	459053	459953	459658
		Northings	6449158	6449051	6448878	6448809	6448787	6437148	6420635	6437406	6437387	6430082	6430088	6429388	6429558
Au	ppb	AA9	3	83	9	2	2	45	9	650	260	85	92	9	53
Au Dp1	ppb	AA10	-	86	-	-	-	43	-	750	230	76	98	-	-
Al	ppm	IC3E	19500	15900	18800	15100	15200	9000	15600	33900	12400	20000	13100	8100	16300
Ba	ppm	IC3E	480	1150	850	800	850	280	230	180	195	280	300	200	280
Ca	ppm	IC3E	260000	288000	278000	305000	296000	310000	283000	181000	284000	213000	264000	218000	274000
Cr	ppm	IC3E	8	42	6	6	3	3	14	22	5	290	210	145	12
Cu	ppm	IC3E	22	320	22	20	21	1100	31	250	1750	160	165	36	43
Fe	ppm	IC3E	8950	8950	10100	8350	8000	13600	11200	67500	20700	35600	26100	15800	10000
K	ppm	IC3E	4350	4800	3850	3850	3750	2750	3750	5900	3500	5750	2850	1450	6200
Mg	ppm	IC3E	5750	5400	6100	5250	5400	5050	6300	6650	5800	41800	25400	72300	8750
Mn	ppm	IC3E	82	3200	175	105	120	410	110	11400	1250	490	600	260	72
Na	ppm	IC3E	4350	4600	6800	4300	4200	1450	2600	1500	2000	2350	1850	2600	1950
Nb	ppm	IC3E	<5	<5	<5	<5	<5	<5	<5	6	<5	18	14	<5	<5
Ni	ppm	IC3E	3	7	8	6	6	7	8	7	10	155	120	140	9
P	ppm	IC3E	320	420	320	320	300	310	220	370	750	350	270	185	260
Pb	ppm	IC3E	6	<5	<5	<5	6	<5	6	14	<5	<5	<5	6	8
S	ppm	IC3E	850	800	650	600	750	600	400	950	700	250	200	200	450
Ti	ppm	IC3E	900	800	900	800	800	550	1700	1750	600	3750	3000	1000	800
V	ppm	IC3E	24	50	24	21	19	18	50	60	18	84	62	34	26
Zn	ppm	IC3E	24	28	22	23	21	19	19	58	23	70	52	32	25
Ag	ppm	IC3M	<0.1	0.3	<0.1	<0.1	<0.1	<0.1	0.2	0.2	0.2	0.2	0.1	<0.1	<0.1
As	ppm	IC3M	2.5	9	5	3.5	2	3.5	3.5	17.5	6	5	3	3	6
Bi	ppm	IC3M	<0.1	<0.1	0.1	<0.1	<0.1	0.5	0.5	13	2.3	0.3	0.1	<0.1	<0.1
Cd	ppm	IC3M	0.2	0.2	0.1	0.2	0.1	0.2	0.2	0.2	0.3	0.1	0.1	0.1	0.2
Co	ppm	IC3M	2.2	42	5.5	4.3	4.3	28.5	10.5	10.5	29.5	36.5	27	22.5	8.5
Cs	ppm	IC3M	1	1.3	0.9	1.1	0.8	0.8	1	2.2	1.7	7.5	3.4	1	1
Ga	ppm	IC3M	5.5	5.5	6	4.7	5	3.5	4.5	11	4.2	7	5	2.6	5.5
In	ppm	IC3M	<0.05	<0.05	<0.05	<0.05	<0.05	0.15	<0.05	0.75	0.25	<0.05	<0.05	<0.05	<0.05
Mo	ppm	IC3M	0.3	4.8	0.2	0.2	0.2	0.7	<0.1	36	0.2	0.2	0.4	0.3	0.5
Rb	ppm	IC3M	19	23	13	15	15.5	11	13	47	18.5	40	16	<0.1	22
Sb	ppm	IC3M	<0.5	6	2	<0.5	<0.5	<0.5	<0.5	0.5	1	<0.5	1	<0.5	<0.5
Se	ppm	IC3M	<0.5	<0.5	1	1	1	0.4	<0.5	<0.5	<0.5	<0.5	<0.5	<0.5	<0.5
Sn	ppm	IC3M	0.7	0.6	1.1	0.7	0.9	0.4	0.7	1.3	0.4	0.9	0.7	0.4	1.5
Sr	ppm	IC3M	500	420	480	410	460	430	460	350	440	480	380	1000	650
Te	ppm	IC3M	<0.2	<0.2	<0.2	<0.2	<0.2	<0.2	<0.2	2	0.3	<0.2	<0.2	<0.2	<0.2
Th	ppm	IC3M	4.6	3.8	4.6	4	3.7	2.5	2.6	14	3.9	2.2	1.55	0.86	3.9
Tl	ppm	IC3M	0.2	0.6	0.1	0.1	0.2	0.2	0.1	6.5	0.66	1.05	0.81	0.14	0.14
U	ppm	IC3M	1.6	2.3	0.94	0.79	1.2	1.05	7.5	2.1	0.61	0.87	0.6	0.69	1.3
W	ppm	IC3M	0.2	0.3	0.2	<0.1	0.1	0.2	0.3	8	0.6	0.6	0.3	0.1	0.4
Y	ppm	IC3M	30.5	20	23.5	20	23.5	12	15	17.5	20	11.5	8	5	20.5
Hf	ppm	IC3R	<1	<1	<1	<1	<1	<1	<1	2	<1	1	1	<1	<1
Dy	ppm	IC3R	4.6	3	4	3.4	3.7	2.5	2.6	9.5	3.9	2.2	1.55	0.86	3.9
Er	ppm	IC3R	2.4	1.85	2.3	1.8	2.1	1.1	1.5	2.3	1.85	1.05	0.75	0.45	1.95
Eu	ppm	IC3R	1.35	0.97	1.25	1.05	1.1	0.89	0.8	2.1	0.91	0.98	0.81	0.35	1.2
Gd	ppm	IC3R	4.6	2.7	3.8	3.3	3.4	2.9	2.6	8	2.8	2.5	1.9	0.9	4.3
Ho	ppm	IC3R	0.76	0.54	0.67	0.54	0.63	0.37	0.43	2.2	0.61	0.34	0.23	0.14	0.6
Lu	ppm	IC3R	0.27	0.23	0.28	0.22	0.26	0.11	0.21	0.6	0.15	0.12	0.09	0.06	0.23
Pr	ppm	IC3R	6.5	4.6	5.5	5.5	5	4.6	4.7	9.5	3.1	7	5.5	2.1	8.5
Tb	ppm	IC3R	0.84	0.51	0.71	0.57	0.63	0.5	0.45	2.3	0.66	0.41	0.3	0.14	0.73
Tm	ppm	IC3R	0.3	0.25	0.3	0.25	0.25	0.15	0.2	0.8	0.2	0.15	0.1	0.05	0.25
Yb	ppm	IC3R	1.95	1.8	2.2	1.65	1.95	0.9	1.55	5.5	1.45	0.95	0.65	0.45	1.8
Ce	ppm	IC3R	27.5	36.5	44.5	37.5	30.5	31.5	31.5	80	25.5	54	45	16	66
La	ppm	IC3R	26	24.5	24	23.5	21	19.5	25.5	43	14.5	39.5	33	12	34.5
Nd	ppm	IC3R	26	24.5	24	22.5	21	18	25.5	34	12.5	24.5	18.5	8	32.5
Sm	ppm	IC3R	5.5	17.5	5	4.3	4.1	3.8	17.5	8.5	3.1	3.9	2.9	1.3	6.5

WD - White Dam, WK - Wilkins, RH - Radium Hill, GG - Green & Gold, LB - Luxemburg

Appendix 6 - Prospect scale RCA assays (Wilkins Case Study)

Element	Units	Analysis	WCS002	WCS004	WCS006	WCS007	WCS008	WCS010	WCS011	WCS012	WCS013	WCS014	WCS015	WCS017	WCS019	WCS020	WCS021	WCS026	WCS027	WCS028	WCS029	WCS030
Sample #			WCS002	WCS004	WCS006	WCS007	WCS008	WCS010	WCS011	WCS012	WCS013	WCS014	WCS015	WCS017	WCS019	WCS020	WCS021	WCS026	WCS027	WCS028	WCS029	WCS030
Eastings (GDA-94)			457728	457723	457564	457392	457088	457194	457170	457126	457043	456810	456873	456956	457008	457186	457069	456701	456819	457001	457503	457371
Northings			6437394	6436768	6437278	6437651	6437984	6437890	6437822	6437511	6437431	6437158	6437523	6437634	6437866	6437123	6437039	6437570	6437790	6437871	6437363	6437254
Au	ppb	AA9	8	2	9	4	9	3	<1	3	4	7	6	7	5	6	4	5	6	4	7	17
Au Dp1	ppb	AA9	6	-	-	-	-	2	1	2	4	-	-	-	-	-	-	-	-	5	-	-
Ba	ppm	IC3E	600	470	460	800	370	340	950	1350	650	550	320	340	410	490	470	320	360	1050	430	500
Ca	ppm	IC3E	297000	306000	303000	299000	296000	284000	284000	312000	294000	277000	241000	279000	277000	281000	271000	258000	272000	278000	261000	281000
Cr	ppm	IC3E	8	9	7	7	7	9	8	6	6	7	10	7	6	9	6	8	8	7	11	8
Fe	ppm	IC3E	11300	7850	7250	6300	8850	8100	8900	6700	7200	8350	20100	7000	6500	8900	9600	8700	8800	7400	11600	10000
K	ppm	IC3E	4700	4200	3450	4350	4200	3000	3500	3950	4350	5100	4950	4150	3600	4900	3350	6150	5350	3650	7100	6250
Mg	ppm	IC3E	8000	7150	5600	7700	6550	5800	6600	6650	7100	6650	5050	5850	6100	6400	5750	6100	5250	6450	7750	10500
Mn	ppm	IC3E	54	80	68	42	96	64	58	50	60	50	54	52	56	64	64	50	64	58	64	84
Na	ppm	IC3E	3450	3900	3600	1900	2150	7200	5500	2450	2200	2950	9050	3300	5800	2100	4050	5400	4200	4900	3700	3450
P	ppm	IC3E	200	310	220	330	220	270	210	200	190	190	370	250	230	240	200	270	195	240	220	250
Ti	ppm	IC3E	850	800	650	650	850	850	850	750	750	850	900	750	650	750	700	800	900	800	1050	900
V	ppm	IC3E	29	23	17	20	25	22	27	22	22	22	39	20	22	22	21	22	23	24	27	24
s	ppm	IC3E	900	800	700	1300	650	750	1050	1200	850	700	550	650	750	750	600	650	600	800	650	700
Ag	ppm	IC3M	<0.1	0.5	<0.1	<0.1	<0.1	<0.1	<0.1	<0.1	<0.1	<0.1	<0.1	<0.1	<0.1	<0.1	<0.1	<0.1	<0.1	<0.1	<0.1	<0.1
As	ppm	IC3M	3.5	2.5	<0.5	1.5	2	1.5	1.5	1	1	<0.5	3.5	2.5	2.5	1.5	1	2.5	2	2	1.5	3
Bi	ppm	IC3M	<0.1	0.2	<0.1	<0.1	<0.1	<0.1	0.1	<0.1	<0.1	<0.1	<0.1	<0.1	<0.1	0.1	0.1	<0.1	<0.1	<0.1	<0.1	<0.1
Cd	ppm	IC3M	0.1	1	0.2	0.1	0.2	0.2	0.1	0.1	0.1	0.1	0.1	0.2	0.1	0.1	0.1	0.1	0.1	0.1	0.1	0.1
Cs	ppm	IC3M	0.9	0.7	0.8	0.7	1.1	0.6	0.7	0.7	0.8	0.9	0.7	0.7	0.7	0.9	0.7	0.9	0.8	0.9	1.1	1.2
Co	ppm	IC3M	6	6.5	6.5	3.6	9.5	6	5.5	4.7	6	5	13.5	6	5.5	5	6.5	8.5	7	6	6	7.5
Cu	ppm	IC3M	38	17.5	105	18.5	27	15	19	13.5	14.5	14	21	16	15	27.5	35	17	12.5	14.5	43.5	84
Ga	ppm	IC3M	17	13	12.5	19.5	11.5	11	23.5	30	17	16	13	11	12.5	13.5	13.5	12	12.5	26	15	16
In	ppm	IC3M	<0.05	0.15	<0.05	<0.05	<0.05	<0.05	<0.05	<0.05	<0.05	<0.05	<0.05	<0.05	<0.05	<0.05	<0.05	<0.05	<0.05	<0.05	<0.05	<0.05
Mo	ppm	IC3M	0.3	0.9	0.2	0.2	0.2	0.2	0.2	0.1	0.1	0.1	0.4	0.1	0.2	0.3	0.8	0.2	0.5	0.1	0.2	0.2
Nb	ppm	IC3M	3.5	5	3	2.5	3	2.5	2.5	2.5	2.5	3.5	3	2.5	2.5	2.5	3	3.5	3.5	2.5	4	3.5
Ni	ppm	IC3M	14	16	14	13	14	13	13	13	13	14	14	14	14	13	13	14	15	14	16	15
Pb	ppm	IC3M	3.5	3.5	3	3.5	5.5	4	5.5	4	4	4	3.5	3.5	4.5	4.5	3	13	3.5	4.5	4	3.5
Rb	ppm	IC3M	27	24	20	23	26	14.5	19	21.5	24.5	32	20.5	20.5	20	26	20.5	35	31.5	20.5	42	36.5
Sb	ppm	IC3M	<0.5	0.5	<0.5	<0.5	<0.5	<0.5	<0.5	<0.5	<0.5	<0.5	<0.5	<0.5	<0.5	<0.5	<0.5	<0.5	<0.5	<0.5	<0.5	<0.5
Se	ppm	IC3M	<0.5	18	1	<0.5	1.5	0.5	0.5	0.5	1	0.5	1	1	1	1.5	1	1.5	2	2	<0.5	1.5
Sr	ppm	IC3M	550	390	430	600	450	440	480	470	480	400	440	440	380	460	430	420	380	490	480	550
Te	ppm	IC3M	<0.2	0.9	<0.2	<0.2	<0.2	<0.2	<0.2	<0.2	<0.2	<0.2	<0.2	<0.2	<0.2	<0.2	<0.2	<0.2	<0.2	<0.2	<0.2	<0.2
Th	ppm	IC3M	5	7.5	3.8	4.5	4.3	4.2	4.9	4.1	4	5	8	4.3	3.1	4.3	7	4.4	4.9	4.2	8	8
Tl	ppm	IC3M	0.1	0.3	0.1	0.1	0.1	<0.1	<0.1	<0.1	<0.1	<0.1	0.1	0.1	0.1	0.1	0.1	0.2	0.1	0.1	0.2	0.2
U	ppm	IC3M	1.05	1.2	0.92	1.75	0.87	0.83	1.1	0.87	0.71	1	1.1	0.72	0.74	0.82	1.2	0.8	1.1	0.84	1.15	1.2
W	ppm	IC3M	0.6	0.9	0.2	0.2	0.3	0.2	0.3	0.2	0.2	0.2	0.2	0.2	0.5	0.3	0.7	0.7	0.3	0.2	0.3	0.3
Y	ppm	IC3M	12.5	14.5	18	12.5	20.5	13	12.5	15.5	12	10	7.5	8	14	11.5	9.5	6	10.5	16.5	10.5	13.5
Zn	ppm	IC3M	15.5	14.5	11	8.5	17.5	10.5	16	9	10.5	11	10	9.5	11.5	11.5	11	11	9.5	12	11	10.5
Ce	ppm	IC3R	33.5	46	37.5	50	27.5	36	42	28.5	26.5	33.5	58	27.5	25.5	48	36.5	29	40	29.5	52	60
La	ppm	IC3R	22.5	27	26	27	21.5	22.5	21.5	23.5	19	20	31	16	20	25	21.5	16	23.5	23.5	28.5	30.5
Dy	ppm	IC3R	2.4	3	2.8	3.2	3.4	2.5	2.8	2.8	2.2	2	1.9	1.75	2.6	2.3	2.1	1.35	2.3	2.9	2.4	3.3
Er	ppm	IC3R	1.05	1.4	1.4	1.2	1.8	1.15	1.2	1.1	1.1	0.95	0.7	0.8	1.25	1	0.95	0.6	0.95	1.45	1.1	1.35
Eu	ppm	IC3R	1	1.05	0.98	1.75	1.05	0.99	1.25	1.35	0.93	0.76	0.95	0.69	0.96	0.96	0.87	0.63	0.92	1.25	1.1	1.3
Gd	ppm	IC3R	3.5	4.4	3.7	5	4.3	3.7	4.3	4.3	3.1	2.9	3.5	2.5	3.6	3.5	3.3	2.1	3.4	4.4	4.1	5
Ho	ppm	IC3R	0.45	0.57	0.55	0.55	0.7	0.45	0.5	0.55	0.45	0.37	0.39	0.32	0.51	0.43	0.37	0.24	0.41	0.59	0.41	0.57
Lu	ppm	IC3R	0.12	0.22	0.16	0.14	0.21	0.14	0.14	0.15	0.13	0.11	0.09	0.1	0.15	0.12	0.12	0.07	0.12	0.17	0.12	0.16
Nd	ppm	IC3R	20.5	25	20.5	33.5	19.5	20	22.5	23.5	17.5	17.5	25	14.5	19	23	19	14	20.5	22.5	25.5	28.5
Pr	ppm	IC3R	5	6.5	5.5	8.5	4.8	5	5.5	6	4.4	4.7	7	3.7	4.7	6	5	3.6	5.5	5.5	6.5	7
Sm	ppm	IC3R	3.7	4.6	3.7	6.5	3.9	3.7	4.3	4.1	3.1	3.1	4.3	2.7	3.5	3.9	3.4	2.4	3.7	4.5	4.5	5.5
Tb	ppm	IC3R	0.5	0.67	0.55	0.73	0.65	0.5	0.59	0.6	0.44	0.41	0.45	0.35	0.52	0.49	0.46	0.3	0.5	0.6	0.54	0.71
Tm	ppm	IC3R	0.15	0.25	0.2	0.15	0.25	0.15	0.15	0.15	0.15	0.1	0.1	0.1	0.15	0.15	0.1	0.1	0.15	0.2	0.15	0.15
Yb	ppm	IC3R	0.95	1.3	1.2	1	1.55	0.95	1.05	1.1	0.9	0.8	0.65	0.75	1.05	0.95	0.85	0.55	0.85	1.25	0.85	1.1
Y	ppm	IC3R	12.5	14.5	18	12.5	20.5	13	12.5	15.5	12	10	7.5	8	14	11	9.5	6	10.5	16.5	10.5	13.5

WCS - Wilkins Case Study samples